1-1-2016

Traffic Signal Control at Connected Vehicle Equipped Intersections

Zhitong Huang

Traffic signal control at connected vehicle equipped intersections

By

Zhitong Huang

A Dissertation
Submitted to the Faculty of
Mississippi State University
in Partial Fulfillment of the Requirements
for the Degree of Doctor of Philosophy
in Civil Engineering
in the Department of Civil and Environmental Engineering

Mississippi State, Mississippi

May 2016

Traffic signal control at connected vehicle equipped intersections

By

Zhitong Huang

Approved:

_____

Li Zhang
(Major Professor)

_____

Thomas D White
(Committee Member)

_____

Qi Zhang
(Committee Member)

_____

Govindarajan Vadakpat
(Committee Member)

_____

James L Martin
(Graduate Coordinator)

_____

Jason M Keith
Dean
Bagley College of Engineering

Name: Zhitong Huang

Date of Degree: May 6, 2016

Institution: Mississippi State University

Major Field: Civil Engineering

Major Professor: Li Zhang

Title of Study: Traffic signal control at connected vehicle equipped intersections

Pages in Study: 173

Candidate for Degree of Doctor of Philosophy

The dissertation presents a connected vehicle based traffic signal control model (CVTSCM) for signalized arterials. The model addresses different levels of traffic congestion starting with the initial deployment of connected vehicle technologies focusing on two modules created in CVTSCM. For near/under-saturated intersections, an arterial-level traffic progression optimization model (ALTPOM) is being proposed. ALTPOM improves traffic progression by optimizing offsets for an entire signalized arterial simultaneously. To optimize these offsets, splits of coordinated intersections are first adjusted to balance predicted upcoming demands of all approaches at individual intersections.

An open source traffic simulator was selected to implement and evaluate the performance of ALTPOM. The case studies' field signal timing plans were coordinated and optimized using TRANSYT-7F as the benchmark. ALTPOM was implemented with connected vehicles penetration rates at 25% and 50%, ALTPOM significantly outperforms TRANSYT-7F with at least 26.0% reduction of control delay (sec/vehicle) and a 4.4% increase of throughput for both directions of major and minor streets. This

technique differs from traditional traffic coordination which prioritizes major street traffic, and thereby generally results in degrading performance on minor streets. ALTPOM also provides smooth traffic progression for the coordinated direction with little impact on the opposite direction. The performance of ALTPOM improves as the penetration rate of connected vehicles increases.

For saturated/oversaturated conditions, two queue length management based Active Traffic Management (ATM) strategies are proposed, analytically investigated, and experimentally validated. The first strategy distributes as much green time as possible for approaches with higher saturation discharge rate in order to reduce delay. For the second approach, green times are allocated to balance queue lengths of major and minor streets preventing queue spillback or gridlock. Both strategies were formulated initially using uniform arrival and departure, and then validated using field vehicle trajectory data. After validation of the modules, the effectiveness of CVTSCM is proven. Then, conclusions and recommendations for future researches are presented at the end.

Keywords: Connected Vehicle, Traffic Signal Coordination, Traffic Progression, Queue Management.

DEDICATION

To my family.

ACKNOWLEDGEMENTS

I would like to express my deepest gratitude to my advisor, Dr. Li Zhang. Dr. Zhang not only provided invaluable guidance during my PhD study but also gave me insightful suggestions when I was faced with difficulties. Thanks also to Dr. Zhang for providing financial support during my PhD study.

I also want to convey thanks to all of my committee members: Dr. Thomas D. White, Dr. Qi Zhang and Dr. Govindarajan Vadakpat. Thanks for your constructive suggestions and for reviewing my dissertation with your helpful comments and suggestions.

I am thankful to the staff and faculty members within the Department of Civil and Environmental Engineering at Mississippi State University. I also want to thank my friends and colleagues at MSU: Dr. Jizhan Gou, Dr. Yi Wen, Ms. Fang Zhou, Mr. Lei Zhang, and Mr. William Case Fulcher etc.

I am grateful for the Dwight David Eisenhower Transportation Fellowship Program for providing financial support for my dissertation research while at the Turner Fairbank Highway Research Center of Federal Highway Administration.

I would like to acknowledge my supervisor and colleagues at Saxton Transportation Operations Laboratory: Mr. Thomas H Philips, Mr. Frank Perry, Mr. Edward M. Leslie, and Dr. Jiaqi Ma, etc.

I would like to express my sincere appreciation for my supervisor at the Federal Highway Administration, Ms. Deborah M Curtis. It was my great fortune to work as a graduate research fellow under Deb's guide. Deb always provided timely help and enlightening suggestions throughout my dissertation research.

Most importantly, I would like to express my earnest acknowledgement to my parents, Qiang Huang and Fengying Gao, and my uncle (Prof. Yuhai Sun). Without their encouragements and support, this dissertation could not have been completed.

TABLE OF CONTENTS

LIST OF TABLES

LIST OF FIGURES

CHAPTER I

INTRODUCTION

1.1 Problem Statement

Traffic congestion has become one of the largest threats to the United States when it comes to economic competitiveness, livability, safety, and long-term environmental sustainability. According to the newest version of the urban mobility report by the Texas Transportation Institute (TTI), from 1982 to 2011 the total cost of traffic congestion in the United States rocketed from 24 to 121 billion dollars [1]. With the continuous increase of auto ownership, the affordability of transportation options, and limits on viable land use for transportation expansion, the future of traffic congestion appears grim. All of these factors result in not only significant economic costs but also increases in air pollution and consumption of precious natural resources.

Congestion on freeways and arterials is a major component and contributor of traffic congestion, and arterials usually experience more blockage than freeways. Specifically, intersection congestion is one of the most outstanding sources of arterial congestion. As indicated by the Federal Highway Administration (FHWA) in the U.S., there are over 260,000 traffic signals which are estimated to result in 5-10% of all traffic delays on major roadways. In state-of-the-practice, traffic signal retiming is one of the most cost-effective methods that can be used to decrease congestion with a ratio of benefit to cost potentially reaching 40 to 1 [2].

Emerging technologies provide opportunities to mitigate traffic congestion. Connected vehicles (previously known as IntelliDrive and Vehicle Infrastructure Integration (VII)), a United States Department of Transportation (US DOT) major research initiative, brings unparalleled safety benefits and also holds promise to alleviate traffic congestion and environmental impacts of future transportation systems.

Connected vehicles can work with advance sensors to communicate with highway infrastructure and other connected vehicles. As a result, it can provide real-time traffic data and warning information to drivers by applying state-of-the-art technologies including advanced communications, on-board computer processing, GPS navigation, advanced vehicle sensors, and smart infrastructures, etc. [3]. There are two major initiatives of connected vehicle: Vehicle-to-Vehicle (V2V) and Vehicle-to-Infrastructure (V2I). V2V focuses on data transfer between vehicles to avoid potential threats. V2I can wirelessly exchange key safety and operating data between vehicles and highway infrastructure [4].

For signalized arterials, the V2I system facilitates communication between connected vehicles and traffic signal control systems thereby exchanging critical operation and safety data by using road side unit (RSU) and vehicle onboard equipment (OBE). This data includes, but is not limited to, signal phase and timing, intersection geometry, and vehicle status information (e.g. position, speed, and acceleration rate, etc.). The information gathered is encoded as several message sets, such as SPaT, MAP, and Basic Safety Message (BSM) data etc., which are defined in the J2735 standard of the Society of Automotive Engineers (SAE) [5]. Therefore, the V2I system provides critical, real-time mobility data which could be utilized to optimize traffic signal system

operation. Models and/or algorithms based on connected vehicle technologies which improve highway system mobility are referred to as one type of connected vehicle mobility applications.

Currently, connected vehicle technology is mostly still in simulation and/or experimental stages and the full implementation of this technology on all vehicles travel on highways (i.e. penetration rates of connected vehicles are 100%) is still decades from completion. However, traffic signal models and algorithms based on connected vehicle technologies can generate obvious benefits in the present when the penetration rate of connected vehicles reaches a minimum value. Goodall indicated that according to results of previous studies the minimum vehicle penetration rate for connected vehicle traffic signal control applications is 20-30%, and that it only takes 5-7 years to be met [6].

Therefore, it is a forthcoming challenge to utilize this emerging technology in its early developmental stage to improve the mobility of transportation systems during a time when the penetration rate of connected vehicles is far from 100%. Unfortunately, it will also take a long time and a significant amount of investment to completely upgrade the existing traffic infrastructure to be fully compatible with connected vehicle technology equipment. There is a need in this beginning stage of connected vehicles to find a solution by utilizing the technology to help our current transportation needs, while also considering existing infrastructure with focus given to a low cost upgrade, which will be one of the objectives of this dissertation.

1.2 Objective

The objective of this dissertation is to create a traffic signal control model for connected vehicle equipped signalized intersections. The proposed model is aimed at implementation at the beginning stage of connected vehicle deployment where the penetration rate of connected vehicles is not 100%. Therefore, a connected vehicle based traffic signal control model (CVTSCM) is developed for this purpose. Specifically, there are two major traffic signal control modules that will be developed for under-saturated and saturated (or oversaturated) conditions. The CVTSCM will address all traffic conditions associated with signalized arterials.

With respect to under-saturated conditions, delays are one of the most important performance measures. Traffic signal coordination is a popular and widely used approach to mitigate delays and congestion in the U.S. and other countries. The objective of traffic signal coordination is to make sure there is continuous movement along an arterial or traverse major streets of a network with minimum delays and stops, which would decrease fuel consumption and vehicle emissions [7]. Proactive traffic signal coordination is one of major types of traffic signal coordination. It real-time adjusts and/or optimizes parameters of traffic signal coordination according to real-time and predicted traffic data. One of the remarkable advantages of connected vehicle technologies is that they can provide accurate and rich traffic information, which can be used to measure current and predict forthcoming traffic conditions in real-time. Therefore, integration of traffic signal coordination with connected vehicle technologies allows for a great leap forward in the state-of-the-practice that could be achieved in the near future. An arterial-level traffic progression optimization model (ALTPOM) is

developed to provide smooth traffic progression for upcoming traffic for an entire arterial in order to improve mobility of the signalized arterial.

When traffic conditions become saturated, serious congestion can appear and Active Traffic Management (ATM) is currently a widely used approach in mitigating traffic congestion in the United States. ATM is defined as "the ability to dynamically manage recurrent and non-recurrent congestion based on prevailing and predicted traffic conditions" [8]. Based on rich, accurate and real-time traffic data provided by connected vehicle technologies, we can measure and/or predict prevailing and upcoming traffic conditions. It is a beneficial choice to integrate ATM with connected vehicle technologies. When traffic conditions are saturated or oversaturated, delay may not be the most relevant performance measure. Managing queue length is more important in order to prevent queue spillback from one intersection to another which would inevitably create gridlock. These situations may result in the performance of transportation systems being significantly degraded. Therefore, two queue length management based active traffic management strategies for connected vehicle equipped signalized intersections are being developed for saturated or oversaturated conditions.

Figure 1.1 shows the entire framework of methodology in this dissertation. When traffic conditions are under-saturated, the arterial-level traffic progression optimization model is used to provide smooth progression for upcoming traffic. When traffic conditions become saturated, queue length management ATM strategies are applied to control queue length dynamics in order to prevent queue spillback and gridlock. The developed traffic signal control model/strategies in this dissertation can handle all traffic conditions of a signalized arterial. It is also expected that the model and strategies

outlined in this dissertation could be easily programmed into a low cost "black box" computer. The "black box" could be directly installed into existing traffic signal cabinets for all National Transportation Communications for ITS Protocols (NTCIP) compatible traffic signal controllers to implement the proposed model and strategies in the field.

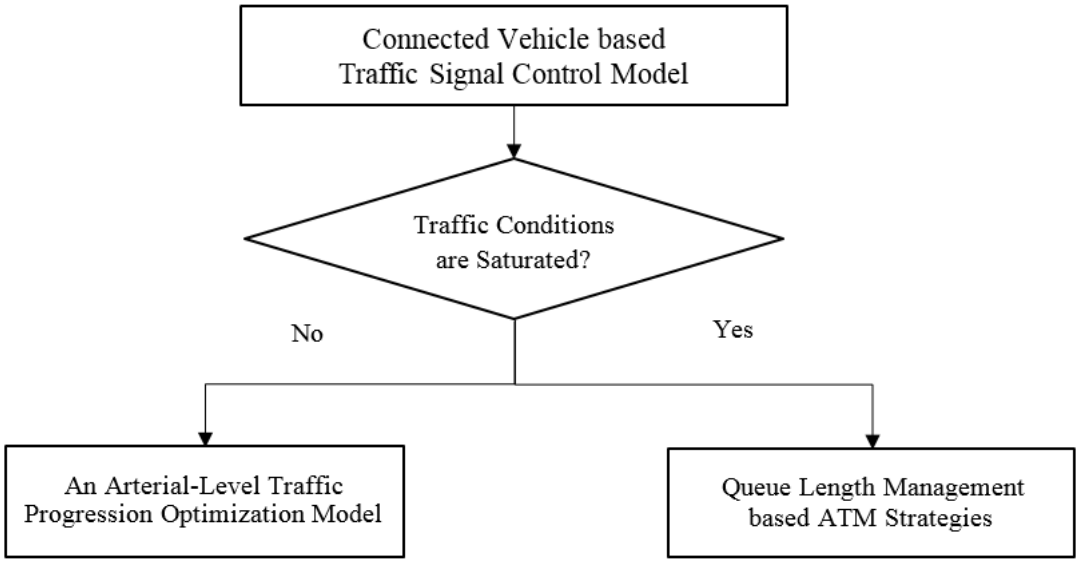

Figure 1.1 The Entire Framework of Methodology in this Dissertation

1.3 Significance of This Dissertation

Traffic signal coordination has proven to be a major and popular approach in the U.S. and other countries to mitigate delays, increase travel speed, and reduce the number of stops for signalized arterials. The most prevalent and widely used traffic signal coordination method is one where all coordination intersections have the same background cycle length (i.e. centralized control). Based on the reviewed literature provided in chapter 2, it has been determined that this dissertation is the first research to implement the use of connected vehicle technologies on centralized control traffic signal

coordination, and thus proposes an arterial-level traffic progression optimization model (ALTPOM). As shown in chapter 4, based on connected vehicle technologies, the ALTPOM can significantly reduce delays, increase speed, and enhance throughput of a signalized arterial with low penetration rates of connected vehicles (25% and 50%). Specifically, ALTPOM significantly outperforms TRANSYT-7F with at least a 26.0% control delay (second per vehicle) reduction, at a minimum 7.8% average speed increase, and no less than a 4.4% throughput improvement, for both directions of major streets and that of minor streets. These results reveal one of the outstanding features of ALTPOM in that it improves performances of both major and minor streets. This feature is unique and differs from traditional traffic coordination, which puts emphasis on major street traffic and generally results in the degrading performance of minor streets. The reason is that ALTPOM not only optimizes the offsets but also proactively and dynamically adjusts splits of all phases.

The most prominent characteristic of ALTPOM is that it optimizes traffic progressions for an entire signalized arterial instead of following what most common traffic progression optimization models do by optimizing traffic progressions for each coordinated intersection individually or sequentially. ALTPOM optimizes the offsets of all coordinated intersections within a signalized arterial simultaneously to improve traffic progressions for the entire arterial. The objective function of ALTPOM is to maximize the total number of arrivals on green after clearing the queue for the whole arterial. ALTPOM's performance for providing traffic progression for an entire arterial is quite exceptional. As indicated by the results in chapter 4, ALTPOM reduced the stopped vehicle percent for the coordinated direction (at least 12.3%) with little impact on the

opposite direction (increases at most 1.8% of the stopped vehicle percent) for the study arterial.

Vehicles' trajectories are critical for traffic signal coordination. Since the arrival times of all traffic are known, we can better arrange green start or end time of a coordinated intersection to let as many vehicles as possible traverse through an intersection without stopping. In this dissertation, a mixed vehicle propagation model is presented based on fusion data of the loop detector data and connected vehicles data to predict vehicle trajectories of the total traffic (both equipped and non-equipped vehicles). ALTPOM utilizes predicted vehicle trajectories of the total traffic to optimize offsets of coordinated intersections.

When considering resident queue length, it has been found to have a non-negligible impact on traffic signal coordination. Even under the green light, the resident queue can result in upcoming vehicles decelerating or coming to a complete stop to join the existing queue, which would seriously interrupt traffic progression of a signal timing plan even if optimized. Therefore, the developed ALTPOM in chapter 3 has specifically considered this impact, whereas traditional methods commonly don't take resident queue length into consideration or are apt to assume the impacts of resident queue to be minor. In this dissertation, to provide smooth progression ALTPOM only considers vehicles arrival on green after resident queue cleared as the performance measure (i.e. number of arrivals on green).

Since connected vehicle technology is still mostly in simulation and/or experimental stages, there is not suitable field data with enough penetration rates of connected vehicles to validate connected vehicle applications at this time, and this

continues to be one of the largest difficulties facing researchers. To solve this restraint and make sure proposed traffic signal control models and strategies could be implemented in the field without significant revision and/or a lot of field experimentation, this dissertation uses simulated Basic Safety Messages (BSM) and BSM equivalent data to validate the developed models and algorithms. Specifically, the ALTPOM in chapter 3 is verified by simulated BSMs provided by Trajectory Conversion Algorithm (TCA) software which is produced by Noblis, Inc [9]. For the two presented ATM strategies in chapter 5, actual vehicle trajectory data collected from US DOT's Next Generation of SIMulation (NGSIM) program [10] is utilized. As indicated by a fact sheet of FHWA, the used data set provides the highest resolution vehicle trajectory data at each 0.1 second with accurate lane locations and positions for each vehicle [8].

Lastly, traffic signal control models/strategies based on connected vehicle technologies for existing traffic infrastructure with a low cost upgrade are needed. The traffic control models/strategies developed in this dissertation meet these goals and requirements.

1.4 Framework of This Dissertation

There are six total chapters in this dissertation with this chapter (Chapter 1) introducing the background, objectives, significance, and framework of the dissertation. Chapter 2 discusses previous related studies in the fields of traffic signal control and optimization for signalized arterials, bridging technologies of connected vehicles, and connected vehicle mobility applications. Next, an arterial-level traffic progression optimization model (ALTPOM) within the connected vehicle environment is presented in chapter 3. Chapter 4 illustrates the methods used to implement and validate the

ALTPOM. Two queue length management based ATM strategies for saturated/oversaturated signalized intersections are developed and validated in chapter 5. Conclusions of this dissertation and recommendations for future research are presented in chapter 6.

CHAPTER II

LITERATURE REVIEW

In this chapter, previous studies related to topics in three major fields are reviewed for this dissertation. Firstly, studies in traffic signal optimization within under-saturated and over-saturated conditions are investigated. The traditional traffic signal control methods provide a foundation for traffic signal control within connected vehicle environments. Then, researchers' work focusing on implementing and evaluating bridging technologies of connected vehicles is reviewed. These technologies can provide vehicle trajectory data, and some of them are already being implemented in the field. Their approaches and experiences are good references for future implementation of connected vehicle technologies. Lastly, connected vehicle applications for improving mobility of transportation systems, especially for traffic signal control, are reviewed.

2.1 Traffic Signal Control and Optimization for Signalized Arterials

Since there are enormous amounts of information on traditional traffic signal control and optimization, this dissertation focused upon sources that would be useful in formulating and supporting the ideas of this research. More specifically, sources focusing upon offset tuning and optimization, traffic signal coordination optimization, and adaptive traffic signal control systems are reviewed in depth.

2.1.1 Offset Tuning and Optimization

Offset is a critical parameter for signal coordination and is the key for traffic progression. In this section, reviews are focused on state-of-the-practice offset optimization and tuning techniques with specific interest given to real-time implementation, which is the major feature of connected vehicle technology.

Li and Furth, et al [11], presented a method to calculate the most-likely optimal offsets of arterials by utilizing the cycle by cycle green usage reports from ATMS. Mitigating the impacts of "early return to green" on progression was the major concern, and the authors decided to apply the Monte Carlo Simulation to generate distribution of time length for "early return to green" at each intersection. Based on those calculations, this paper pin pointed the optimal offset distribution and selected the most likely offsets to occur. The proposed optimization method for offsets in this reference was an offline approach.

Shoup and Bullock [12] presented an offline fine-tuned offsets method for an arterial based on travel time data. This reference indicated this method mitigated the impacts of "early return to green" and downstream queue on progression. Initial offsets were determined based on the end point of the green phase and the link free flow travel time. Then the scholars adjusted the offsets according to the average disruptive travel time over several cycles (i.e. stop delay of the first vehicle of a platoon). For this approach, only one-directional progression was considered.

Liu and Hu, et al. [13] chose to utilize a data-driven approach to optimize offsets of an arterial. The deterministic delay model for two successive intersections was formed first. This reference mathematically formed a relationship between vehicle actuation and

coordinated a phase green time start point to calculate the corresponding conditional distribution. Weight factors were used for two directions of the major street. The objective of this model was to decrease the delay of a major direction without significantly increasing the delay of the reverse direction. The proposed optimization method in this reference was also an offline approach.

Day, Haseman, et al. [14], presented two methods to evaluate and improve traffic progression for a corridor. The first method was the Purdue Coordination Diagram (PCD). PCD used the high resolution detector data and signal phase data to generate a figure which combines arrival profiles and green time profiles. Based on the percentages of arrivals on green and the total number of arrivals on green, PCD was performed to assess progression and to enhance it by offset adjustments. For the second method, Bluetooth MAC address matching technology was used to re-identify vehicles for travel time assessment. The presented optimization approach for offsets in this reference is also offline.

Gettman, Head, et al. [15], proposed two real-time offset adjustment algorithms, Distributed Offset Adjustment (DOA) and Network Offset Adjustment (NOA), which were actual algorithms in ACS-lite. DOA considered adjusting the offset between a pair of upstream and downstream intersections individually, and NOA adjusted a group of offsets for a highway corridor. DOA and NOA both used incremental step sizes to adjust offsets, such as 2, 4 or 6 seconds. Captured flow, i.e. expectation of arrival on green, was the objective function of this reference. The algorithms presented in this reference were online approaches, but they were still found to be responsive.

Abbas, Bullock, et al. [16], proposed an algorithm for real-time offset adjustment for actuated traffic signal coordination systems. The key concept of this algorithm was that the smaller the difference between distributions of advanced detector occupancy and actuation profiles led to better progression based on diffusion theory. The reference calculated the skewness of absolute differences between detector occupancy and actuation profiles, which was used as a criterion for applying the proposed algorithm. The presented algorithm adjusted offsets accordingly to move green time to cover higher occupancy summation. The proposed algorithm in this reference was responsive.

Liu, Han, et al. [17], proposed an offset optimization model for congested arterial networks based on fixed-time control. The authors of this reference calculated ideal offset, maximum offset (to prevent queue spillback), and minimum offset (to avoid unused green due to no arrivals). An adjustment factor to the ideal offset was presented by the authors of this reference as the penalty function. The objective function of this reference was to minimize the penalty function for the entire network. The constraints of this model were maximum and minimum offsets as well as relationships between inbound and outbound offsets of two adjacent intersections. A case study was conducted to validate the proposed model. Compared with fixed-time control optimized by SYNCHRO, the presented model provided better performance than SYNCHRO with respect to system average delay (improved around 10%) and throughput (enhanced less than 5%). Although this paper used real-time adaptively optimized offsets, it didn't consider the controller transition and it optimized offsets cycle by cycle which is unrealistic for field implementation.

Abbas and Jung, et al. [18], used the stop bar detector's count and occupancy profiles as well as microscopic shockwave theory to identify early, good, and later offsets. The scholars presented a simple method to adjust offset that adds and subtracts the preset time period for early and late offsets, respectively. The simulation study was performed and CORSIM was used as the simulator. According to the results, this method can decrease 5-6% delay when compared with using a fixed offset.

Takahashi and Nakarnura, et al. [19], applied a genetic algorithm to dynamically optimize offsets by considering variations of traffic flow. A highway arterial with twenty-one intersections was used as the test network, and the average travel time was chosen as the performance measure. Two strategies were performed: the first strategy used the offset patterns of the previous traffic volume as the initial solution of genetic algorithm for current traffic level, and the second approach considered the differences of offsets between previous and current traffic levels. A simulation case study was then conducted and based on the results the second strategy was found to have better results than that of the first method.

2.1.2 Optimization for Traffic Signal Coordination

Traffic signal coordination is an effective approach to decrease delays and congestion. It is widely used for urban areas in the U.S. and worldwide. Popular optimization models for traffic signal coordination are reviewed in this section, such as MAXBAND, MULTIBAND, PROS, etc.

Little [20] presented models for maximizing bandwidths for an arterial and a network. Pre-time signal control was applied in these models with speed and cycle length used as decision variables. Little built the models as a mix-integer programming problem

with branch-and-bound algorithms as the solving algorithm. The details of developing models and performing branch-and-bound algorithms were presented in the study, and a ten signals arterial and a seven signals network were used as samples to illustrate presented models and solving algorithms. For the presented models, no residual and accumulated queues were considered.

Little, Kelson, et al. [21], introduced the methodology of MAXBAND which was a software package to set up signal timings for arterials and triangular networks to achieve maximum bandwidths. The model of MAXBAND could generate cycle length and speed within a given range. It also produced optimal directional bandwidths based on user defined weights. This model was developed based on the previous model presented by Little [20]. Compared to the previous model, this model had several strengthened features: 1) It could choose optimized left turn patterns; 2) the impact of queue clearance time was considered; and 3) according to Webster's theory (distributing green times based on volume/capacity ratios) it could produce green splits when volumes and capacities were provided. The branch and bound algorithm was also used for solving the presented model.

Instead of the previous methods that optimized identical directional bandwidth for the entire arterial, Gartner, Assmann, et al. [22], presented a method which optimized directional bandwidth for each section of arterials, named MULTIBAND. A case study was conducted and NETSIM was selected to be used as the simulator. Two computer programs, MAXBAND and MULTIBAND, were used to optimize signal settings for an arterial. According to results, compared to MAXBAND, MULTIBAND had significant

enhancements with respect to delays (16% for major streets; 11% for all traffic) and number of stops (25% of major streets; 15% of all traffic).

Gartner, Little et al. [23, 24], presented models for optimizing network signal settings by mixed-integer linear programming and based on pre-time control. Their work was divided into two parts which were introduced by two references. For " Part I: The Network Coordination Problem" [23], the green splits and cycle length were given and offsets were only decision variables, so the researchers used average delay as the objective function with some assumptions being made. The key assumptions were: 1) arrival pattern was cyclical; 2) the intersections were under-saturated; and 3) the queue could be cleared during the green. A simple traffic flow model was proposed to mimic platoon length, and the scholars presented a link performance function that built a relationship between delays and offsets. To avoid nonlinear problems, the model was converted to piecewise. The solving algorithm was selected to be the branch and bound algorithm, and then a simple network was used as a numerical example. With respect to "Part II: The Network Synchronization Problem" [24], when compared to models from part I an extent feature was that offsets, splits, and cycle length were used as decision variables simultaneously. Another strengthened place was that the researchers presented a saturation deterrence function which considered overflow queue (resident queue) due to stochastic effects. However, over-saturated conditions were not considered in the models of part II. The branch and bound algorithm were also used as the solving algorithm. The same numerical example with Part I was used to evaluate the models of Part II. According to results, simultaneously optimizing offsets, splits, and cycle length reduced

11.6% average vehicle delay when compared with sequentially optimizing these variables.

Wallace and Courage [25] presented a progression opportunities (PROS) method to optimize fixed-time traffic signal coordination. PROS at the time instant of an intersection indicated a number of downstream intersections vehicles could pass through without stopping at the designed progression speed. Compared with uniform bandwidth of an arterial provided by the maximum bandwidth method, PROS method used all opportunities of an intersection so that vehicles could traverse through downstream intersections without having to stop. To evaluate the effectiveness of the PROS method, a case study was conducted. When PROS was used as the objective function to optimize traffic signal coordination, only offsets could be optimized. Results of PROS had better performance than that of the maximum bandwidth method, but only to a limited degree. To overcome this shortcoming, the authors of this reference proposed an expanded PROS method that utilized an objective function which combined PROS and utility functions (e.g. delay etc.), thereby expanding the PROS method so that both offset and splits could be optimized. Based on results of the case study, it was shown that the expanded PROS method could significantly outperform the maximum bandwidth method, especially for study arterials. The maximum improvement for bandwidth and delays for study arterials were 30.4% and 21.4%, respectively.

Bleyl [26] presented a computer program for optimizing traffic progression for an arterial. In this program, the scholar considered the two directional distances and took into account that the desired progressive speeds between two intersections may be different in the real world. According to the desired progressive speeds of two directions,

Bleyl used average travel time in two directions to represent the "spacing" between two intersections. This reference converted a traditional time-space diagram to a time-average travel time diagram. If the ratio of two axes (time and desired travel time) was 1:1 then the 45-degree progression line is the best solution, since the actual travel time was equal to the desired travel time. If the best solution was unobtainable then the program generated the maximum available progression signal timing plans. After that the program would adjust directional offsets according to differences of directional travel times and average travel time. For this reference, accumulative queue and residual queue are not considered.

Lieberman, Chang, et al. [27], designed a real-time traffic signal control policy with special attention to oversaturated arterials, although it was found to also be suitable for under-saturated conditions. The method was named as a real-time/internal metering policy to optimize signal timing (RT/IMPOST). There were three major objectives of RT/IMPOST: 1) maximize system throughput; 2) completely utilize link storage capacity; and 3) provide equal service for minor street traffic. The key concept of this reference was to optimally control and stabilize queue length dynamics. Two optimization models were formulated: 1) a mixed integer linear programming (MILP) model to generate optimal offsets and queue length for each approach on major streets; and 2) a non-linear programming (NLP) model which dynamically adjusted phase durations of arterial approaches each cycle in order to maintain queue length for each approach close to the optimal queue length generated by MILP. The whole policy was repeated when the system state was significantly changed. In this reference, the minimum updated interval was eight cycles and a case study was conducted. Compared with the

results of PASSER, TRANSYT and SYNCHRO, RT/IMPOST significantly improved mean travel speed and decreased total delays. For this reference, it was based on the fixed-time control mode and was a responsive traffic signal control strategy.

Messer, Whitson, et al. [28], developed a program for multiple phases arterial progression optimization. Four general phase options were considered. The program generated phase sequences and movement green time durations for maximum progression with respect to a specific selected cycle length. The Brooks' interference algorithm was used for generating the maximum bandwidth and two performance measures, the percentage of efficiency and attainability, were presented. The percentage of efficiency was the ratio of two directional bandwidths to double cycle lengths. The attainability evaluated the performance of select signal plans using available progression green time within the arterial system. This program was tested in the field at a study site and generated optimal results as expected.

2.1.3 Adaptive Traffic Signal Control System

Adaptive traffic signal control systems are one of the hottest topics for traffic signal practitioners and researchers. It is based on different advanced traffic surveillance systems designed to actively and proactively control traffic according to real-time and predicted traffic data. RHODES, ACS-lite, SCOOT, SCATS, OPAC, and InSync are major adaptive traffic signal control systems implemented in the U.S. and worldwide. These systems and their core algorithms are reviewed in this sub-section.

Mirchandani and Head [29] presented an introduction, methodology, architecture and prototype called RHODES, a traffic adaptive signal control system. RHODES is a traffic adaptive signal control system with a hierarchical structure comprised of three

control levels: Network load control, network flow control, and intersection control. RHODES has several algorithms to predict platoon arrivals and individual vehicle arrivals for network flow control and intersection control. All predictions were based on real-time collected detector data, while models for intersection control (COP) and network flow control (REALBAND) were briefly introduced. A simulation study was conducted to evaluate the performance of RHODES and when compared with the semi-actuated control system RHODES reduced average vehicle delay for low and high loads to 50% and 30%, respectively.

Sen and Head [30] presented a controlled optimization of phases (COP) algorithm to optimize intersection traffic signal control, and was utilized in RHODES. The COP was solved by forward recursion of dynamic programming, and it was found that delay, stops and queue length could be used as performance measures. For this algorithm, it can skip phases for optimization by setting the green time of a phase to 0. A numerical case and a simulation were performed to illustrate and validate this algorithm. Semi-actuated, fully actuated, and COP were applied for the study intersection within the simulation. Delay was chosen as the performance index, and based on the simulation results the COP algorithm could significantly reduce delay compared to semi- and fully- actuated control. However, a drawback for this algorithm is that the left turn phase may be skipped during light volume traffic for optimization. The waiting left turn vehicles would then be required to wait another cycle to progress through the intersection and real-time drivers would likely find this solution bothersome.

Luyanda and Gettman, et al. [31], introduced the major algorithmic architecture of the ACS-lite system. ACS-lite has three key algorithmic components: a time-of-day

(TOD) tuner, a run-time refiner, and a transition manager. The TOD tuner was used to update a used phase plan (cycle, splits, and offsets) offline according to traffic volumes and the phase plan performance. The run-time refiner was used to optimize the current phase plan by implementing incremental adjustments which slightly modified the parameters of the current phase plan. The run-time refiner also determined the most suitable time to switch to a scheduled or unscheduled phase plan. The transition manager decided to use the best built-in transition method of controllers in order to impact traffic as little as possible. ACS-lite was a cost-effective solution developed by FHWA and was a product that applied an adaptive control system within the current closed-loop traffic signal control system. The ACS-lite has limitations since the currently used traffic signal system was not upgraded significantly for adaptive traffic signal control at the time. For example, it was found to be more of a traffic-responsive system.

Robertson and Bretherton [32] introduced the SCOOT traffic responsive control system, and they pointed out that SCOOT was developed based on TRANSYT. Three major principles of SCOOT are: 1) to assess real-time cyclical flow profiles; 2) a continuously updating online queue model; and 3) to adjust signal settings in an incremental mode. Bandwidth, average queues, and vehicle stops were three major optimization criteria for SCOOT. According to the results of the studies, the scholars presented that SCOOT could save 12% for delay on average, when paired with good fixed-time plans.

Jhaveri and Perrin, et al. [33], evaluated the benefits of the Split, Cycle and Offset Optimization Technique (SCOOT) by comparing that of plan-based coordinated actuated control with respect to network and corridor levels. The simulation studies were

conducted using CORSIM and focused on a test network and corridor as well as two actual highway networks and corridors. The signal timing for the plan-based coordinated actuated control were generated from SYNCHRO, while delay, queue length and travel time were selected as performance measures. According to the results, SCOOT had significant benefits compared to plan-based signal timings, and had better performance on the network than on the corridor. When compared to plan-based coordinated actuated control, when the volume/capacity (v/c) ratio was around 0.9, SCOOT reached maximum benefits while also achieving other minor positive results at and above saturation.

The Roads and Traffic Authority (RTA) of New South Wales, Australia developed the Sydney Co-ordinated Adaptive Traffic System (SCATS) software [34]. Wilson and Millar, et al. [34], assessed the benefits of SCATS coordinated signal control by micro-simulation. Three control modes were evaluated in the simulation: fixed-time coordinated control, SCATS isolated actuated control (each intersection independently controlled by vehicle actuation mode), and SCATS coordinated control. Delay and number of stops were selected as performance indexes. Based on the simulation results, the performances of the three modes were similar under light traffic. SCATS isolated actuated control and coordinated control had better performances than fixed-time control when traffic increased. For the heavy traffic, SCATS coordinated control had the best results since it can best adapt to traffic variations.

Gartner, Pooran et al. [35], presented field implementation procedures for the Optimized Policies for Adaptive Control (OPAC) traffic signal control system in Northern Virginia. Control strategies of different versions of OPAC were also described in the paper. For OPAC, the upstream detectors of each link in intersections were needed

for collecting real-time vehicle counts and occupancy. To evaluate the effectiveness of OPAC implementation, field tests were conducted. The performances of fixed traffic signal timing plans were optimized by TRANSYT and used as the benchmark. Due to the frequent communication disruptions of several intersections as a result of system upgrades by a phone company and the simultaneous construction activities of OPAC deployment, the OPAC system was not as fine-tuned as it needed to be for the study. However, based on results from the field OPAC outperformed the fixed traffic signal timing optimized by TRANSYT with a 5-6% decrease on average for delays and stops.

Chandra and Gregory [36] describe the functions and benefits of InSync, which was developed by Rhythm Engineering in 2008. It is a newly emerging adaptive traffic signal control system, and was installed in some parts of the United States. InSync had global and local optimization devices and adjusted signal timing with second by second adjustments according to real-time traffic. The local and global optimizers aimed to improve individual intersections and corridors. The authors of this reference indicated that implementing InSync had significant benefits with respect to travel time, number of stops, fuel consumption and emission, and reduced accidents.

2.2 Bridging Technologies of Connected Vehicle

Connected vehicle technologies are still in the stages of simulation and the beginnings of field testing. Some promising technologies can provide accurate high resolution (second to second or even sub-second to sub-second) real-time individual vehicle data. This data cannot be provided by traditional traffic surveillance systems, even though they are very helpful in real-time traffic management and control. It is encouraging that state DOTs have begun installing more and more such sensors on the

road, and that data from those technologies are available now for application development, debugging and testing. Three major bridging technologies of connected vehicles are reviewed in this section: video detector systems, probe vehicles, and mobile sensors.

2.2.1 Video Detection Systems

Video Detection System (VDS) is one of the technologies that might bridge real-time data availability between existing systems and connected vehicles. In addition to VDS installed with some traffic signal control systems at intersections, traffic cameras are also a major element of the advanced traveler information system (ATIS) and are widely installed in the United States. VDS can collect real-time traffic data and simulate pulse from the traditional loop detectors. One of the main benefits of VDS is that it offers field of view by providing real-time video image streams from the field. However, VDS is considered a controversial technology as researchers generally have very strong opinions, both negative and positive, about its performance and limitations as indicated below.

Panda [37] indicated that damaged roadbeds and restricted sensing space are two major drawbacks of inductive loop detectors (the most utilized traffic sensor systems). The author of this reference also presented the new design of video sensors which improved accuracy and decreased cost more than the previous design which struggled with affordability and reliability. His paper described the new video sensor design's physical architecture and corresponding software. With the hardware and software of this new video sensor it can detect incidents and measure many types of traffic data such as real-time speed, volume, queue length, etc. It can also provide central control of a large

network in a Traffic Control Center (TCC). According to the field tests, the performance of this video sensor system was similar to that of the inductive loop detector. The field tests also indicated that different engineers can successfully manage traffic in TCC via this integrated video sensor system.

Oh and Leonard [38] evaluated performances of a video image processing system called PEEK Video Trak 900. The evaluation was concentrated on volume and speed data accuracy collected by the test system. According to results of the field studies, the speed data collected by the test system was more accurate than volume data. The tracking strip type and location were critical for data accuracy, however this study indicated that performance of the test system during nighttime was not good.

Sharma, Bullock, et al. [39], proposed an algorithm to detect inclement weather conditions based on video image vehicle detection systems (VIVDS). The authors of this reference indicated that the signal timings need to be revised during inclement weather to improve safety and operation efficiency. The presented algorithm was planned to automatically identify inclement weather and change signal timing plans accordingly. The algorithm obtained real-time images from VIVDS and then analyzed the difference between normal day images and real-time images. When the difference of these images reached a preset threshold, an inclement weather (snow day, etc.) was identified. This algorithm was validated in the field and can successfully detect when the snow is present.

Several research projects about video detection systems (VDS) were also conducted by a research team at Purdue University. In 2001, Grenard, Bullock, et al. [40], evaluated the performances of chosen VDS at signalized intersections. Within this project two problems of VDS operation during nighttime were identified: 1) the effective length

of the detection zone increased at nighttime compared to in the daytime; and 2) VDS lost detection calls when vehicles traveled past stop bars within several feet. The authors of this reference also indicated the VDS should not be used for providing dilemma zone protection due to inaccurate detection during nighttime.

In 2006 during in a follow-up project, Rhodes, Bullock et al. [41], assessed the stop bar detection accuracy of Three vendor-selected VDSs at a signalized intersection: Autoscope (version 8.10), Peek UniTrak (version 2), and Iteris Vantage (Camera CAM-RZ3). Two test beds in Indiana were selected to conduct field studies. Based on these field studies, the authors of this report made some major conclusions: 1) VDS generated a moderate to high number of missed calls and false calls; 2) the loop detector had much better performance than VDS; and 3) three tested VDSs had similar results.

Rhodes and Jennings, et al. [42], investigated the influence of camera position and lighting on video detection accuracy. Vehicle detection activated early during daytime and nighttime was identified due to the impact of vehicle headlights. This issue resulted in several problems: 1) effective length of detection zone was stochastically varied; 2) gap time was unpredictable; and 3) headway of traffic flow was shorter than actual value which resulted in measured traffic volume falsely increased compared to the true value. This reference recommended the nearside overhead stop bar as the camera deployment location.

2.2.2 Probe Vehicles

For implementing connected vehicle technologies for traffic signal control and operations, obtaining vehicle trajectories from connected vehicles is critical to collecting the data needed for modeling and optimization. Similar with connected vehicles, probe

vehicles could provide high resolution vehicle trajectory data (second by second or even 0.1 second by 0.1 second). The major difference between probe vehicle and connected vehicle is that probe vehicles cannot communicate with each other or with the infrastructure. Previous studies based on probe vehicles/vehicle trajectories are very useful references for connected vehicle researchers.

Unal and Cetin [43] presented a method to estimate maximum queue length and delays at an isolated intersection for both under-saturated and oversaturated conditions by implementing the time and space data of probe vehicles in a queue. The proposed method was based on fixed-time control and was an offline approach. Shockwave theory was applied to estimate the critical points of the queue dynamics. This reference developed equations to estimate maximum queue length and delays for over- and under-saturated conditions. A simple test case was conducted and according to results the presented method could effectively estimate queue length and delays at an isolated signalized intersection. As the penetration rate of the probe vehicle increased, the estimation errors of the queue length decreased; however, the increase of the probe vehicle percentages had no obvious impact on the estimation errors of the total delay.

Cheng, Qin et al. [44], presented a method for estimating signal timing and queue lengths of signalized intersections by using vehicle trajectory data. The presented method was based on the shockwave approach, and critical points which represented changes of traffic states were extracted to build a shockwave diagram. Three types of critical points were identified: vehicle start to deceleration, vehicle joins queue, and residual queue discharging. The method for extracting critical points and approaches for estimating signal timing data and cycle by cycle maximum queue lengths were presented. This

reference used simulation data and NGSIM data to evaluate the proposed method. The presented method could successfully detect start of green and red time instants, and it could also estimate maximum queue length with a 18.4% to 24.2% mean absolute percentage error.

Izadpanah, Hellinga et al. [45], proposed a method to identify and estimate shockwave according to vehicle trajectory data. Two critical steps were proposed: 1) identify intersection points of vehicle trajectory and shockwave; and 2) group intersection points by a linear clustering algorithm to estimate shockwave speed and spatial/temporal extents of shockwave. The scholars used the data of a signalized intersection generated by INTEGRATION and a freeway NGSIM data set to validate the proposed method. With respect to the signalized intersection compared with the analytical estimation, the proposed method had 0.32% and 27.3% differences in shockwave speed estimation for queue accumulation and dissipation. However, the proposed method could not detect the shockwave of a vehicle moving forward. For the freeway, the proposed approach had 17.5% shockwave speed estimation difference with a method presented by Lu and Skabardonis [46] with respect to the same NGSIM dataset (freeway US 101).

Cheng, Qin et al. [47], proposed a cycle by cycle queue length estimation method based on the shockwave theory. Vehicle trajectory data was the input for the presented approach and critical points which represented changes of traffic states were extracted from vehicle trajectories for queue length estimation. Five types of critical points were identified when a vehicle started deceleration, vehicles joined the queue, the residual queue began discharging, the arrival vehicles were impacted by residual queue discharging, and arrival vehicles could directly traverse stop bar without delays. The

proposed method was evaluated by simulation data, NGSIM data and GPS data. Results indicated that the presented method could estimate queue length with 17.5% to 25.5% mean absolute percentage error.

Quiroga and Bullock [48] proposed an offline method to estimate the control delay of signalized intersections by using GPS data provided by probe vehicles equipped with GPS. The presented method included forward and backward average acceleration algorithms. The forward average acceleration algorithm used current and n-1 in advance GPS data (the total number of used GPS data was n) to identify when and where vehicles start to accelerate or decelerate. For the backward average acceleration algorithm, it utilized current and n-1 pasted GPS data to determine when and where vehicles stop accelerating and decelerating. This reference analyzed sensitivities of the proposed forward and backward average acceleration algorithms for variations of thresholds that identify whether or not vehicles accelerated or decelerated and the total number of used GPS data. This reference also studied the relationships between stop delay and control delay, between stop delay and approach delay, and between approach delay and control delay which were all found to be linear relationships. However, the first two did not pass the origin of coordinated systems. This reference also indicated that the component of the control delay from a vehicle left stop bar to the vehicle finished acceleration could not be ignored.

Liu and Ma [49] proposed a virtual vehicle probe model to estimate signalized arterials' time-dependent travel time. In this model, the collected and archived "event-based" vehicle actuation and signal status field data were used. The presented model simulated behaviors of a virtual probe vehicle traversing an arterial to measure time-

dependent travel time. The virtual probe vehicle had three states: acceleration, deceleration and constant speed. This paper presented a formula to estimate the speed and position of the virtual probe vehicle at each time stamp. A field study was performed and the results found the presented model could provide accurate travel time estimation of signalized arterials. However, the presented model can only measure "past" travel time of signalized arterials and cannot predict signalized arterials' travel time.

Ni and Wang [50] proposed a trajectory reconstruction model for travel time estimation based on point-based speed data. The major feature of this model was that it estimated vehicle trajectory by forming speed surface using both space and time. After vehicle trajectory for a path was estimated the travel time of the path was obtained. This reference utilized the finite difference method to solve the proposed model. The model was then validated by two NGSIM data sets collected in California and GA400 data collected in Georgia. This reference also applied two popular types of travel time estimation models to the data sets: the instantaneous and linear models. Based on results, the proposed trajectory reconstruction model smoothly approximated ground truth data with no statistically significant difference, and the mean absolute percentage error (MAPE) was 6.3% compared with the ground truth data. For instantaneous and linear models, field data was well estimated when congestion didn't appear, but there was an obvious difference between travel time estimated by instantaneous and linear models when congestions became severe. Results generated by these two models were proven statistically different with the ground truth data. Compared with the field data, the MAPE of instantaneous and linear models were 14.0 % and 11.7 %, respectively. It should be

noted that the accuracy of the proposed model in this reference was determined by density of deployed point detectors.

2.2.3 Mobile Sensor

Mobile sensor is another newly emerging surveillance technology used in transportation systems. Herrera, Work, et al. [51], indicate mobile sensors provide high accurate position and speed data (an example of mobile sensor would be a GPS enable cell phone). Herrera, Work, et al., pointed out virtual trip lines (VTL) are data collection sites and that their geographic locations are stored in a mobile sensor and mobile sensor equipped vehicles crossing VTL would update their speed and position data.

Herrera, Work, et al. [51], proposed a traffic monitoring system based on GPS enabled smart phones and the scholars conducted field experiments, named Mobile Century, on the freeway to prove the concept of the presented system. A segment of I-880 close to Union City, California was selected as the study site. Three sets of field data were collected: vehicle trajectory and speed data collected by onboard GPS-enabled smart phones, loop detector data, and video camera data. Virtual trip lines (VTL) were implemented to collect cell phone data. In this research, the travel time data obtained by processing video camera data was referred to as the ground truth data since loop detectors had detection errors in general. Based on the results of the field study, the data collected by GPS-enabled smart phones was more accurate than that obtained by loop detectors. It also indicated that the proposed system could provide enough traffic data without sacrificing the privacy of phone owners. More importantly, the field results showed that only 2-3% penetration rate of GPS-enabled smart phones was adequate to provide accurate speed data.

Sun and Ban et al. [52], proposed a method based on a variation formulation approach to reconstruct signalized arterial short vehicle trajectories by sampling vehicle trajectories collected by mobile traffic sensors. Then a shockwave diagram for vehicles queueing, discharging and dissipating was formed. The researchers presented optimization based and delay based approaches to estimate shockwave boundaries which were required by the variation formulation method. This reference used both simulation data and NGSIM data for validation. Results showed that the performance of the optimization based approach were better than that of the delay based method. The authors of this reference indicated that one disadvantage of the proposed method was that the rear end of queue needed to be pre-estimated by historic data.

Ban, Herring et al. [53], developed a method to estimate delay patterns of signalized intersections based on collected travel time. Virtual trip lines were deployed to collect travel time upstream and downstream of an intersection. Two major steps were in the proposed method. First, the researchers identified the start of each cycle (i.e. the start of red time in a cycle) according to significant delay increase at the beginning of red. Then, the scholars used piecewise line curves to fit collected travel time data to estimate delay patterns. To this end, the reference presented a least square based linear fitting algorithm. The researchers computed delay for the difference between actual travel time and free flow travel time. The scholars utilized simulation data and field data to validate the proposed method. When penetration rate of probe vehicles in the simulation data was larger than 40%, performances of the proposed algorithm was better than a linear interpolation method for delay pattern estimations. When the penetrate rate of probe vehicles was over 60%, the estimated signal timing was close to actual signal timing. For

the field test, the penetration rate was 45%-65%. With respect to delay pattern estimations 88% vehicles had less than 15% estimation errors. For the cycle length approximation, differences between 81% estimated cycle lengths and actual cycle lengths were within 15%. In this reference, the proposed method assumed uniform arrival in a cycle. It required at least 2 and 4 probe vehicles in a cycle to estimate delay patterns for under-saturated and saturated conditions. However, this reference didn't consider acceleration and deceleration delays for delay pattern estimation.

Ban, Hao et al. [54], proposed a method to estimate real time queue length of signalized intersections by applying travel time obtained from mobile sensors. One of the major assumptions of the presented method was that the arrival pattern of vehicles was uniform. Queue Rear No-delay Arrival Time (QRNAT) and Queue Front No-delay Arrival Time (QFNAT) were two major concepts of the developed method. QRNAT was the scheduled departure time of the last queued vehicle released from the intersection if the green time was long enough. QFNAT was the scheduled stop bar arrival time, i.e. impacts of accumulative queue length of resident queues were not considered of the vehicle which was the first vehicle stopped at the stop bar at the beginning of red time. By using shockwave theory, the formula for computing minimum and maximum queue lengths of a cycle with respect to distance and number of vehicles were developed, and equations for estimating the time instants that the minimum and maximum queue length of a cycle achieved were formulated as well. To validate effectiveness of the proposed method, the scholars conducted a field test and a simulation study. Based on the results, the developed method could estimate the actual queue patterns per cycle. It was also indicated that as the penetration rate of probe vehicles increased or traffic conditions

became more congested the possibility of successfully implementing the proposed method was increased and the estimation error was reduced, but not significantly.

Hao, Ban et al. [55], presented another method based on kinematic equation to estimate the location in a queue and the time a vehicle joins a queue according to travel time data collected by mobile sensors. One upstream virtual trip line (VTL) and two downstream VTLs of an intersection were used to collect data. The scholars concentrated on queue discharging process, and they obtained location in a queue and acceleration rate of a vehicle by solving corresponding kinematic equations. In this reference, simulation data, field data and NGSIM data were used for validating the proposed method. A queue estimation method developed previously by one of the authors (Ban [54]) was used for comparison with the proposed method of this reference. Based on the results, performances of the presented method were better than that of the previous queue estimation method under high penetrate rates of probe vehicles. But the presented method had a poorer performance than the previous method when penetration rate of probe vehicles was found to be less than 45%. The presented method of this reference only required a probe vehicle in a cycle.

Hao and Ban [56] presented a method to estimate long queue length at signalized intersections based on data collected by mobile sensors. Specifically, the researchers estimated queue length over the upstream mobile sensor data collection site. Two critical steps existed in the presented approach: 1) reconstructed vehicle trajectory and 2) to use a delay based model to estimate queue length. With respect to reconstructed vehicle trajectory, this reference estimated undetected vehicles' deceleration and acceleration trajectories over the upstream mobile sensor. The reference utilized the simple car

following model of Newell and the shockwave method to rebuild vehicle deceleration and acceleration trajectories. Field data was used to validate the proposed method and, according to results, the proposed method was found to be effective. Its success rate (i.e. the percentage of successfully implemented proposed method in all cycles) was 20% more than a method proposed previously by one of authors in this reference (Ban [54]). The scholars pointed out that deploying the upstream mobile sensor at an appropriate location was critical.

2.3 Connected Vehicle Mobility Applications

2.3.1 Traffic Signal Control based on Connected Vehicle Technology

In his dissertation, Goodall [6] presented a traffic signal control algorithm, the predictive microscopic simulation algorithm (PMSA), based on the connected vehicle environment which implemented rolling horizon technology. The proposed algorithm collected the speed, location and heading of connected vehicles within DSRC communication distance, i.e. 300 meters (which translated to 15 seconds travel time based on speed of the study corridor). After that, the proposed algorithm predicted cumulative delays of the upcoming 15 seconds for possible phasing configurations by microscopic simulation. Then the phase with the minimum delay was chosen as the optimal phase for next time period. An operation constraint was added so no phase would experience red time for more than 120 seconds. Simulation studies were conducted to evaluate the effectiveness of the proposed algorithm for different penetration rates of connected vehicles and congestion levels of intersections as well as demand variations due to incidents or annual traffic flow changes. Based on the results of simulation study, the proposed algorithm was found to be more effective when the penetration rate of

connected vehicles was at least 25% and traffic conditions were under-saturated. It was also shown that the proposed algorithm worked better when met with unexpected demand due to incidents or annual variations of traffic demand than traditional actuated coordinated traffic control system. This reference also tested the performance of the presented algorithm when utilizing an objective function with multiple variations (i.e. delay, stop, and deceleration) instead of with delay only. The results indicated that the developed algorithm with multiple variables objective function could not outperform that of the developed algorithm with a delay only objective function.

Joyoung Lee [57] studied an IntelliDrive (now connected vehicle) based Intersection Control Algorithm in his dissertation to assess the potential benefits. In the dissertation, Joyoung presented cumulative travel time responsive (CTR) control algorithm for real-time intersection traffic signal control. The cumulative travel time (CTT) of all vehicles traversing an intersection is estimated by adaptive Kalman filter. CTTs are grouped by NEMA possible phase combinations and determine the highest CTT phase combinations. A switch to the phase combination with the highest CTT is made if that phase is not the current phase. The phase timing plan is considered the optimized timing plan. The adaptive Kalman filter is used to estimate the total travel time coming from vehicle trajectories with the developed method being applied to NGSIM trajectory data from two arterial test sites. It was concluded that the number of sites was too small and the trajectory data from VISSIM were actually used to feed the adaptive Kalman filter. Joyoung indicated the CTR algorithm could beat actuated control for moderate and congested traffic conditions when the penetration rate of connected vehicles was over 30%.

In a pool fund study also from University of Virginia, Smith, etc. [58], evaluated how to incorporate IntelliDrive^{SM} (now Connected Vehicle) into traffic signal control algorithms. Three algorithms are evaluated in their report. In their first approach, a VISSIM simulation model with two intersections was used to illustrate how to improve the spillback from one oversaturated intersection to the next upstream intersection on the main street which would experience de facto red conditions. They extracted simulation data to monitor the queue length of the oversaturated intersection, and if a spillback existed the green phase for the affected phases was cut short (ECG) or started late (LSG). They also explored the early start of minor street green (SSG). Combinations of two of the three strategies are evaluated as well. Their evaluation results indicated that except for a 5-9 % increase for LSG on stops and delays, other strategies reduced 6-28% of delays and 7-41% of stops. For the second approach, similar to InSync [59], the vehicle clustering algorithm (VCA) first computes cumulative waiting time (CWT) for each movement within a red light. When the CWT exceeds a specific predetermined value, it requests a green light for this phase. Second, it makes sure to clear vehicles before it maxes out. Finally, at green intervals it determines green extension time by the last vehicle's distance and speed. The last vehicle within vehicle clusters in the dilemma zone was searched by VCA then identified and grouped in pseudo-platoons. They also extracted simulation data from VISSIM models with four intersections to provide precise information for this purpose and evaluate the algorithms. They improved their VCA by using a k-means clustering algorithm to determine the optimal time to end the green phase. According to results, their performance under normal traffic volume increases so that delay decreased by 6.8% and speed increased 2.8%. However, no statistical analysis

is performed to confirm those results, so those better performances might not be warranted or consistent. In addition, they indicated about an 11% jump in fuel consumption. The third model explored is the Predictive Microscopic Simulation Algorithm (PMSA). They used the information at the current time to simulate the delays in the next 20 seconds, and the phase with the least delays is selected and implemented. Their simulation studies indicated that there were average delay reductions and speed increases at the level of 0.1% to 8.3% depending on market penetrations. The highest performance index is the delay reduction of 8.3% at the penetration rate of 75% (not 100%). The performance changes are statistically significant at a 95% confidence level when the penetration rate is more than 25%. Their simulation study indicated that when the mainline traffic volumes increased 25%, the benefit increased significantly up to 26% delay reductions and 14% speed increases.

Cesme and Furth [60] described approaches using several rules widely accepted when responding to traffic demand and fine-tuning traffic signal timing. This includes green truncation in cases of intersection spillback, early green and double realization for left turn phases prone to pocket spillback, and dynamic coordination for groups of signals spaced too closely together. Simulation tests based on a benchmark network shows 45% delay reductions compared to the coordinated control plan calculated by SYNCHRO, TRANST-7F and PASSER.

He, Head et al. [61], proposed a multi-modal online traffic signal control model based on vehicle to infrastructure (V2I) communication which was named PAMSCOD. There were two major components in this model. The first one was a platoon identification algorithm which used critical headway to identify moving platoons. The

second element was a mixed integer linear programming model to generate signal timing based on platoons. The objective function of the mixed integer linear programming model was that minimizing total delays of the entire arterial would be the summation of both signal delay and queue delay of each intersection. This reference indicated it provided dynamic progression and that no common cycle length existed. VISSIM was used as the simulator to evaluate the effectiveness of PAMSCOD. Signal timing plans optimized by Synchro were used as the benchmark cases. According to results, when the penetration rate of connected vehicle was over 40% the performance of PAMSCOD was better than signal timings generated by Synchro. Compared with coordinated signal timing generated by Synchro, 8% average vehicle delay and 25-30% average bus delay were decreased by implementing PAMSCOD. PAMSCOD reduced 20-30% average vehicle delay and increased 3% average bus delay when compared with coordinated signal timing with transit priority output by Synchro.

Priemer and Friedrich [62] presented an adaptive signal control algorithm based on vehicle to infrastructure (V2I) data. Based on vehicle arrival data from V2I and stop bar, the algorithm optimized phase sequence for the next 20 seconds in order to minimize queue lengths while the algorithm was implemented for every 5 seconds. In this reference, the V2I communication zone is 280 meters from the stop bar. The algorithm of this reference was decentralized which did not have cycle length and offset. The minimum green time and the maximum waiting time were two constraints. A weight factor was used to facilitate platoons and emergency vehicles traversing intersections. The authors of this reference also used a queue length estimation approach when the penetration rate of connected vehicle was low. The dynamic programming integrated

with complete enumeration was selected to solve the developed algorithm of this reference. The reference conducted a simulation study to evaluate the presented algorithm, and the pre-time signal timing plan optimized by TRANSYT-7F was utilized as the benchmark scenario. Based on results, when compared to the benchmark scenario a maximum of 24% mean delay decrease and 5% mean speed increase was achieved by the proposed algorithm of this reference. The significant improvements required the minimum penetration rate of connected vehicle to be around 25%.

Feng, Khoshmagham et al. [63] proposed an online adaptive traffic signal control algorithm in the connected vehicle environment that optimized phase sequences and phase duration. The algorithm was solved for two levels. For the first level, the duration of a barrier group (i.e. duration of major or minor streets' phases) was determined, and for the second the duration and sequence of each phase in the barrier group was optimized. This reference also presented an algorithm to estimate unequipped vehicles' position, speed, and acceleration based on the status of connected vehicles. A simulation study was conducted to evaluate the proposed algorithm in different penetration rates and under medium and high traffic demand conditions. The performances of a fine-tuned actuated controller were referred to as the benchmark. Based on results, in heavy traffic conditions the proposed algorithm of this reference could decrease delays 6% and 16.6% in the low and high penetration rates, respectively. However, the medium traffic condition performances of the presented algorithm could not beat that of the actuated controller, except in the case of 100% penetration rate.

He, Head et al. [64], proposed a mixed integer linear program model for multi-modal traffic signal control optimization. The presented model considered priority,

actuated controller features, and signal coordination simultaneously. The scholars utilized priority to materialize signal coordination. Passenger vehicles, buses, and pedestrian were three traffic modes considered in the model. The model of this reference was decentralized, and it was designed to optimize the entire arterial coordination by decomposing the problem to optimize each intersection within the arterial separately. This model was formulated by assuming deterministic and constant arrival rate. Then the authors of this paper released this constraint and assumed that the arrival rate of passenger vehicle and arrival times of priority vehicles were in a predetermined uncertain set. A simulation case study was conducted. Actuated coordination, actuated coordination with transit signal priority, the proposed model were three strategies utilized in the case study. According to results, actuated coordination obtained the minimum passenger vehicles' delay in all scenarios, and the least bus delays in high traffic volume scenario. The proposed model outperformed actuated coordination with transit signal priority strategy and proved to work well within the high volume scenario. Compared with the actuated coordination with transit signal priority strategy, the proposed model of this reference decreased 24.9% bus delay, 14% pedestrian delays and obtained comparable passenger vehicles delay.

2.3.2 Other Mobility Applications of Connected Vehicle Technology

In addition to traffic signal control and optimization, other mobility applications of connected vehicle are also reviewed such as estimation and prediction of real-time traffic conditions and critical traffic data, and traffic operations and management.

Li, etc. [65], estimated queue length under different penetration rates of connected vehicle. Their estimation combined the connected vehicle data and loop detector, and is

based on an event driven approach. Their study indicated that when the penetration rate is high the fusion data does not help the estimation accuracy.

Christofa, Argote, et al. [66], proposed methods to identify arterial queue spillback and presented corresponding signal control strategies (gap-based and shockwave-based) based on connected vehicle data. For the gap-based method, it estimated distance between the last stopped connected vehicle in the queue and the real last vehicle in queue (i.e. gap length) by using connected vehicle trajectory data. With respect to the shockwave-based approach (in addition to using connected vehicle trajectory data) the method estimated the maximum queue length based on the time and position of the last connected vehicle in queue, signal timing data of the upstream intersection, and the shockwave theory. A maximum acceptable queue length was determined by the difference of the link length, the maximum value of estimated accumulated queue length of the next cycle, and a predefined safety distance. After possible queue spillback is determined, the proposed signal control strategy redistributes the green time of the upstream intersection. Based on the simulation results, the two proposed queue spillback identification methods could effectively detect more than 80% possible queue spillback. In addition, the simulation results showed that the shockwave-based method was more effective when the penetration rate of connected vehicles was between 10% to 20%, and the gap-based approach was more beneficial in other ranges of penetration rates of connected vehicles. The results of the simulation case study also indicated that the presented signal control strategy could enhance traffic conditions by avoiding and decreasing the impacts of queue spillback appearing.

Khoshmagham, Feng et al. [67], proposed a method to estimate travel time by using extended tardity function and partial vehicle trajectory in connected vehicle environment. The major feature of this method was to protect privacy since the method of this reference considered vehicles' ID changes in a 5 minute interval. When a vehicle's ID changed it was recognized as two vehicles. Only vehicles' trajectories in DSRC communication range was used to estimated travel time. A software-in-the-loop simulation study was conducted to verify the effectiveness of the proposed method of this reference. Estimated travel time in link, intersection, and section levels were then evaluated. Compared to the ground truth results, in the worst case, the presented approach of this reference generated 11.03% mean absolute percentage errors with respect to the intersection level. A major advantage of the proposed method of this reference was that its performance was stable when penetration rates of connected vehicle varied.

Arnaout, Khasawneh, et al. [68], proposed an agent-based method to decrease traffic congestions under IntelliDrive (the previous name of connected vehicle) environments. Specifically, this reference presented a simple speed control algorithm for an IntelliDrive vehicle which implemented Cooperative Adaptive Cruise Control on a one-lane highway in order to impact traffic flow dynamics and reduce vehicle oscillation behaviors. The IntelliDrive vehicle adjusted speed according to the velocity and distance of the immediate front vehicle and subsequent front vehicles within communication range. The scholars conducted a simulation study to test the proposed approach. Based on the results, the proposed method could eliminate or decrease vehicle oscillations and improve the average speed of vehicles.

2.4 Summary of Literature Review

In this chapter, three categories of literature which are related to this dissertation were reviewed: traffic signal control and optimization models/algorithms for signalized arterials, bridge technologies of connected vehicles, and connect vehicle mobility applications.

For traffic signal control and optimization models/algorithms for signalized arterials, offset tuning and optimization, traffic signal coordination optimization and adaptive traffic signal control system are scanned. Since major benefits of connected vehicle technologies are providing rich, accurate, and real-time traffic data, for offset tuning and optimization, literatures related to the real-time application or other methods which could be extended to be implemented online are of major concern. Popular traffic signal coordination methods were viewed such as MAXBAND, MULTIBAND, and PROS, etc. For the adaptive traffic signal control system, previous researches related to the most prevalent adaptive traffic signal control systems in the U.S. were reviewed (RHODES, ACS-lite, SCOOT, SCATS, OPAC, and InSync).

The major bridge technologies of connected vehicle were reviewed: video detection system (VDS), probe vehicles, and mobile sensor. VDS is the most widely implemented technology within these three technologies. We can easily find VDS at signalized intersections and interstate highways in the U.S. One of the main benefits of VDS is that it offers field of view or provides real-time video image streams from the field. The second major advantage of VDS is considerable reduction in maintenance costs and labor when compared with the loop detection system, though its reliability and accuracy during nighttime and bad weather (such as heavy rain and snow, etc.) are not

good. VDS is also a controversial technology and researchers generally possess very strong negative and positive opinions about its performance and limitations.

Probe vehicle and mobile sensor could also offer real-time vehicle trajectory and other critical data (such as speed and location, etc.), but they cannot communicate with each other or with infrastructure. The methods and approaches based on probe vehicles and mobile sensor, however, provide good references for developing traffic control models/algorithms based on connected vehicle technologies.

For connected vehicle mobility applications, studies related to traffic signal control based on connected vehicle technologies are the major concern. It can be seen that traffic signal control models/algorithms generated decent results based on rich real-time traffic data provided by connected vehicle technologies, especially for online traffic signal control. Yet, there are only a few papers concerned with traffic signal coordination, such as Cesme and Furth [60], He, Head et al. [61], and He, Head et al. [64]. With respect to these three papers, they used a decentralized method to materialize traffic signal coordination, i.e. no common cycle length requirements for coordinated intersections. On the other hand, He, Head et al. [61], and He, Head et al. [64] were two bodies of research more concentrated on traffic signal priority. However, the most widely implemented traffic signal coordination method in the U.S. is the centralized method where all coordinated intersections have the same cycle length. There is no previous research implementing connected vehicle technology on the centralized traffic signal coordination method at the time of this dissertation.

Traffic signal control strategies are different between under-saturated and saturated/over-saturated conditions. All reviewed traffic signal control models and

algorithms based on connected vehicle technologies only considered one condition (under-saturated or saturated/over-saturated condition) or they did not consider proposing two methods for under-saturated and saturated/over-saturated conditions.

Therefore, there is a need to propose traffic signal control models/algorithms to implement connected vehicle technologies for traffic signal coordination, especially for centralized traffic signal coordination. A comprehensive traffic signal control framework is necessary to use different control models/algorithms for different traffic conditions. These two requirements are taken into consideration and different traffic signal control methods for under-saturated and saturated/over-saturated conditions are developed to form a connected vehicle based traffic signal control model (CVTSCM) in this dissertation. They are illustrated in the following chapters.

CHAPTER III

ARTERIAL-LEVEL TRAFFIC PROGRESSION OPTIMIZATION MODEL

3.1 Background and Entire Framework of ALTPOM

In this chapter, one of the major modules of the connected vehicle based traffic signal control model (CVTSCM), an arterial-level traffic progression optimization model (ALTPOM), is presented. As indicated by its name, the prominent feature of ALTPOM is that it optimizes traffic progression for an entire signalized arterial simultaneously instead of one intersection by one intersection. Specifically, ALTPOM optimizes offsets of all coordinated intersections at the same time. To optimize these offsets, the splits of coordinated intersections are first adjusted to balance the predicted upcoming demands on all approaches. Then, offsets of all coordinated intersections are optimized according to adjusted splits and predicted traffic data. To accomplish this, there are two major modules in the ALTPOM: split adjustment and offset optimization. ALTPOM is recursively implemented in real time for a user defined projection horizon. The duration of a projection horizon could be defined according to specific field traffic fluctuations and/or experiences of local traffic engineers.

Figure 3.1 shows the entire framework of the ALTPOM in a projection horizon in five steps. The first step is to collect real-time traffic data. In addition to install an RSU for a coordinated intersection, an upstream detector is expected to be installed on each approach of a coordinated intersection. The upstream detector is used to collect upstream

arrival profiles for each approach. It is assumed that all approaches of coordinated intersections are already installed with upstream detectors. With respect to the second step, critical upcoming traffic data is predicted based on the collection of real-time traffic data. The predicted data for a coordinated intersection includes impending traffic demands, vehicle trajectories of all traffic, and average approach travel time, etc. Based on predicted data, splits are adjusted to balance upcoming traffic demand for all approaches. Then, new splits and predicted vehicle trajectories for all upcoming traffic are input into the offset optimization module to generate optimal offsets. The adjusted splits and optimized offsets are implemented for all coordinated intersections in the final step.

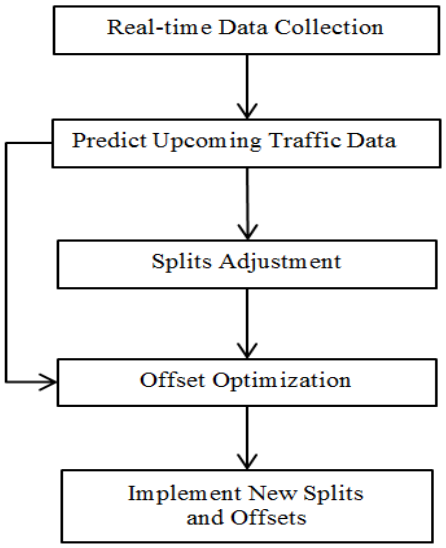

Figure 3.1 The Entire Framework of the ALTPOM for a Projection Horizon

Cycle length, splits, and offsets are the parameters to define traffic signal coordination operations. According to *Traffic Signal Timing Manual*, there are three

major methods to determine coordination cycle length: manual method, critical intersection method, and network approaches. For manual method, it chooses coordination cycle length according to progression speed and distances between intersections. Critical intersection method determines coordination cycle length according to the intersection with the highest demand within all intersections. With respect to network approaches, coordination cycle length is decided by considering multiple intersections at a time. Popular traffic signal programs, such as Synchro, PASSER^{TM} II and TRANSYT-7F, are typically used to find the optimal coordination cycle length [69].

However, coordination cycle length is not frequently changed in real-time and usually changes according to time of day which is predetermined by operational policies of individual state DOT and local transportation agencies. Traffic signal coordination is usually used for multiple arterials and/or a network as shown in Figure 3.2. On the next page Figure 3.2 (a) shows traffic signal coordination implemented for two intersected arterials, while Figure 3.2 (b) provides a case that traffic signal coordination is applied for a network. The intersections highlighted by a red circle are referred to as intersected coordinated intersections, which are crossing points of two signalized arterials. Since all coordinated intersections of an arterial have the same cycle length and two intersected arterials have one common intersection, these two arterials have the same cycle length as well. As shown in Figure 3.2 (a), arterials A and B have the same cycle length, and so do arterials C, D, E, and F of Figure 3.2 (b). If cycle length of an arterial is adjusted or optimized, then cycle length of multiple arterials or a network need to be updated as well. Then, corridor-level and/or network-level traffic signal control is necessary. In this dissertation, ALTPOM aims to optimize traffic progression for the arterial-level (not

corridor-level or network-level) so the cycle length is not adjusted or optimized in ALTPOM. ALTPOM provides a foundation for developing corridor-level or network-level traffic signal control models in the future.

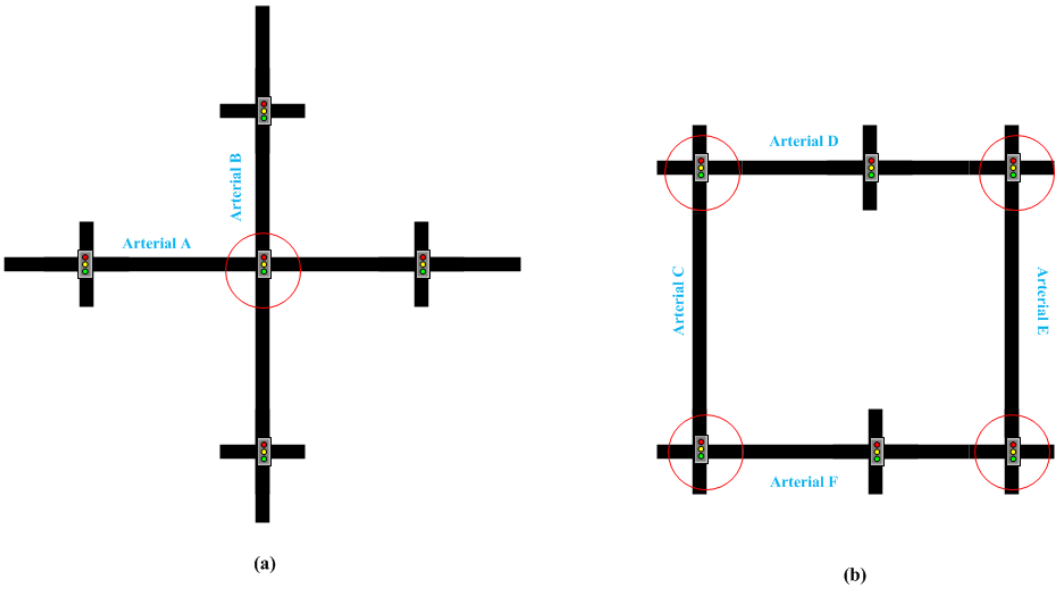

Figure 3.2 Typical Traffic Signal Coordination Implementation

3.2 Real-Time Splits Adjustment

3.2.1 Upstream Detectors Layout

In this dissertation, the target timeline for connected vehicle technologies is when the rudimentary stage of the penetration rate of connected vehicles is not high. The fusion data of loop detector and connected vehicles is collected and used to estimate traffic conditions for all approaches. There are two major purposes behind deploying upstream detectors: 1) to collect the total number of vehicles entering an approach within a projection horizon; and 2) to record upstream arrival profiles in order to estimate all

vehicles' trajectories based on the trajectories of connected vehicles. In this research, upstream arrival profiles are accumulated for each cycle. It is not possible to identify every unequipped vehicle or equipped vehicle based on loop detector data. However, if connected vehicle and loop detector data are used in tandem it is possible to identify specific detector actuation caused by a connected vehicle.

Connected vehicles use dedicated short range communications (DSRC) to exchange data for V2V and V2I. Roadside unit (RSU) is the device which materializes communication between infrastructure (such as traffic signal controllers) and connected vehicles. The device is usually located close to an intersection or further out to extend the communication range when a RSU is already installed at the intersection. The communication range between a RSU and connected vehicles via DSRC has limitations, and is typically restricted within 1,000 to 1,500 ft. According to J2735, the BSM message of each connected vehicle provides a 3-dimensional position and the speed data of that vehicle is the transition rate of 10 times per second [5]. The vehicle trajectories of each connected vehicle within the DSRC communication zone are generally available, so if an upstream detector is deployed within that same zone then the arrival of a connected vehicle can be detected. At this same time, the actuation of the upstream detector caused by the connected vehicle could be identified.

Figure 3.3 shows the layout of upstream detectors within a signalized arterial. From Figure 3.3, it can be seen that for an approach connecting two coordinated intersections there are two DSRC communication zones covering this approach. In this case, an upstream detector would be installed at the upstream endpoint of this approach.

For other approaches, the upstream detectors are installed at the upstream boundary of a DSRC communication zone.

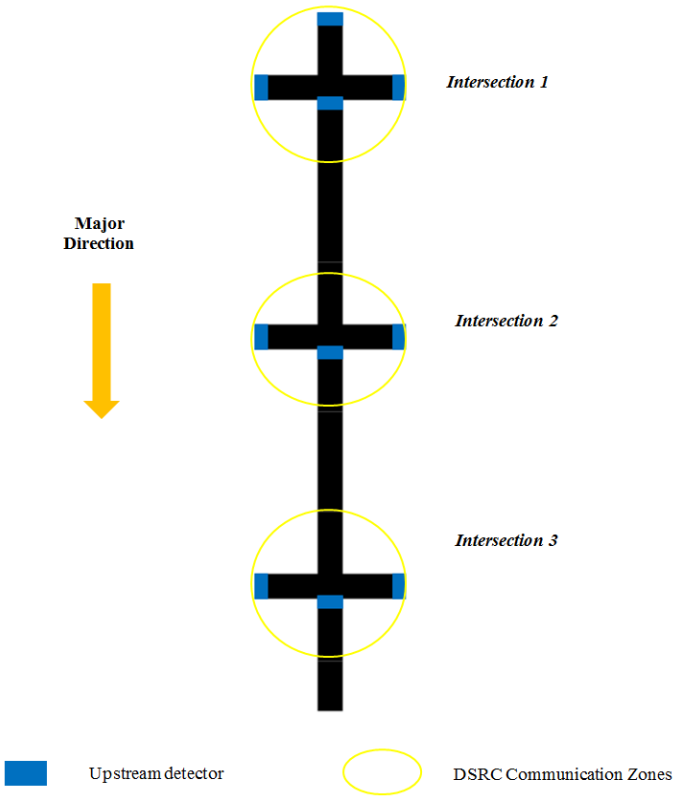

Figure 3.3 Upstream Detectors Layout

3.2.2 Real-Time Splits Adjustment

Figure 3.4 shows the entire framework of splits adjustment for a coordinated intersection in this dissertation. Three data sets are needed to collect, measure, and predict for splits adjustment. The first is the signal phasing plan and timing interval data of phases, such as minimum and maximum green time, yellow time, all red time, etc. The second data set is upcoming traffic demands (i.e. number of arrivals) within the next

projection horizon for each phase. The final data set is the field data which determines discharge/departure characteristics of corresponding lane groups of a phase, such as lane configuration, discharge headway, startup lost time, etc.

Signal phase and timing data are easier to obtain and compare with the other two data sets. They can be obtained from Departments of Transportation (DOTs), local transportation agencies, or field traffic signal controllers.

With respect to predict real-time upcoming traffic demand within the next projection horizon for each phase, a simple procedure is utilized. Since upstream detectors are deployed for each approach of a coordinated intersection, the upstream arrival profiles of an approach during the last projection horizon could be obtained. In general, traffic propagates from upstream intersection to downstream intersection. We directly extract upstream arrival profiles of the last projection horizon from the installed upstream detector, and those extracted arrival profiles are referred to as the upcoming upstream arrival profiles for the next projection horizon. Then, the forthcoming total number of vehicles for an approach in the next projection horizon could be generated by summarizing the collected upstream arrival profiles. After the upcoming total demand of an approach is obtained, estimation for traffic demands of each movement needs to be made, by evaluating real-time turning percentages for an approach.

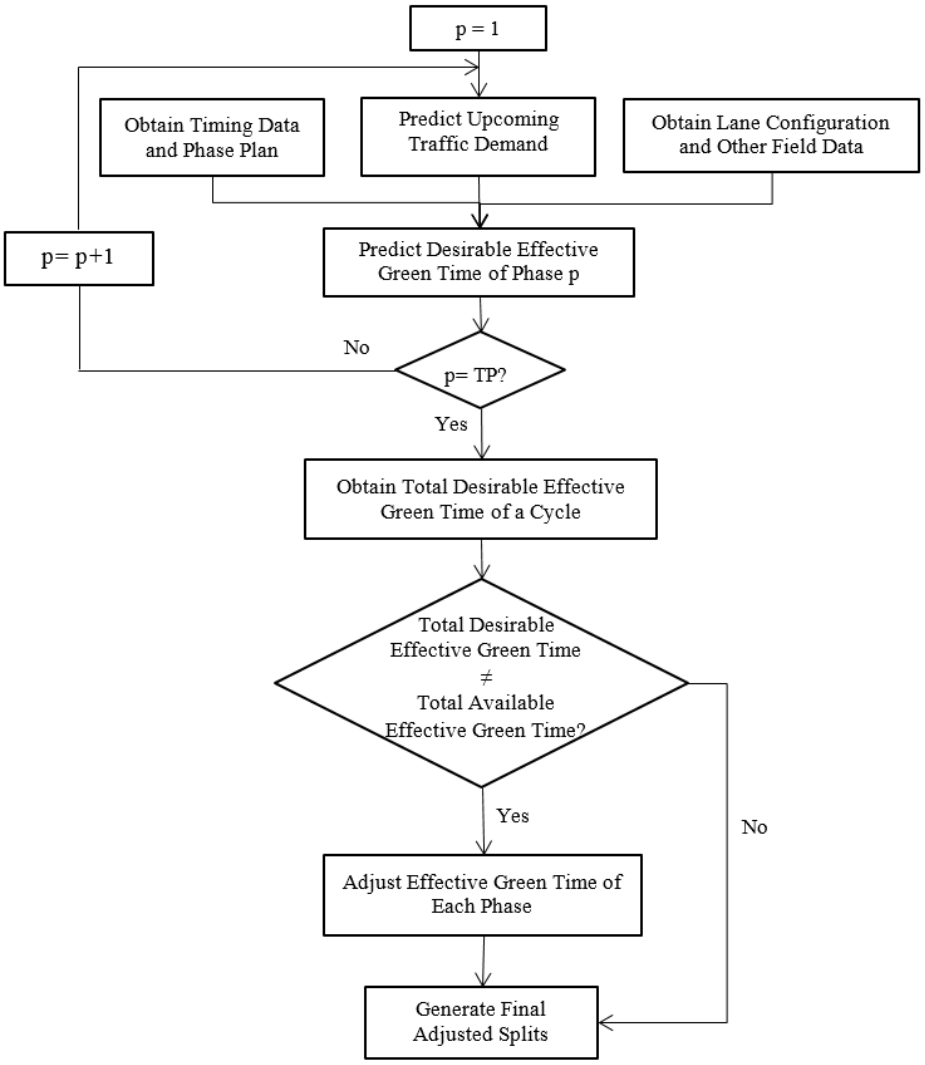

Figure 3.4 The Framework of Split Adjustment for a Coordinated Intersection

With respect to $TP_{p,m}$%, it is very difficult to get real-time turning percentages based on traditional transportation detection devices which could be used as an input for online traffic signal control models. Usually the average historic turning percentages of a time period collected from the field are used for traffic signal adjustment/optimization. Within the connected vehicle environment, estimating this data becomes easier than before by utilizing vehicle trajectories. According to J2735 as defined by SAE, connected

vehicles position can be obtained from Basic Safety Message (BSM) at the rate of 10 times a second [5]. Vehicles' turning direction could be identified by vehicle trajectories. Then it becomes a matter of counting the number of discharged connected vehicles turning left, right, and going through an approach in the last projection horizon (i.e. served demand). Connected vehicles in the queue for each movement at the beginning of each projection period are also collected as the unserved demand. The total traffic demand of each movement is the sum of served and unserved demands. After that, real-time turning percentages are generated off of the collected data. It is assumed $TP_{TM,m}\%$ will not significantly change during each project period T.

$$TP_{TM,d,m}\% = \frac{CQ_{TM,d,m} + \sum_{j=1}^{T} NCV_{j,TM,d,m}}{\sum_{TM=1}^{3} CQ_{TM,d,m} + \sum_{TM=1}^{3}\sum_{j=1}^{T} NCV_{j,TM,d,m}} * 100\% \quad (3.1)$$

$$TP_{p,m}\% = \sum_{d=1}^{TD}\sum_{TM=1}^{3} TP_{TM,d,m}\% * \alpha_{p,TM,d,m} \quad (3.2)$$

Where,

TM: Turning movement (left =1, through =2, and right=3);

j: The time index of a projection horizon (j =1, 2, ⋯, T),

d: Approach of each intersection (d= 1, 2, 3, ⋯, and TD)

TD: Total number of approaches for an intersection,

p: The index of phases for an intersection (p =1, 2, 3, ⋯ and TP),

TP: Total number of phases for an intersection,

m: The index of coordinated intersections (m= 1, 2, 3, ⋯, M),

M: Total number of coordinated intersections in a signalized arterial,

T: The duration of a projection horizon (seconds),

$TP_{TM,d,m}\%$: Turning Percentage of turning movement TM for approach d at intersection m (%),

$CQ_{TM,d,m}$: Number of connected vehicle in the queue at the beginning of a projection horizon for turning movement TM of approach d at intersection m (vehicles),

$NCV_{j,TM,d,m}$: Number of connected vehicles discharged at time index j from turning movement TM of direction d at coordinated intersection m (vehicles),

$\alpha_{TM,p,m}$: The binary variables, ($\alpha_{TM,p,m} = 1$, if phase p severs turning movement TM of approach d at intersection m; $\alpha_{TM,p,m} = 0$, otherwise),

$TP_{p,m}\%$: Turning percentage of phase p at intersection m (%).

The accuracy of estimated real-time turning percentages is expected to be enhanced along with an increase in penetration rates of connected vehicles. After real-time turning percentages are obtained, total demand is estimated for each phase using the formula below.

$$DM_{p,m} = TP_{p,m}\% * \sum_{j=1}^{T} N_{j,d,m} \quad (3.3)$$

Where,

$DM_{p,m}$: Total demand for phase p at intersection m (vehicles),

$N_{j,d,m}$: Number of vehicles actuated the upstream detector at the jth time index of the direction d at coordinated intersection m (vehicles).

After predicting upcoming traffic demand, estimates for discharge characteristics of a phase for the next projection horizon need to be made. The last data set in Figure 3.4 is needed (i.e. discharge headway), and this data could be directly obtained and measured from the field. As shown in Figure 3.5, when considering the randomness of the vehicle discharging process, discharge headway was selected which covers the preferred cumulative percentage of discharge headway distribution, e.g. 80%, to discharge capacity of a phase for the next projection horizon.

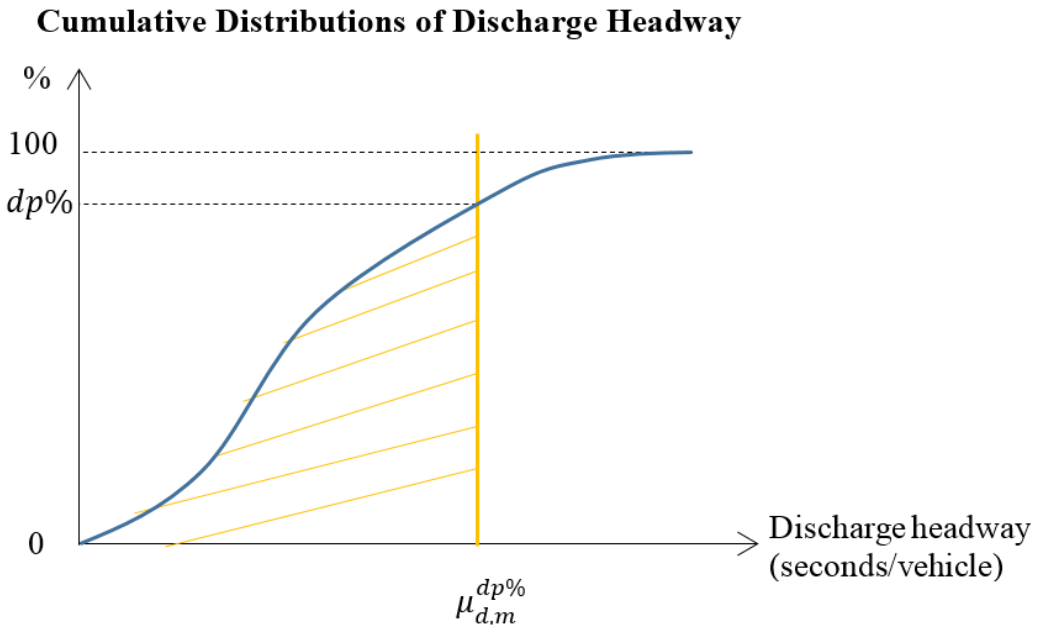

Figure 3.5 Discharge Headway Estimation

Attention should be given to identifying corresponding lane groups of each phase or movement within a phase based on lane configuration of an approach due to its importance for estimating the discharge capacity of a phase for the next projection horizon. According to a report conducted by Battelle and TTI, the static and real-time

intersection geometric data and turning movement attributes are the major element of MAP data which could be provided by SPaT system at the broadcast rate of once per second. This report pointed out that the intersection number of lanes and turning movement attributes may be varied due to an unforeseen lane closure, incident, and/or turning restriction based upon time of day [70]. It is expected that the number of feasible lanes for each phase be updated when MAP information is changed. Then, total vehicles could be discharged in a phase for the next projection horizon is calculated as below:

$$DC_{p,m} = \frac{G_{de_{p,m}} * T}{C * \mu_{d,m}^{dp\%}} * NL_{p,m} \quad (3.4)$$

Where,

$DC_{p,m}$: The discharge capacity of phase p at intersection m (vehicles),

C: The cycle length (seconds),

$NL_{p,m}$: Number of lanes for phase p at intersection m,

$dp\%$: Desired cumulative percentages that a selected discharge headway should cover (%),

$\mu_{d,m}^{dp\%}$: The selected discharge headway to estimate desirable green time (seconds/vehicle/lane),

$G_{de_{p,m}}$: The duration of desirable effective green time of phase p at intersection m (seconds).

According to a paper by Newell, it was indicated that the minimum intersection delay could be achieved under the condition that a phase be switched when its queue

cleared [71]. As in Figure 3.6, when the total number of arrivals is equal to the total number of departures (i.e. at point A), existing queue length is cleared.

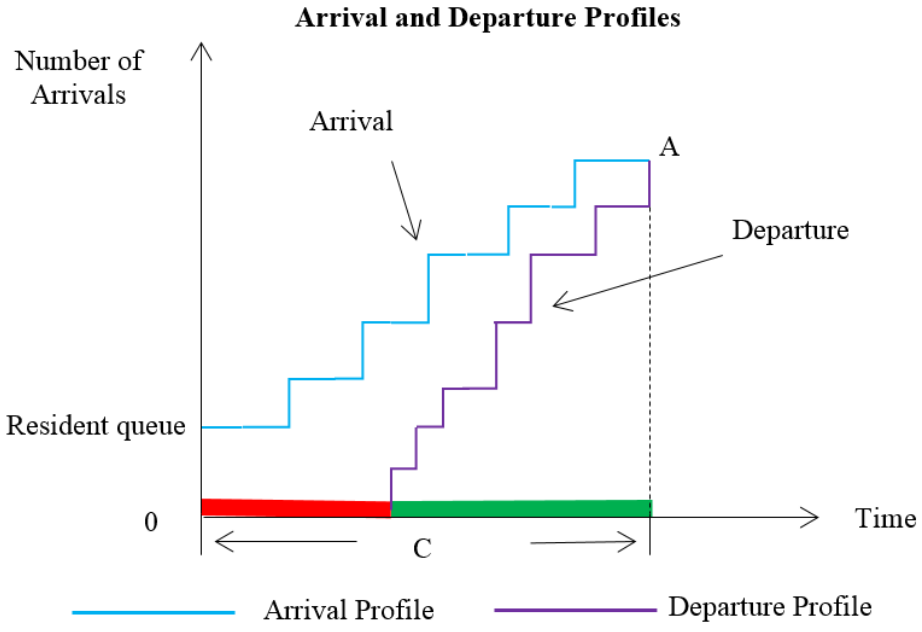

Figure 3.6 Estimation of Desirable Effective Green time of A Phase

The intersection point of arrival profiles and departure profiles are the desirable effective green time for a phase. Let equation (3.3) equals to equation (3.4) such that the equation to estimate desirable effective green time is derived as below.

$$DM_{\mathrm{p,m}} = DC_{p,m}$$

$$\mathrm{TP}_{\mathrm{p,m}}\% * \sum_{j=1}^{T} N_{j,d,m} = \frac{G_{de_{p,m}} * T}{C * \mu_{d,m}^{dp\%}} * NL_{p,m}$$

$$G_{de_{p,m}} = \frac{\mu_{d,m}^{dp\%} * \mathrm{TP}_{\mathrm{p,m}}\% * \sum_{j=1}^{T} N_{j,d,m}}{T * NL_{p,m}} * C \qquad (3.5)$$

To estimate effective green time of a phase, two additional conditions are needed to be considered: 1) a phase contains turning movements in multiple approaches; and 2) turning movements in a phase are not in the same lane group. In these situations, the method mentioned above needs to apply for estimating desirable effective green time for each lane group or each approach of a phase. The larger green time requested by a lane group or an approach will be selected as the desirable effective green time for the phase in order to meet the demand of every lane group or every approach in a particular phase.

Then, adjusted effective green times are required to meet minimum green time and ring barrier restraints. Two more steps are conducted, with the first being the estimated desirable effective green time of a phase when compared with the minimum effective green time. If the estimated desirable effective green time is less than the minimum effective green time of a phase, then the minimum effective green time is used as the desirable effective green time of the target phase. Since signal timing data has already been obtained, it is easy to compute minimum effective green time of a phase. A formula presented by *Traffic Engineering* textbook is utilized [72].

$$G_{e_{p,m}} = G_{a_{p,m}} + y_{p,m} + ar_{p,m} - l_{1_{p,m}} - l_{2_{p,m}} = Split_{p,m} - L_{p,m} \quad (3.6)$$

Where,

$G_{a_{p,m}}$: Maximum green time of phase p at intersection m (seconds),

$y_{p,m}$: Yellow time of phase p at intersection m (seconds),

$ar_{p,m}$: All red time of phase p at intersection m (seconds),

$l_{1_{p,m}}$: Startup lost time of phase p at intersection m (seconds),

$l_{2_{p,m}}$: Clearance lost time of phase p at intersection m (seconds),

$Split_{p,m}$: Split of phase p at intersection m (seconds),

$L_{p,m}$: Total lost time of phase p at intersection m (seconds).

Then equation (3.5) is rewritten as below:

$$G_{de_{p,m}} = \max\left(\frac{\mu_{d,m}^{dp\%} * \mathrm{TP_{p,m}}\% * \sum_{j=1}^{T} N_{j,d,m}}{T * NL_{p,m}} * C, G_{e,min_{p,m}}\right) \quad (3.7)$$

Where,

$G_{e,min_{p,m}}$: The minimum effective green time of phase p at intersection m (seconds).

From Figure 3.4, it can be seen that it is possible to get the total desirable effective green time of a cycle after predicting all phases in a cycle. If the total available effective green time conflicts with the total desirable effective green time, then adjustments to the desirable effective green time of each phase are needed to be made again.

$$TG_{e_m} = C - L_m \quad (3.8)$$

$$TG_{de_m} = \max\left(\sum_{P=1}^{4} G_{de_{p,m}}, \sum_{P=5}^{TP} G_{de_{p,m}}\right) \quad (3.9)$$

$$G_{e_{p,m}} = TG_{e_m} * \frac{G_{de_{p,m}}}{TG_{de_m}}, \qquad if TG_{de_m} \neq TG_{e_m} \tag{3.10}$$

Where,

TG_{e_m}: Total available effective green time of a cycle at intersection m (seconds),

L_m: Total lost time of a cycle at intersection m (seconds),

TG_{de_m}: Total desirable effective green time of a cycle at intersection m (seconds).

The adjusted effective green time of each phase would then be checked for minimum green time again. Splits for each phase are computed after the estimated effective green time of each phase is obtained, and must be checked to ensure that they conform to the barrier restrictions of a signal controller. Figure 3.7 shows a typical four legs intersection layout and its phasing plan. Equation (3.11) indicates barrier restrictions.

$$\begin{cases} Split_{1,m} + Split_{2,m} = Split_{5,m} + Split_{6,m} \\ Split_{3,m} + Split_{4,m} = Split_{7,m} + Split_{8,m} \end{cases} \tag{3.11}$$

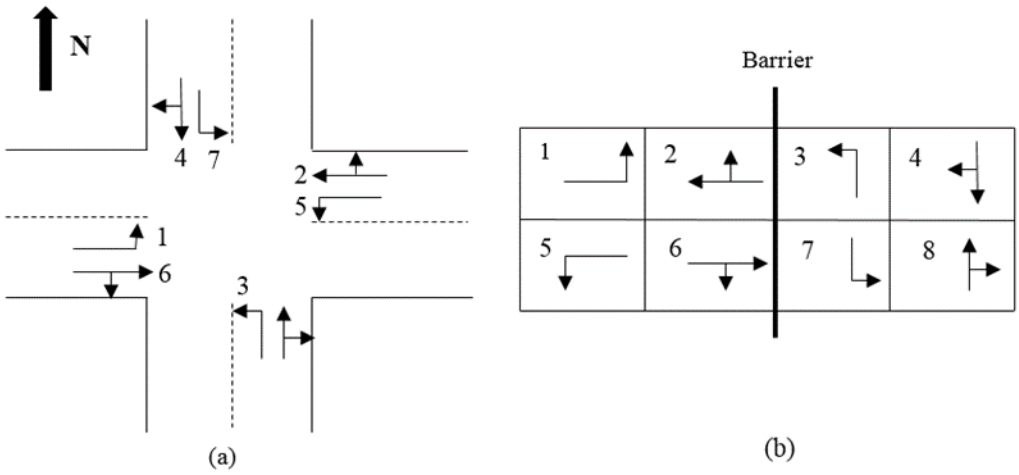

Figure 3.7 A Typical Phasing Plan for an Intersection

Since the built-in logic of an actuated controller would take care of phase overlap, this study adjusts splits to ensure splits of phases in the same position of different rings have the same duration, e.g. phases 1 and 5 in Figure 3.7 (b). The same duration of two phases will be determined by the phase which requires a larger split.

$$\begin{cases} Split_{1,m} = Split_{5,m} \\ Split_{2,m} = Split_{6,m} \\ Split_{3,m} = Split_{7,m} \\ Split_{4,m} = Split_{8,m} \end{cases} \tag{3.12}$$

3.3 Real-Time Offset Optimization

After splits are adjusted to balance upcoming traffic demand of all approaches, focus will shift to optimize offsets of all intersections in the entire arterial simultaneously to provide smooth progression for the whole arterial. When offset of a signal controller is changed, a transition period will occur and traffic flow is disrupted during this transition period which causes unnecessary extra delay. To mitigate the transition period's side

effect, attention is given to restraining the value change of the offset within a small interval to facilitate the direct transition. To this end, the dissertation optimizes offsets of a coordinated intersection within a predefined interval $[-\beta, +\beta]$, e.g. [-5, +5]. In this approach, the transition period is completed immediately.

$$O_m = O_{current,m} + \Delta O_m$$
$$-\beta_m \leq \Delta O_m \leq \beta_m \quad (3.13)$$

Where,

O_m: Offset of intersection m which will be implemented in the next projection horizon (second),

$O_{current,m}$: Current offset of intersection m (second),

ΔO_m: Offset adjustment factor (seconds),

$-\beta_m, \beta_m$: The lower and upper bound of offset adjustment for intersection m defined by users (seconds).

There are three major steps in the proposed offset optimization module. Step 1: predict upcoming vehicle trajectories based on a traffic propagation model. Step 2: forecast the number of arrivals on green at stop bar after all queues are cleared, and predict discharging profiles of the target intersection. Repeat Steps 1 and 2 for all coordinated intersections from the first intersection to the last according to traffic flow propagation sequences. Step 3: offset optimization for the entire arterial.

3.3.1 Step 1: Predict Upcoming Vehicle Trajectories based on a Traffic Propagation Model

In this step, vehicle trajectories of total upcoming vehicles (connected vehicles and unequipped vehicles) are predicted. A traffic propagation model is presented based on fusion data of loop detectors and connected vehicles. Since the upstream detectors are installed, arrival profiles of all vehicles (connected vehicles and un-equipped vehicles) are available. Aforementioned, traffic conditions of a signalized arterial in a short time interval are reasonably assumed to be stable. The procedures of forecasting vehicle trajectories of connected vehicles and unequipped vehicles are different as explained and illustrated below.

Figure 3.8 shows the procedures to predict all vehicles' trajectories and average approach travel time within the connected vehicle environment in this dissertation. Orange lines represent connected vehicle trajectories.

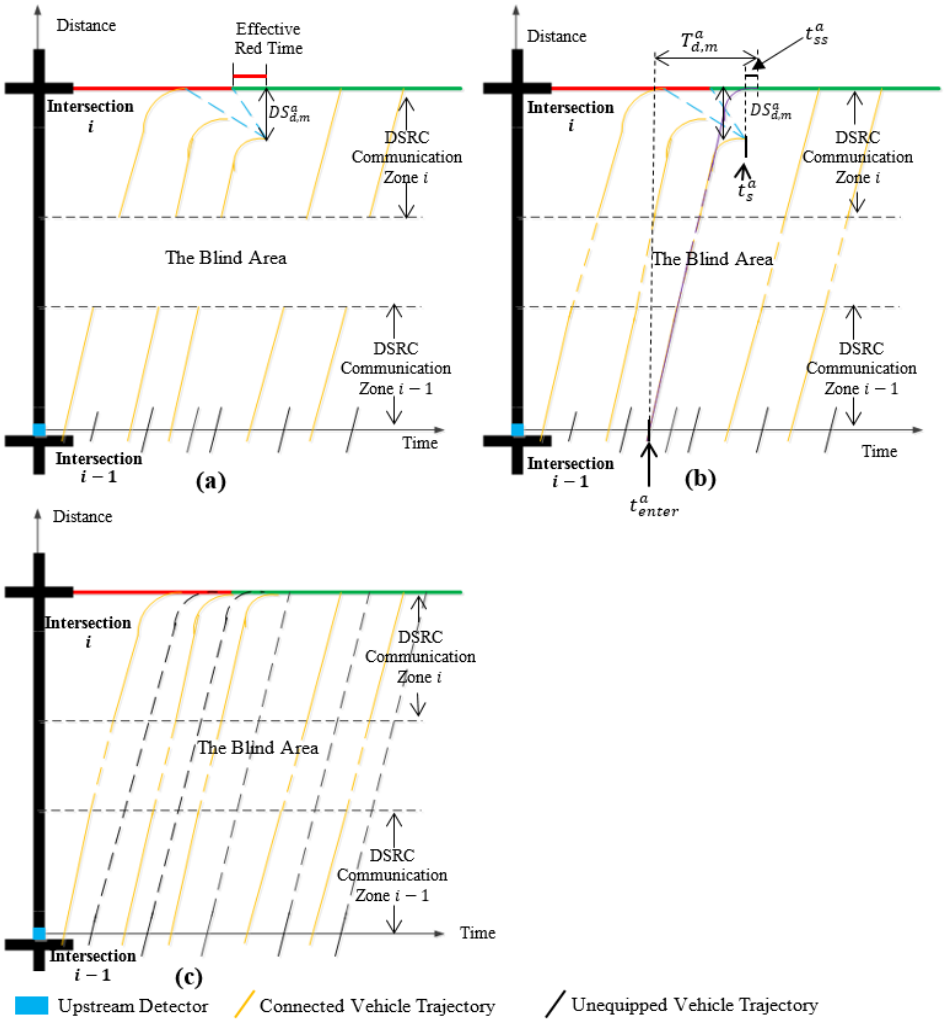

Figure 3.8 Vehicles Trajectories and Approach Travel Time Estimation

As shown in Figure 3.8 (a), vehicle trajectories and travel time of a connected vehicle on an approach can be divided into three zones or segments: trajectories and travel time in DSRC communication zone i, trajectories and travel time in the blind area, and trajectories and travel time in DSRC communication zone $i-1$. DSRC communication zones i and $i-1$ are the effective DSRC communication range for an intersection (i) and its upstream intersection $(i-1)$. If DSRC communication zones i and $i-1$ cannot cover the entire approach, then there is a blind area between two

successive intersections and as such no connected vehicles' trajectory data is available, as shown in Figure 3.8 (a).

As a result, vehicle trajectories of connected vehicles must be predicted within this area as described in the following. The time instants on the x axis and corresponding locations on the y axis of each connected vehicle that leaves the communication zone $i-1$ and enters zone i could be obtained. By connecting these two points, an estimated trajectory in the blank area of a connected vehicle is formed as shown in Figure 3.8 (b). The time difference between these two points is the travel time of a connected vehicle within the blind area. After trajectory of a connected vehicle within the blind area is estimated, the complete trajectory of a connected vehicle between two adjacent intersections is generated. If DSRC communication zones i and $i-1$ can cover the entire approach, then the complete vehicles' trajectories are available and the procedures described above are not needed.

To protect privacy, the connected vehicle temporal ID may be changed for a specific time interval. According to information obtained by communications with several connected vehicle experts, each connected vehicle generates an ID by its onboard equipment (OBE) and the connected vehicle ID is updated every 5 minutes according to current practice (Deborah Curtis, Walton Fehr, and Thomas Timcho, unpublished data). If a connected vehicle changes its ID within an approach, its trajectory data would be discarded since no complete vehicle trajectory data is available.

The objective function of the proposed model is maximizing the total number of vehicle arrivals on green after existing queues are discharged for an entire arterial. Close attention is paid to the predicted arrival time of a vehicle at stop bar is before or after the

existing queue cleared. The estimated stop bar arrival profiles and the complete forecasted vehicle trajectories of all vehicles from the upstream detector to the stop bar of an approach must be generated. As such, the average approach travel time needs to be estimated first.

From Figure 3.8 (a), it can be seen that some connected vehicles may meet resident queue and completely stop before the stop bar. To estimate approach travel time for these connected vehicles without existing queue impacts, an estimate of their scheduled arrival time at the stop bar must be made. In this dissertation, a stopped vehicle is defined as when a vehicle's travel speed is less than a user defined speed (such as 5 ft/sec [3.4 mph]), or 7.35 ft/sec [5 mph], etc). Based on vehicle trajectories, the location of a connected vehicle stop for the first time can be obtained, and distance between the location and stop bar can also be found if the connected vehicle stops within the DSRC communication zone. The travel time of a connected vehicle within this distance is calculated as the equation below. The purple vehicle trajectory of Figure 3.8 (b) is the predicted scheduled vehicle trajectories from the upstream detector to the stop bar. The yellow vehicle trajectory, which is partly covered by the purple vehicle trajectory, is the actual vehicle trajectory of a connected vehicle.

$$t_{ss}^{a} = \frac{DS_{d,m}^{a}}{UV_{d,m}} \tag{3.14}$$

Where,

t_{ss}^{a}: The travel time of connected vehicle a from the location it stops first time to the stop bar (seconds),

$DS_{d,m}^{a}$: The distance between the location that connected vehicle a completely stop first time and the stop bar (ft),

$UV_{d,m}$: The free flow speed of approach d at intersection m (mph).

Then, the complete connected vehicle trajectory is estimated as in Figure 3.8 (c). If a connected vehicle enters the DSRC communication zone i under the stop and go conditions and it is under free flow travel status in zone $i-1$, then the connected vehicle is considered as an unequipped vehicle. After complete vehicle trajectories of all available connected vehicles are estimated, the average travel time of an approach is computed as below.

$$T_{d,m}^{a} = t_{s}^{a} - t_{enter}^{a} + t_{ss}^{a} \tag{3.15}$$

$$T_{d,m} = \frac{\sum_{a=1}^{A} T_{d,m}^{a}}{A} \tag{3.16}$$

Where,

$T_{d,m}^{a}$: Travel time of connected vehicle a at approach d of intersection m (seconds),

t_{enter}^{a}: The time instant that connected vehicle a arrives at the upstream detector on the approach d of intersection m (second),

t_{s}^{a}: The time instant that connected vehicle a completely stops for the first time within DSRC communication zone i at approach d of intersection m (t_{s}^{a} is the time instant that connected vehicle a traverses the stop bar of intersection m, if the vehicle doesn't completely stop),

$T_{d,m}$: Average travel time at approach d of intersection m (seconds),

A: Total number of connected vehicles which complete vehicle trajectories are available at approach d of intersection m for the last projection period (vehicles).

For unequipped vehicles, only upstream arrival profiles are available. Since real-time average travel time of the target approach has already been estimated, stop bar arrival profiles of unequipped vehicles can be calculated based on upstream arrival profiles second by second. The specific equation is listed below. One major advantage of this procedure is that it only requires one connected vehicle with complete trajectory in the last projection horizon to estimate the average approach travel time. As a result, the required penetration rate for this procedure is very low. For example, there is an approach with traffic volume 1000 vehicle per hour and the projection horizon is 15 minutes. This method only needs 0.4% penetration rate of connected vehicle.

$$Arr\_sb_{\left((i+T_{d,m}) mod\ C\right),d,m} = Arr\_up_{i,d,m} \tag{3.17}$$

Where,

i: The time index in a cycle($i = 0,1,2,\cdots,C-1$),

$Arr\_sb_{i,d,m}$: Stop bar arrival profiles for time index i at approach d of intersection m (vehicles),

$Arr\_up_{i,d,m}$: Upstream arrival profiles for time index i at approach d of intersection m (vehicles).

Two critical vehicle trajectory points of an unequipped vehicle are predicted: that the vehicle activates the upstream detector and that it arrives at the stop bar of an approach. Then, these two critical vehicle trajectory points are connected to form approximate vehicle trajectories. After that, complete vehicle trajectories can be built for all vehicles as shown in Figure 3.8 (c).

In this dissertation, it is assumed that the distance between the first coordinated intersection and its nearest upstream intersection is large enough that no impact of upstream intersection will be made on the first coordinated intersection. Predicting upcoming vehicle trajectories for the first intersection are slightly different when compared to the rest of intersections. Since upstream arrival profiles of the first intersection are not impacted by splits and offset changes of any coordinated intersection within the study arterial, upstream arrival profiles of the first intersection in the last projection horizon could be directly referred to as the upcoming arrival profiles. The predicted impending upstream arrival profiles of the first intersection are accumulated for each cycle of a projection horizon to estimate approaching vehicle trajectories. In this dissertation, all arrival profiles are accumulated for each cycle to generate an accumulative and cyclical arrival profiles.

With respect to the rest of the intersections on a signalized arterial, accumulative and cyclical upstream arrival profiles for these intersections are impacted by any changes of splits and offsets of its upstream intersection. As a result, upstream arrival profiles of these intersections need to be predicted and are approximated by the discharge profiles of its upstream intersection. The predicted upstream arrival profiles of these intersections, i.e. forecasted discharge profiles of its upstream intersection, are described in Step 2.

3.3.2 Step 2: Predict Number of Arrivals on Green at Stop Bar

For an entire arterial, the number of arrivals on green at stop bar after the existing queue clears is the performance index to optimize offsets in this dissertation. This method improves the Purdue Coordination Diagram (PCD) method presented by Day, Haseman et al. [14], in which the number of arrivals on green are estimated without considering existing queue length impacts. The PCD method could work well when traffic volume is low, which results in short or no residual queue length. The short queue length is quickly cleared which has little influence on traffic progression, but when traffic volume becomes heavy (but still under-saturated) notable random resident queue length causes a large part of vehicles arrival on green to completely stop or cause deceleration when joining an existing queue. Even when traffic volume is low, the stochastic nature of vehicles' arrival from major and minor streets may cause residual queue for some cycles. In this situation, maximizing the number of arrivals on green without considering the impacts of resident queue is not the best choice as the objective function for offset optimization. Maximizing the number of arrivals on green after the existing queue clears is the better choice as the objective function for offset optimization.

3.3.2.1 Step 2-1: Estimate Initial Queue Length of a Projection Horizon

To predict the number of arrivals on green after the existing queue is cleared at a coordinated approach, initial queue length at the beginning of the next projection horizon should be estimated. Since each coordinated approach has an upstream detector installed in addition to a stop bar detector for actuated controllers, the number of vehicles traveling on an approach could be measured by the difference between accumulative counts of the

upstream detector and the stop bar detector. It is assumed that there are neither missing counts nor double counts.

$$TNVL_{d,m} = AccV_{up_{d,m}} - AccV_{stop_{d,m}} \tag{3.18}$$

$$MNVL_{d,m} = TNVL_{d,m} \tag{3.19}$$

Where,

$TNVL_{d,m}$: Total number of vehicle travel on approach d of intersection m currently (vehicles),

$AccV_{up_{d,m}}$: Accumulative traffic counts for the upstream detector on approach d of intersection m currently (vehicles),

$AccV_{stop_{d,m}}$: Accumulative traffic counts for the stop bar detector on approach d of intersection m currently (vehicles),

$MNVL_{d,m}$: Maximum number of vehicles may travel on link (vehicles).

In addition to collecting the number of vehicles traveling on an approach, the initial queue length at the beginning of each projection horizon is also determined by traffic signal indication (green or red) and the remaining green time. If traffic indication is red, all vehicles currently traveling on an approach would stop and become the resident queue length for the next projection horizon. On the other hand, if traffic signal indication is green, an estimation needs to be made for how many vehicles currently traveling on the link could traverse the intersection within the remaining green time. Based on the number

of vehicles currently traveling on link and with second by second arrival profiles being recorded by the upstream detector, arrival times of these vehicles at the upstream detector could be obtained. Then, an estimated scheduled departure time at stop bar could be made for these vehicles according to equation below.

$$VD_{veh,d,m} = VA_{veh,d,m} + T_{d,m} \tag{3.20}$$

Where,

veh: The index of all vehicles,

$VA_{veh,d,m}$: Arrival time of vehicle veh at the upstream detector on approach d of intersection m (second),

$VD_{veh,d,m}$: Scheduled departure time of vehicle veh at approach d of intersection m (second).

Based on estimated vehicle scheduled departure time, an approach into four possible regions could be divided as shown in Figure 3.9: 1) queuing region; vehicles are in the queue in this region; 2) deceleration region; vehicles will join the queue; 3) free flow region 1; vehicles are traveling at free flow speed and they could be released during the remaining green time; and 4) free flow region 2; vehicles are traveling at free flow speed as well, but they cannot pass the target intersection during the remaining green time. The length of the remaining green time determines vehicles in which regions and how many vehicles in these regions could be released. The rest of the vehicles traveling on this approach are the initial queue at the beginning of the next projection horizon.

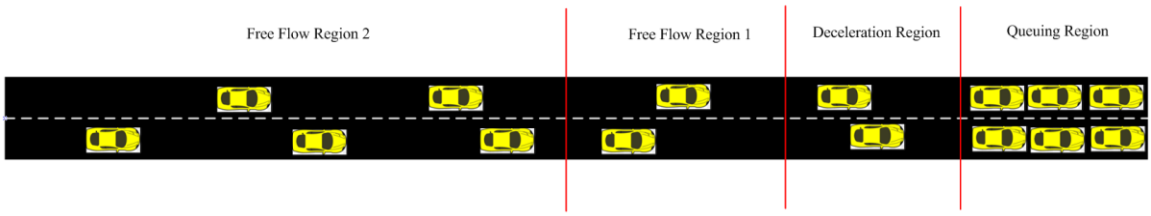

Figure 3.9 Four Possible Regions of an Approach

If $VD_{veh,d,m}$ of a vehicle is earlier than the present time, it indicates that this vehicle is in the queuing region. By checking the $VD_{veh,d,m}$ of all vehicles traveling on an approach, an estimated number of vehicles in the queuing region can be made, but this number may be not be equal to the total number of vehicles in the queueing region. If scheduled arrival time of a vehicle at stop bar is later than the present time, it indicates this vehicle should travel on this approach according to estimated average approach travel time, but it could be located in any of the four possible regions of Figure 3.9. Vehicles' positions are estimated one by one from the earliest arrival on the approach to the final one by using the equations listed below. Equation (3.21) estimates duration of the remaining green time. Equations (3.22) and (3.23) estimate the number of vehicles in the queuing region that could be released during remaining green time. With respect to equations (3.24) and (3.25), they calculate the total number of vehicles in the queuing and deceleration region that could be released during the remaining green time. The final two equations (3.26) and (3.27) estimate the number of vehicles in the free flow region 1 that could be discharged during the remaining green time.

$$RG_{cp,m} = \begin{cases} t_{yield_m} - t_{curret} + 1, & signal\ indication\ is\ green \\ 0 & ,otherwise \end{cases} \quad (3.21)$$

$$VIQ0_{p,m} = \mathrm{TP_{p,m}}\% * \sum_{v=1}^{W_{d,m}} NQ_v \tag{3.22}$$

$$NQ_v = \begin{cases} 1, & if\ VD_{v,p,m} < t_{current}, \quad \frac{\mathrm{TP_{p,m}}\% * \sum_{v=1}^{W_{d,m}} NQ_v}{DR_{p,m} * NL_{p,m}} < RG_{cp,m}, and\ W_{d,m} \le MNVL_{d,m} \\ 0, & otherwise \end{cases} \tag{3.23}$$

$$VIQC_{p,m} = VIQ0_{p,m} + TP_{p,m}\% * \sum_{v=W_{d,m}+1}^{E_{d,m}} ND_v \tag{3.24}$$

$$ND_v = \begin{cases} 1, & \begin{array}{l} if\ t_{current} < VD_{v,p,m} < t_{current} + \frac{VIQ0_{p,m} + TP_{p,m}\% * \sum_{v=W_{d,m}+1}^{v-1} ND_v}{DR_{p,m} * NL_{p,m}} \\ , \frac{VIQ0_{p,m} + TP_{p,m}\% * \sum_{v=W_{d,m}+1}^{E_{d,m}} ND_v}{DR_{p,m} * NL_{p,m}} < RG_{cp,m}, and\ W_{d,m} < E_{d,m} \le MNVL_{d,m} \end{array} \\ 0, & otherwise \end{cases} \tag{3.25}$$

$$VFFRC_{p,m} = TP_{p,m}\% * \sum_{v=E_{d,m}+1}^{Q_{d,m}} NF_v \tag{3.26}$$

$$NF_v = \begin{cases} 1, & if\ t_{current} + \frac{VIQC_{p,m}}{DR_{p,m} * NL_{p,m}} \le VD_{v,p,m} \le t_{current} + RG_{cp,m}, and\ E_{d,m} < Q_{d,m} \le MNVL_{d,m} \\ 0, & otherwise \end{cases} \tag{3.27}$$

Where,

$RG_{cp,m}$: The remaining green time of the coordinated phase cp at intersection m (seconds),

t_{yield_m}: The time instant of the yield point at intersection m, i.e. the last second of the coordinated green (second),

$t_{curre\,t}$: The current time (second),

$W_{d,m}$, $E_{d,m}$, $Q_{d,m}$: variables which indicate estimated total number of vehicles in the queuing region, deceleration region, and free flow region 1 of approach d at intersection m, respectively, (vehicles),

N_v: a binary variable,

v: The index of vehicles,

$VIQ0_{p,m}$: Estimated number of vehicles in the queuing region for of phase p at intersection m (vehicles) and these vehicles could be released during remaining green time (vehicles),

$DR_{p,m}$: The discharge rate per second per lane for phase p at intersection m (vehicles),

$NL_{p,m}$: Number of lanes for phase p at intersection m,

$VIQC_{p,m}$: Estimated number of vehicles in the queuing and deceleration region for phase p at intersection m which could be released during the remaining green time (vehicles),

$VFFRC_{p,m}$: Estimated Number of vehicles in the free flow region 1 could be discharged during the remaining green time (vehicles).

After the predicted number of vehicles currently traveling on the target approach could be released during the remaining green time, initial queue length of an approach for the next projection horizon is generated by the equation below.

$$rq_{0,p,m} = \max(MNVL_{d,m} * \%TP_{p,m} - VIQC_{p,m} - VFFRC_{p,m}, 0) \quad (3.28)$$

Where,

$rq_{0,p,m}$: The initial queue length of the phase p at intersection m for the next projection horizon (vehicles).

3.3.2.2 Step 2-2: Estimate Number of Arrivals on Green and Forecast Discharge Profiles

For the first intersection, upstream arrival profiles of the coordinated approach are extracted from the upstream detector. With respect to the rest of coordinated intersections, the upstream arrival profiles are predicted discharge profiles of its upstream intersection. To predict number of arrivals on green after existing queue cleared and discharge profiles for an intersection, the second by second queue length dynamics forecasted by equations (3.29) and (3.30) must be used. Discharge profiles are predicted by equation (3.31).

$$rq_{i,p,m} = \max\left(rq_{i-1,p,m} + Arr_{sb_{i,d,m}} * TP_{p,m}\% - DC_{i,p,m}, 0\right), i \geq 1 \tag{3.29}$$

$$DC_{i,p,m} = \begin{cases} \dfrac{1}{QDH_{p,m}} * NL_{p,m} * NC, & SI_{i,p,m} = 1 \\ 0, & SI_{i,p,m} = 0 \end{cases} \tag{3.30}$$

$$dis_{i,p,m} = \begin{cases} DC_{i,p,m} & rq_{i,p,m} > 0 \text{ and } SI_{i,p,m} = 1 \\ rq_{i-1,p,m} + Arr_{sb_{i,d,m}}, & rq_{i-1,p,m} > 0, rq_{i,p,m} \leq 0, \text{and } SI_{i,p,m} = 1 \\ Arr_{sb_{i,d,m}} * SI_{i,p,m}, & rq_{i-1,p,m} = 0,\ rq_{i,p,m} < 0 \text{ and } SI_{i,p,m} = 1 \\ 0, & SI_{i,p,m} = 0 \end{cases} \tag{3.31}$$

Where,

$rq_{i,p,m}$: The queue length of time index i for phase p at intersection m of the next projection horizon (vehicles),

$DC_{i,p,m}$: The discharge capacity of time index i for phase p at intersection m of the next projection horizon (vehicles),

$QDH_{p,m}$: Queue discharge headway per lane for phase p at intersection m (seconds/vehicle),

$SI_{i,p,m}$: Signal indication for time index i of phase p at intersection m ($SI_{i,p,m} = 1$: green light; $SI_{i,p,m} = 0$: red light),

NC: Number of cycles within a projection horizon,

$\mathrm{dis}_{i,p,m}$: The discharge profiles of time index i for phase p at intersection m of the next projection horizon (vehicles).

Equation (3.31) shows four conditions for calculating discharge profiles of a phase. The first three conditions are during green light: 1) the existing queue cannot be cleared within this second. The discharge profile of this second is the total capacity of this second; 2) the existing queue is cleared within this second. The discharge profile of this second is the sum of resident queue length in last second and the number of arrivals in this second; and 3) no queue exists in the last second. In this second, the number of arrivals is also less than the discharge capacity. The discharge profile of this second is the number of arrivals in this second. The fourth condition indicates that no vehicle can be released during the red light.

After second by second queue length is estimated, the calculation of when existing queues are cleared can be known. For multilane intersections, the lane with the largest queue length of an approach is the critical lane of that approach since it needs the longest time to clear an existing queue. It determines the queue clearance time of that

approach. As a result, it has significant impacts on estimating number of arrivals on green after queue cleared and it generates the largest stop delay for that approach. The number of vehicles arrival on green after the existing queues are discharged could be predicted as below.

$$NAG_{cp,m} = \sum_{i=0}^{C-1} Arr\_sb_{i,d,m} * TP_{p,m}\% * SI_{i,p,m} * \delta_{p,m} \tag{3.32}$$

$$\delta_{p,m} = \begin{cases} 1, if\ rq_{i-1,p,m} = 0 \\ 0, \quad otherwise \end{cases} \tag{3.33}$$

Where,

$NAG_{O_m,cp,m}$: Total number of arrivals on green after existing queue dispersed for coordinated phase cp of intersection m for next projection horizon (vehicles).

As shown in Figure 3.10, discharge profiles for a typical four leg intersection consists of three individual discharge profiles: the major street through movement, minor street left turn, and minor street right turn. The steps 2-1 and 2-2 are conducted for the major street vehicle through movement. Step 2-2 is performed for minor streets left and right turns. It is assumed that traffic volumes on minor streets are not heavy, and the cyclical residual queue should be quickly cleared. The initial queue at the beginning of a projection horizon has very little impact on predicting discharge profiles for minor streets.

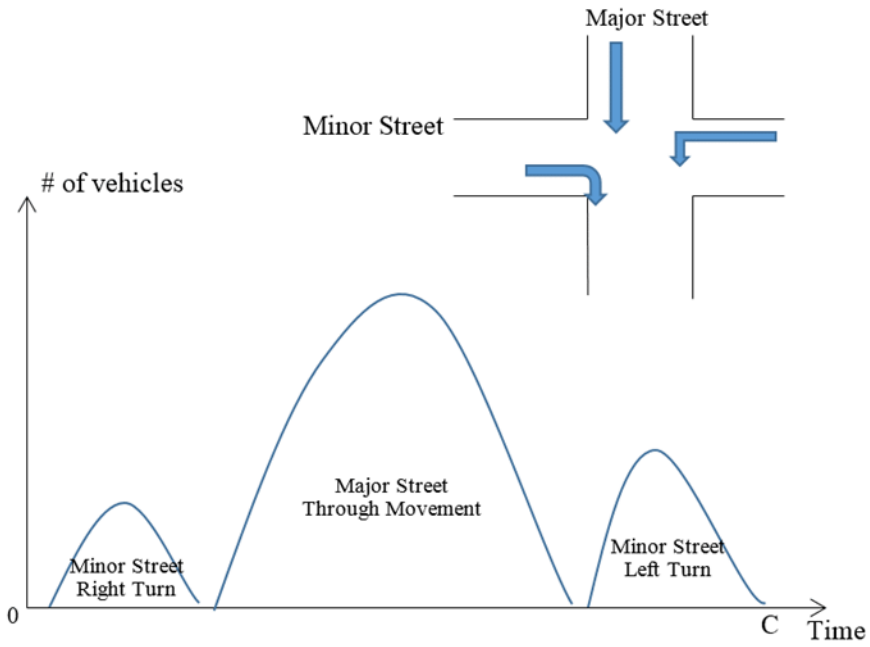

Figure 3.10 Discharge Profiles of an Intersection

3.3.3 Step 3: Offset Optimization

Based on Steps 1 and 2 for each intersection of a signalized arterial, it is possible to estimate the number of arrivals on green at stop bar after the existing queue is cleared in the coordinated approach for each potential offset of that intersection. In this dissertation, one directional progression is taken into consideration. Steps 1 and 2 are performed from the first intersection to the last intersection according to the sequences of traffic flow propagation.

The objective function of this study is to maximize the total number of arrivals on green after existing queue is cleared for the entire arterial. The dynamic programming algorithm is used to solve the proposed model. The specific procedures are described below.

Stage $m = 0, 1, 2, \cdots, M$

The stage of this model is divided based on the number of intersections within the study arterial. A stage is procedures for predicting number of arrivals on green after existing queue is cleared in the coordination direction for each potential offset of an intersection.

State decision variable:

The decision variable for each state is feasible offsets of an intersection.

State performance equation:

$$f(O_m, VSplit_m) = NAG_{cp,m} \tag{3.34}$$

Where,

$VSplit_m$: The split vector which contains splits of 8 phases of intersection m (seconds),

$f(O_m, VSplit_m)$: Number of arrivals on green after existing queue cleared when the offset of an intersection is O_m and splits of the intersection are $VSplit_m$ (vehicles).

State cumulative performance equation

$$cf(O_m, VSplit_m) = f(O_m, VSplit_m) + cf(O_{m-1}, VSplit_{m-1}) \tag{3.35}$$

Where,

$cf(O_m, VSplit_m)$: Cumulative number of arrivals after existing queue cleared from intersection 0 to m (vehicles). The offsets and splits of intersection m and $m-1$ are ($O_m, VSplit_m$) and ($O_{m-1}, VSplit_{m-1}$), respectively.

Objective function and the entire model

$$\mathrm{Z} = \max \sum_{m=1}^{M} NAG_{cp,m}(\Delta O_m, VSplit_m) \tag{3.36}$$

s.t.

$$G_{de_{p,m}} = \max\left(\frac{\mu_{d,m}^{dp\%} * \mathrm{TP_{p,m}}\% * \sum_{j=1}^{T} N_{j,d,m}}{T * NL_{p,m}} * C, G_{e,min_{p,m}}\right)$$

$$\mathrm{TP_{TM,d,m}}\% = \frac{CQ_{TM,d,m} + \sum_{j=1}^{T} NCV_{j,TM,d,m}}{\sum_{TM=1}^{3} CQ_{TM,d,m} + \sum_{TM=1}^{3}\sum_{j=1}^{T} NCV_{j,TM,d,m}} * 100\%$$

$$\mathrm{TP_{p,m}}\% = \sum_{d=1}^{TD}\sum_{TM=1}^{3} \mathrm{TP_{TM,d,m}}\% * \alpha_{p,TM,d,m}\; TG_{e_m} = C - L_m$$

$$TG_{de_m} = \max\left(\sum_{P=1}^{4} G_{de_{p,m}}, \sum_{P=5}^{TP} G_{de_{p,m}}\right)$$

$$G_{e_{p,m}} = TG_{e_m} * \frac{G_{de_{p,m}}}{TG_{de_m}}, \qquad if\, TG_{de_m} \neq TG_{e_m}$$

$$\begin{cases} Split_{1,m} + Split_{2,m} = Split_{5,m} + Split_{6,m} \\ Split_{3,m} + Split_{4,m} = Split_{7,m} + Split_{8,m} \end{cases}$$

$$O_m = O_{current,m} + \Delta O_m$$

$$VIQ0_{p,m} = \mathrm{TP_{p,m}}\% * \sum_{v=1}^{W_{d,m}} NQ_v$$

$$NQ_v = \begin{cases} 1, & if\ VD_{v,p,m} < t_{current}, \quad \dfrac{\mathrm{TP_{p,m}}\% * \sum_{v=1}^{W_{d,m}} NQ_v}{DR_{p,m} * NL_{p,m}} < RG_{cp,m}, and\ W_{d,m} \leq MNVL_{d,m} \\ 0, & otherwise \end{cases}$$

$$RG_{cp,m} = \begin{cases} t_{yield_m} - t_{curret} + 1, & signal\ indication\ is\ green \\ 0, & otherwise \end{cases}$$

$$VIQC_{p,m} = VIQ0_{p,m} + TP_{p,m}\% * \sum_{v=W_{d,m}+1}^{E_{d,m}} ND_v$$

$$ND_v = \begin{cases} 1, & if\ t_{current} < VD_{v,p,m} < t_{current} + \frac{VIQ0_{p,m} + TP_{p,m}\% * \sum_{v=W_{d,m}+1}^{v-1} ND_v}{DR_{p,m} * NL_{p,m}} \\ & , \frac{VIQ0_{p,m} + TP_{p,m}\% * \sum_{v=W_{d,m}+1}^{E_{d,m}} ND_v}{DR_{p,m} * NL_{p,m}} < RG_{cp,m}, and\ W_{d,m} < E_{d,m} \le MNVL_{d,m} \\ 0, & otherwise \end{cases}$$

$$VFFRC_{p,m} = TP_{p,m}\% * \sum_{v=E_{d,m}+1}^{Q_{d,m}} NF_v$$

$$NF_v = \begin{cases} 1, & if\ t_{current} + \frac{VIQC_{p,m}}{DR_{p,m} * NL_{p,m}} \le VD_{v,p,m} \le t_{current} + RG_{cp,m}\ , and\ E_{d,m} < Q_{d,m} \le MNVL_{d,m} \\ 0, & otherwise \end{cases}$$

$$rq_{0,p,m} = \max(MNVL_{d,m} * \%TP_{p,m} - VIQC_{p,m} - VFFRC_{p,m}, 0)$$

$$rq_{i,p,m} = \max\left(rq_{i-1,p,m} + Arr_{sb\,i,d,m} * TP_{p,m}\% - DC_{i,p,m}, 0\right), i \ge 1$$

$$DC_{i,p,m} = \begin{cases} \frac{1}{QDH_{p,m}} * NL_{p,m} * NC, & SI_{i,p,m} = 1 \\ 0, & SI_{i,p,m} = 0 \end{cases}$$

$$dis_{i,p,m} = \begin{cases} DC_{i,p,m} & rq_{i,p,m} > 0\ and\ SI_{i,p,m} = 1 \\ rq_{i-1,p,m} + Arr_{sb\,i,d,m}, & rq_{i-1,p,m} > 0, rq_{i,p,m} \le 0, and\ \ SI_{i,p,m} = 1 \\ Arr_{sb\,i,d,m} * SI_{i,p,m}, & rq_{i-1,p,m} = 0, \quad rq_{i,p,m} < 0\ \ and\ SI_{i,p,m} = 1 \\ 0, & SI_{i,p,m} = 0 \end{cases}$$

$$NAG_{cp,m} = \sum_{i=0}^{C-1} Arr\_sb_{i,d,m} * TP_{p,m}\% * SI_{i,p,m} * \delta_{p,m}$$

$$\delta_{p,m} = \begin{cases} 1, if\ rq_{i-1,p,m} = 0 \\ 0, \quad otherwise \end{cases}$$

$$-\beta_m \le \Delta O_m \le \beta_m$$

$$\beta_m, O_m \ge 0$$

$$G_{e_{p,m}}, G_{de_{p,m}}, G_{e,min_{p,m}} > 0$$

Where,

Z: The maximum number of arrivals on green after the existing queue is cleared in the coordination direction for the entire arterial (vehicles).

For the ALTPOM, forward recursion approach of the dynamic programming algorithm is utilized for solving the presented model. After obtaining the maximum number of arrivals on green after existing queue is cleared for an entire arterial, the optimal offset of each intersection for the next projection horizon are extracted by backtracking.

Figure 3.11 shows the algorithm framework of the offset optimization module. In Figure 3.11, there are there layers of loops. The inner loop shows the procedures to estimate number of arrivals on green when offsets of intersections m and $m-1$ are O_m and O_{m-1}. When these two variables are determined, the initial queue length of the coordinated approach of intersection m is estimated. Then, the number of arrivals on green after the existing queue is cleared for the coordinated direction is predicted. After doing this for all intersections, the accumulative number of arrivals on green after queue cleared for the coordinated direction from the first intersection to the last intersection $(M-1)$ is estimated. After upcoming arrival profiles for the next intersection is forecasted, the inner loop is repeated until all feasible offsets of intersection $m-1$ are taking into consideration for estimating possible number of arrivals on green when offset of intersection m is O_m. Then, the maximum accumulative number of arrivals on green when offset of intersection m is O_m and the corresponding offset of intersection $m-1$ are identified.

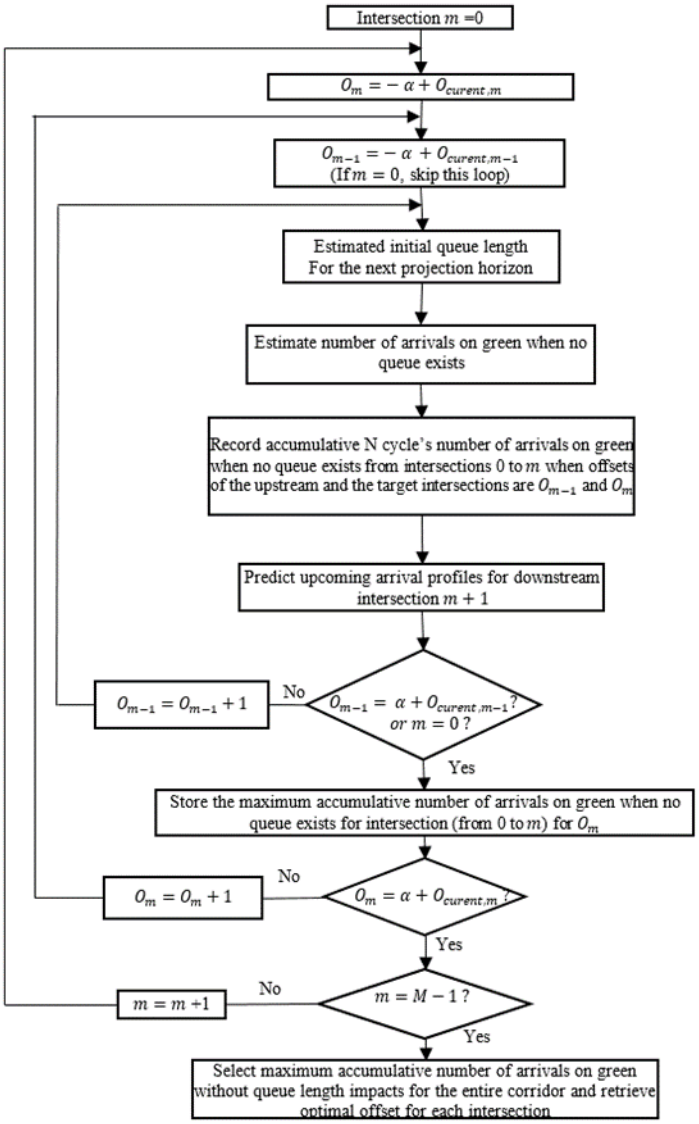

Figure 3.11 Implementation of Dynamic Programming for the ALTPOM

The purpose of the inner loop is to calculate the maximum accumulative number of arrivals on green for a potential offset of intersection m by considering impacts of different offsets of its upstream intersection. It is noticed that, as we mentioned before, there is no inner loop for the first intersection, since it is not affected by its upstream intersection which is far. Next, the algorithm enters the middle loop. The middle loop is

used to estimate the maximum accumulative number of arrivals on green for all potential offsets of intersection m by considering impacts of different offsets of intersection $m-1$. The outer loop is the procedure to estimate the maximum accumulative number of arrivals on green for each potential offset of an intersection by repeating inner and middle loops. These three layers of loops start from the first intersection and terminate at the last intersection $M-1$. After obtaining all possible accumulative numbers of arrivals on green after queue cleared for each of potential offsets of the final intersection, the maximum accumulative number of arrivals on green after queue cleared for the entire arterial could be identified. The corresponding optimal offset for each intersection for the next projection horizon is obtained by backtracking. After adjusted splits and optimized offsets are generated by ALTPOM, these splits and offsets are implemented at the beginning of the next projection horizon. The entire procedure of ALTPOM for each projection horizon is completed. Then, ALTPOM is repeatedly performed for each projection horizon which is defined by users.

In this chapter, ALTPOM is developed and details of modules within ALTOPOM are illustrated. In next chapter, the effectiveness of ALTPOM needs to be assessed and the procedures of interfacing ALTPOM with a selected traffic simulator will be presented. Case studies will be conducted to evaluate the performances of ALTPOM.

CHAPTER IV

IMPLEMENTATION AND VALIDATION OF THE ALTPOM

In the last chapter, an arterial-level traffic progression optimization model (ALTPOM) for signalized arterials based on connected vehicle technologies was presented. This chapter will focus on the proposed model as it is evaluated within the connected vehicle environment. The procedures to implement the ALTPOM within a selected microscopic traffic simulator are introduced first. The chosen traffic simulator will simulate the connected vehicle environment, and then the ALTPOM will be assessed by case studies. Next, the results of the case studies are analyzed.

Since ALTPOM optimizes traffic progression of an entire arterial, all performance measures evaluated in this chapter are mobility related performance indexes. These including control delay per vehicle, stop delay per vehicle, travel time per vehicle, average speed, stop vehicle percent, volume, and level of service. With the exception of the specific indication, performance measures are used in this chapter instead of mobility related performance measures in order for simplification.

4.1 Implementation of the ALTPOM within Connected Vehicle Simulation Environment

To evaluate the effectiveness of the ALTPOM, the first step is to select a suitable traffic simulator with connected vehicle simulation features. The next step is

implementing the proposed model within the chosen connected vehicle simulation environment.

4.1.1 The Selected Simulator

A microscopic traffic simulator, Enhanced Transportation Flow Open-source Microscopic Model (ETFOMM), is selected as the simulator. ETFOMM was developed based on CORSIM algorithms and concepts with advanced technology and computing features, such as the connected vehicle simulation feature. As indicated by a poster, ETFOMM has the following major features which CORSIM doesn't have: 1) provides cloud service; 2) it can operate using different platforms (such as windows x86, windows x64, AndroidTM, iPad, iPhone, Mac, etc.); 3) owns parallel computing capacity; and 4) has optional simulation time step (the smallest time step is 0.01 second) [73].

Trajectory Conversion Algorithm (TCA) software produced by Noblis, Inc can simulate DSRC communication between connected vehicles and RSUs according to data sets such as vehicle trajectory, RSUs' location information, strategy information, etc. Based on TCA, in addition to transmitting Basic Safety Messages (BSMs), equipped vehicles also can generate ITS Spot messages and/or European Cooperative messages by DSRC and/or cellular. This software can also consider communication latency and loss rate according to users' settings [9].

New Global Systems for Intelligent Transportation Management Inc. (NGS Inc.) is the developer of ETFOMM. NGS integrated TCA with ETFOMM so it can now provide an ideal connected vehicle simulation environment, which is utilized to develop, debug, and evaluate ALTPOM within variable penetration rates of connected vehicle conditions.

4.1.2 Implementation of ALTPOM

In this sub-section, an illustration of the procedures that implement ALTPOM within the chosen connected vehicle simulation environment is demonstrated. By referring to Zhang's presentation [74] and discussion with technical supporters and other users of ETFOMM (Yifeng Zeng, Xiang Li, and Lei Zhang, Unpublished data), a data flow diagram (Figure 4.1) is presented to illustrate the interface between the ALTPOM and the connected vehicle simulation environment, i.e. ETFOMM with TCA.

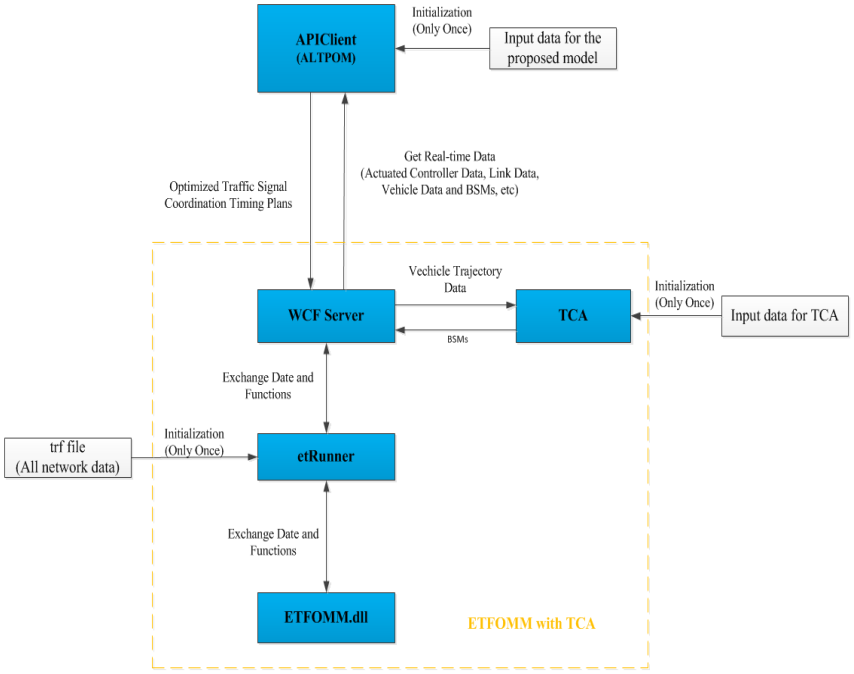

Figure 4.1 The Data Flow Diagram of Implementing the ALTPOM within ETFOMM

In Figure 4.1 the blue rectangles are the five major modules of ETFOMM with TCA. ETFOMM.dll is the simulation engine of ETFOMM which contains a set of get/set functions [75]. etRunner is the major control program between a Windows Communication Foundation (WCF) server and ETFOMM.dll [76]. As indicated by the

API Report, in ETFOMM, applications developed by users and ETFOMM simulations can exchange data by WCF service. WCF is a run-time and .NET Framework application [75]. The WCF server is functioning as a data exchange center to provide a bridge for data sharing among different modules within ETFOMM. TCA is already integrated with ETFOMM by NGS Inc., as mentioned before, with the major function of TCA is simulating DSRC communication within the connected vehicle environment. ETFOMM provides an application programming interface (API, i.e. APIClinet) where users can use different programming languages, such as C++, C#, Python, etc. [74]. In this dissertation, the author uses C++ to implement the proposed ALTPOM within the API provided in ETFOMM.

Figure 4.1 also shows connections between these five modules. etRunner could load ETFOMM.dll and the WCF server, while also providing functions to exchange data in every simulation step [74]. During the beginning initializations, etRunner read data from a trf file containing simulation network data such as link, lane, node, traffic signals, simulation duration, and critical simulation parameters, which are set by users, etc. etRunner shares this data with ETFOMM.dll.

As shown in Figure 4.1, TCA reads vehicle trajectory data of equipped vehicles from the WCF server. Then TCA produces simulated BSMs data and sends it back to the WCF server. At the initialization, critical input data for TCA, such as penetration rates of connected vehicles, locations of RSUs, and effective communication distance between a RSU and connected vehicles, etc., is read by the TCA module of ETFOMM.

As shown in Figure 4.1, ETFOMM.dll, etRunner, WCF server, and TCA are in an orange rectangle with dash lines. The orange rectangle indicates these modules are

encapsulated by ETFOMM and users cannot directly access these four modules. In this dissertation, the proposed ALTPOM is coded as the APIClient of ETFOMM with more than 7,000 lines of C++ programmed code. At the initialization process, parameters for the proposed model are read into the APIClient. The data includes the coordinated path, geometric data of coordinated intersections, interval of each optimization, and the start time of implementing the proposed model, etc. The proposed model retrieves real-time simulation data from the WCF server, such as BSMs, actuated controller data, and link data etc. These data sets are then processed by the proposed model. ALTPOM is then repeatedly executed according to a user defined interval as mentioned in Chapter 3. Based on collected and processed real-time data, the proposed model predicts forthcoming traffic conditions and generates optimized traffic signal coordination plans at the beginning of each interval. These signal timing plans are sent back to the WCF server. The WCF server shares these optimized signal timing plans with etRunner, which sends these signal timing plan back to the signal controller algorithms inside of ETFOMM.dll. Then, ETFOMM.dll advances the simulation according to the optimized signal timing plans. This loop continues until the simulation is completed.

Figure 4.2 shows the simulation execution process of ETFOMM with TCA. Three modules (etRunner64.exe, APIClient.exe, and TCA_Interface.exe) are running for each simulation step in order to process and exchange real-time simulation data.

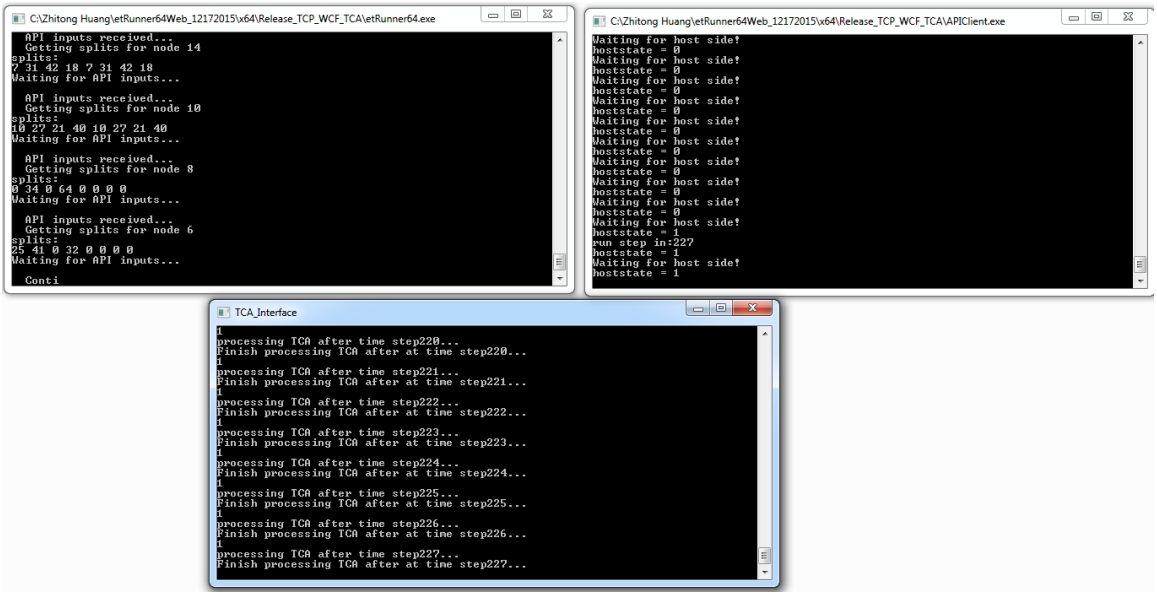

Figure 4.2 Simulation Process of ETFOMM with TCA

4.2 Case Studies

After interfacing ALTPOM with the ETFOMM with TCA, case studies are conducted to assess the effectiveness of ALTPOM. Results of the case studies are presented and analyzed. The volume sensitivity study of ALTPOM is also performed.

4.2.1 The Selected Study Site

State Street (U.S. Route 51) is the north/south major arterial in the city of Jackson, the capital of Mississippi. State St. connects the downtown area of Jackson and residential areas, and as such carries major commuter traffic between downtown and residential areas. The stretch of State St. between Manship St. to Amite St. is selected as the study site. Figure 4.3 shows the study site which was obtained using Google Map.

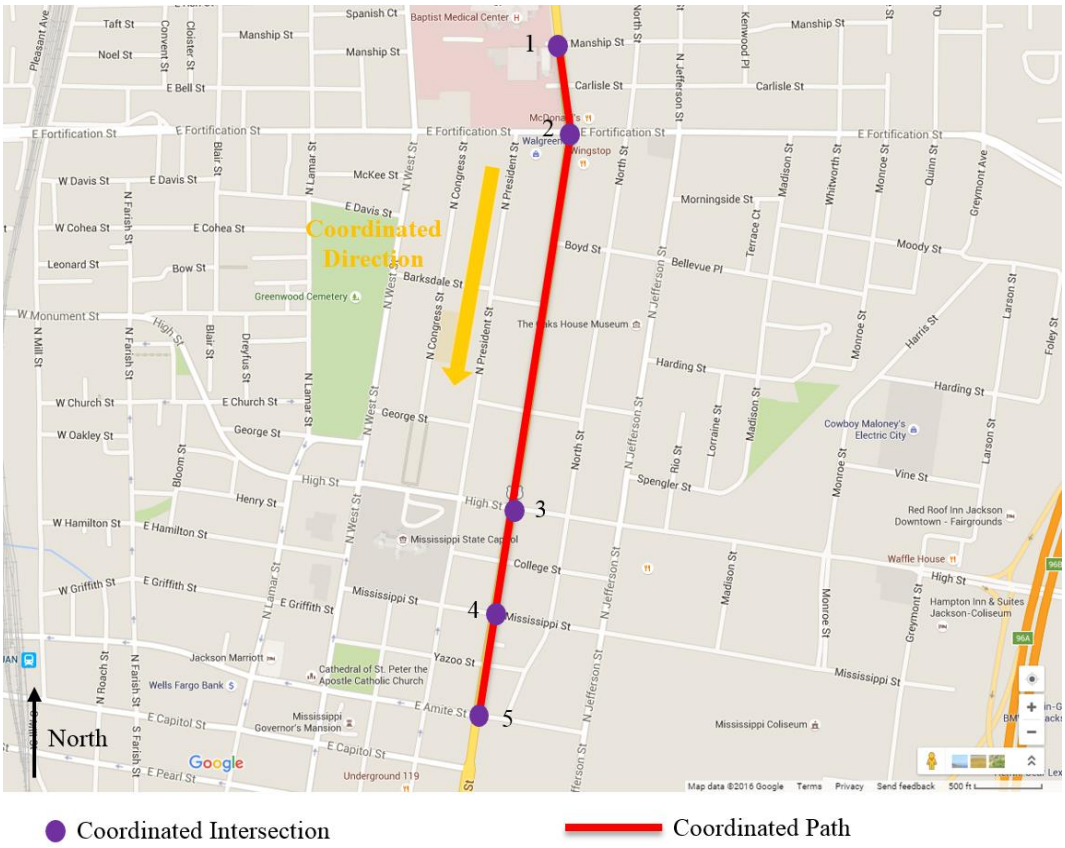

Figure 4.3 The Study Site

(Obtained from: https://www.google.com/maps/place/Jackson,+MS/@32.3079968,-90.1865325,16z/data=!4m2!3m1!1s0x86282b7f90741b21:0x713cde441f038a0)

Aforementioned, ALTPOM is utilized for one directional traffic signal coordination. The south bound of the study site is the coordinated direction which is shown in Figure 4.3 to facilitate morning peak traffic. As shown in this figure, there are five intersections within the study site, which are listed below:

- Intersection 1: Manship St. at State St.
- Intersection 2: Fortification St. at State St.
- Intersection 3: High St. at State St.

- Intersection 4: Mississippi St. at State St.
- Intersection 5: Amite St. at State St.

4.2.2 Scenarios Development

To build a simulation network of the study site, curial field data was collected, such as intersections geometry data, traffic volume, speed, turning percentages, and signal timing plans, etc. The built simulation network is well calibrated based on collected field data, which was participated by the author in another report [77]. That work details the full procedures taken for data collection and simulation network calibration.

Three scenarios are developed for evaluating the proposed model:

- Scenario 1 (base case): Since the 5 intersections are not coordinated in the field, the field signal timing plans provided by Mississippi Department of Transportation (MDOT) are utilized as the input of TRANSYT-7F to generate an optimized traffic signal coordination plan. The performance measures of this scenario are used as the benchmark to assess the effectiveness of the presented ALTPOM.
- Scenario 2 (low penetration rate case): In this scenario, the penetration rate of connected vehicle is 25%. The optimized traffic signal timing plan by TRANSYT-7F is used as the original coordination plan and the input for the proposed model. To warm up the study network, the beginning time to implement the proposed model is 900 seconds. The proposed model is

repeatedly implemented for every 10 cycles to optimize traffic progressions of all study intersections.

- Scenario 3 (high penetration rate case): In this scenario, the penetration rate of connected vehicle is 50%. All settings of Scenario 3 are the same as those of Scenario 2, except where the penetration rates of the two scenarios differ.

The entire simulation time for the three scenarios is 5400 seconds (90 min), which approximate the local peak hour time. In this dissertation, the effective communication range between a RSU and an OBE is 1,500 ft. Results of the case studies are reported below.

4.2.3 Results and Analysis of the Case Studies

For the case studies, important mobility performance measures are collected and analyzed, such as control delay, average speed, stopped vehicle percent, volume and level of service (LOS), etc. According to the Highway Capacity Manual (HCM), control delay is caused by the existence of a traffic signal control device which is a major measurement to assess level-of-service (LOS) for signalized and un-signalized intersections. It includes deceleration delay, stop delay, queue moving time, and acceleration delay [78]. Stopped vehicle percent is the performance measure related to fuel consumption and emission. It evaluates the effectiveness of traffic progression for a traffic signal timing plan. Therefore, in this dissertation these two performance measures are the performance indexes given the most concern.

Table 4.1 provides the results of three scenarios for major streets. It can be seen that by implementing the proposed model, all performance measures of the coordinated

direction of the study arterial are improved for both low and high penetration rate cases when compared with the signal timing plan optimized by TRANSY-7F (base case). In addition to the coordinated direction, all performances of the opposite direction and both directions are also enhanced. Under the 25% penetration rate of connected vehicle (low penetration rate case), all delay measures per vehicle for all directions (the coordinated direction, opposite direction, and both directions) are significantly decreased when compared with that of the base case. Correspondingly, LOS improves from D to C, from E to C, and from D to C for the coordinated direction, opposite direction, and both directions. Average speeds for the coordinated direction, opposite direction, and both directions are increased 14.5%, 25.9%, and 18.7%. The throughput of the coordinated direction, opposite direction, and both directions improved 4.9%, 5.0%, and 4.9%.

Compared to the base case with respect to stopped vehicle percent, low penetration rate case decreases 12.3% and 6.9 % for the coordinated direction and both directions. There is only one insignificant degrading performance where the opposite direction increased 1.4% for the stopped vehicle percent. These results indicate ALTPOM provides smooth progression for the coordinated direction without significantly impacting the opposite direction.

Table 4.1 Results of Three Scenarios for Major Streets

			Control Delay Per Vehicle	Stop Delay Per Vehicle	Travel Time Per Vehicle	Average Speed	Stopped Vehicles Percent	Volume	LOS***
Unit			Seconds/Vehicle			MPH	%	VPH	----
Entire Arterial	Coordinated Direction	Base Case	48	42.9	89	13.1	53.5	4295	D
		Low Penetration Rate Case	24.7	19.8	60.7	15	46.9	4506	C
		*Difference	-23.3	-23.1	-28.3	1.9	-6.6	211	----
		*Difference (%)	-48.5%	-53.8%	-31.8%	14.5%	-12.3%	4.9%	----
		High Penetration Rate Case	20.6	16.1	56.6	16	45.7	4414	C
		**Difference	-27.4	-26.8	-32.4	2.9	-7.8	119	----
		**Difference (%)	-57.1%	-62.5%	-36.4%	22.1%	-14.6%	2.8%	----
	Opposite Direction	Base Case	64	52.3	98.5	11.2	43.8	3365	E
		Low Penetration Rate Case	21.6	17.2	52.3	14.1	44.4	3533	C
		*Difference	-42.4	-35.1	-46.2	2.9	0.6	168	----
		*Difference (%)	-66.3%	-67.1%	-46.9%	25.9%	1.4%	5.0%	----
		High Penetration Rate Case	21.9	17.5	53	14.2	43.7	3580	C
		**Difference	-42.1	-34.8	-45.5	3	-0.1	215	----
		**Difference (%)	-65.8%	-66.5%	-46.2%	26.8%	-0.2%	6.4%	----
	Both Direction	Base Case	55	47	93.2	12.3	49.2	7660	D
		Low Penetration Rate Case	23.3	18.7	57	14.6	45.8	8039	C
		*Difference	-31.7	-28.3	-36.2	2.3	-3.4	379	----
		*Difference (%)	-57.6%	-60.2%	-38.8%	18.7%	-6.9%	4.9%	----
		High Penetration Rate Case	21.2	16.7	55	15.2	44.8	7994	C
		**Difference	-33.8	-30.3	-38.2	2.9	-4.4	334	----
		**Difference (%)	-61.5%	-64.5%	-41.0%	23.6%	-8.9%	4.4%	----

* Performance difference and difference percentages between Scenarios 1 and 2;
** Performance difference and difference percentages between Scenarios 1 and 3.
*** LOS is determined according to Highway Capacity Manual 2010 [78].

From Table 4.1, we can see that the ALTPOM further enhances the performance of major streets in the study arterial along when there is an increased penetration rate of connected vehicle. With 50% connected vehicle penetration rate (the high penetration case), the control delay per vehicle declines 4.1 seconds (16.6%) and 2.1 seconds (9.0%) for the coordinated direction and both directions when compared with the low penetration rate case. For the opposite direction, the control delay per vehicle is comparable at a slight difference of only 0.3 second more. This trend is the same for other performance measures such as stop delay per vehicle. The ALTPOM seems to provide better progression with higher penetration rates of connected vehicle. For the high penetration rate case, stopped vehicles percent for both coordinated direction and the opposite direction's is reduced with the latter overcoming a slight reduction when compared with the low penetration case. With respect to LOS, the low and high penetration rate cases have the same performance which improves LOS from D to C, from E to C, and from D to C for the coordinated direction, opposite direction, and both directions when compared to the base case. However, it seems that the impact of increased penetration rates of connected vehicle on throughput is not significant. For both directions, low and high penetration rate cases increased volume for 4.9% and 4.4 % when comparing with the base case.

In traditional traffic coordination, smoothing the major street traffic generally results in the performance of minor streets degrading, but this is not the case in the proposed models. ALTPOM not only optimizes the offset but also proactively and dynamically adjusts splits of all phases. This overcomes the traditional shortcomings

where increased performance of major streets usually means sacrificing performance of minor streets.

State St. is a major N/S arterial in the heart of City of Jackson, Mississippi. EB and WB of all intersections on State St. are considered as minor streets. Table 4.2 provides results from three scenarios for EB, WB, and both directions of minor streets. Based on the results, it was concluded that all performances in EB and both directions of minor streets are significantly improved when applying the proposed model. All delay measures are decreased in the range from 26.0% to 61.9%. With respect to LOS, there is at least one level improvement, while both mobility and throughput of EB and both directions of minor streets are improved. The average speed and throughput are increased at least 7.8% and 7.4 %. The performances in EB and both directions of minor streets are also increased along with the penetration rate of connected vehicle growth. For the control delay per vehicle, the high penetration rate case saved an extra 9.9 seconds and 3.7 seconds compared to the low penetration rate case for EB and both directions of minor streets.

Since the proposed model only provides progression for major streets, low and high penetration rate cases have the comparable performance with the base case with respect to stopped vehicles percent. The ALTPOM also raises the throughput of minor streets for EB and both directions of minor streets. The impact of the penetration rate of connected vehicle on throughput is minor. Though, it is found that the low penetration case slightly outperforms the high penetration rate case.

Table 4.2 Results of Three Scenarios for Minor Streets

			Control Delay Per Vehicle	Stop Delay Per Vehicle	Travel Time Per Vehicle	Average Speed	Stopped Vehicles Percent	Volume	LOS***
Unit			Seconds/Vehicle			MPH	%	VPH	----
Entire Arterial	EB	Base Case	83.2	90.4	133.1	6	83.8	1954	F
		Low Penetration Rate Case	52.5	43.4	73.6	6.9	84.8	2231	D
		*Difference	-30.7	-47	-59.5	0.9	1	277	----
		*Difference (%)	-36.9%	-52.0%	-44.7%	15.0%	1.2%	14.2%	----
		High Penetration Rate Case	42.6	34.4	62.6	7.7	83.4	2220	D
		**Difference	-40.6	-56	-70.5	1.7	-0.4	266	----
		**Difference (%)	-48.8%	-61.9%	-53.0%	28.3%	-0.5%	13.6%	----
	WB	Base Case	41.7	34.2	58.9	6.8	80.6	1646	D
		Low Penetration Rate Case	40.8	33.1	57.9	6.9	80.4	1647	D
		*Difference	-0.9	-1.1	-1	0.1	-0.2	1	----
		*Difference (%)	-2.2%	-3.2%	-1.7%	1.5%	-0.2%	0.1%	----
		High Penetration Rate Case	45.4	37.4	62.6	6.4	81.6	1645	D
		**Difference	3.7	3.2	3.7	-0.4	1	-1	----
		**Difference (%)	8.9%	9.4%	6.3%	-5.9%	1.2%	-0.1%	----
	Both Direction	Base Case	64.2	64.7	99.2	6.4	82.3	3600	E
		Low Penetration Rate Case	47.5	39	66.9	6.9	82.9	3878	D
		*Difference	-16.7	-25.7	-32.3	0.5	0.6	278	----
		*Difference (%)	-26.0%	-39.7%	-32.6%	7.8%	0.7%	7.7%	----
		High Penetration Rate Case	43.8	35.7	62.6	7.1	82.6	3865	D
		**Difference	-20.4	-29	-36.6	0.7	0.3	265	----
		**Difference (%)	-31.8%	-44.8%	-36.9%	10.9%	0.4%	7.4%	----

* Performance difference and difference percentages between Scenarios 1 and 2;
** Performance difference and difference percentages between Scenarios 1 and 3.
*** LOS is determined according to Highway Capacity Manual 2010 [78].

With respect to WB of the study arterial, the low penetration rate case raises the performance of WB to a limited degree when compared with the base case. In contrast, all performance indexes, except LOS, in the high penetration rate case for WB are decreased.

Figures 4.4 and 4.5 displays control delay and LOS in different directions of the study arterial with respect to three scenarios. It can be seen that under the low and high penetration rates of connected vehicles the proposed ALTPOM significantly reduces control delay and improves LOS at least one level for all different directions of the study arterial except WB. For WB, the proposed model has the comparable performance with signal timing optimized by TRANSYT-7F with the LOS of WB for three scenarios at the same level (D). From Figures 4.4 and 4.5, with respect to the effects of penetration rate of connected vehicles, it is found that the control delays of different directions of the study arterial, except WB, are further decreased along with an increase of penetration rate of connected vehicles, although LOS of low and high penetration rate cases are the same for all directions.

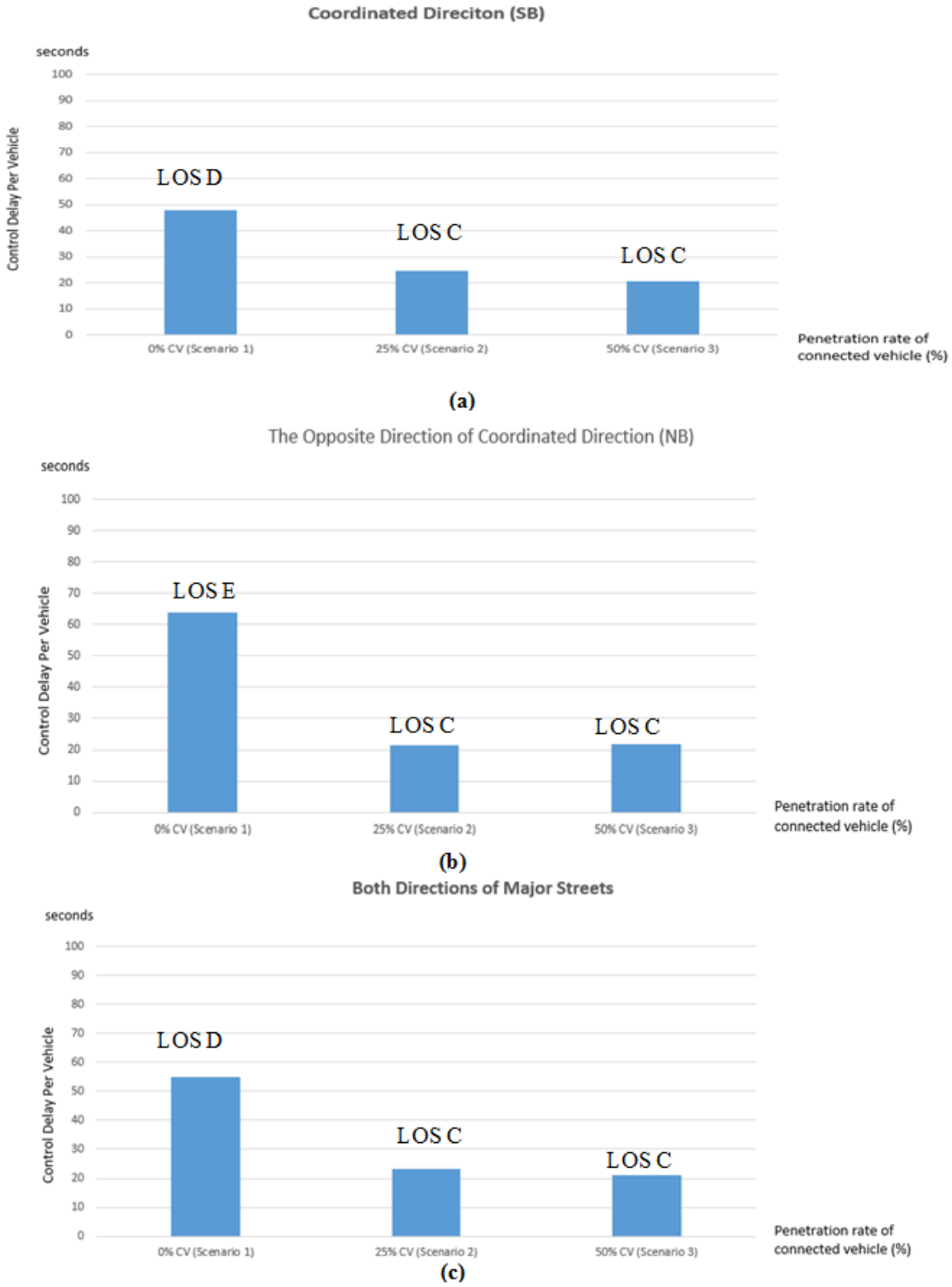

Figure 4.4 Control Delays per Vehicle and LOS of Major Streets

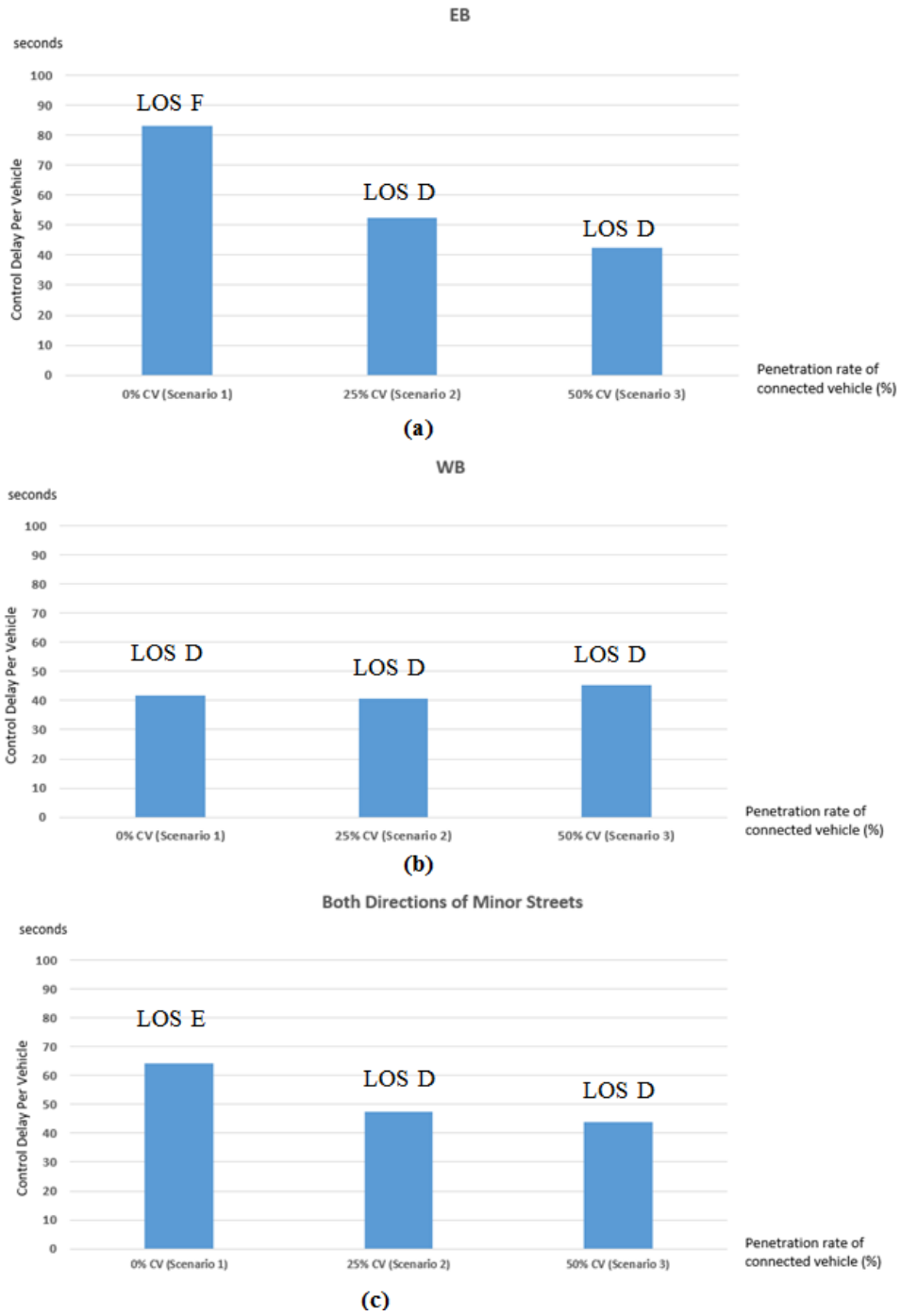

Figure 4.5 Control Delays per Vehicle and LOS of Minor Streets

Figures 4.6 and 4.7 show the effects of the proposed model for traffic progression of the study arterial. According to Figure 4.6 (a) and (c), under connected vehicle

environment the ALTPOM provides better progression for the coordination direction and both directions of major streets than that of the base case. For the opposite direction of the coordinated direction, the proposed model has little impact, as shown in Figure 4.6 (b). For (a), (b), and (c) of Figure 4.7, the proposed model provides comparable performance with the base case which is expected, since traffic coordination only impacts on major streets.

Therefore based on Table 4.1, Table 4.2, and Figures from 4.4 to 4.7, it can be concluded that the proposed ALTPOM is effective at improving mobility performances of both major and minor streets. It also provides smooth traffic progression for the coordinated direction with little impact on the opposite direction.

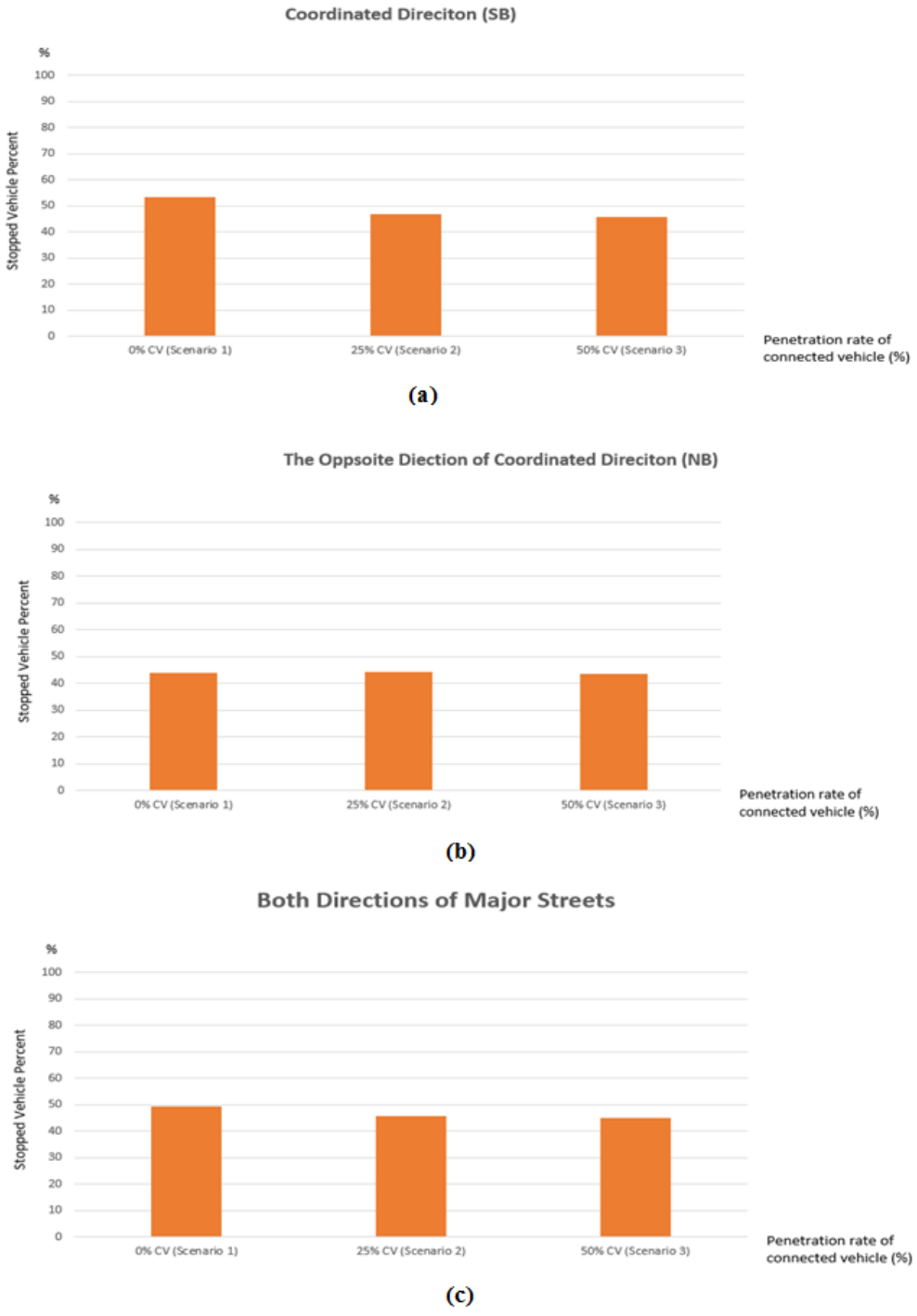

Figure 4.6 Stopped Vehicle Percent of Major Streets

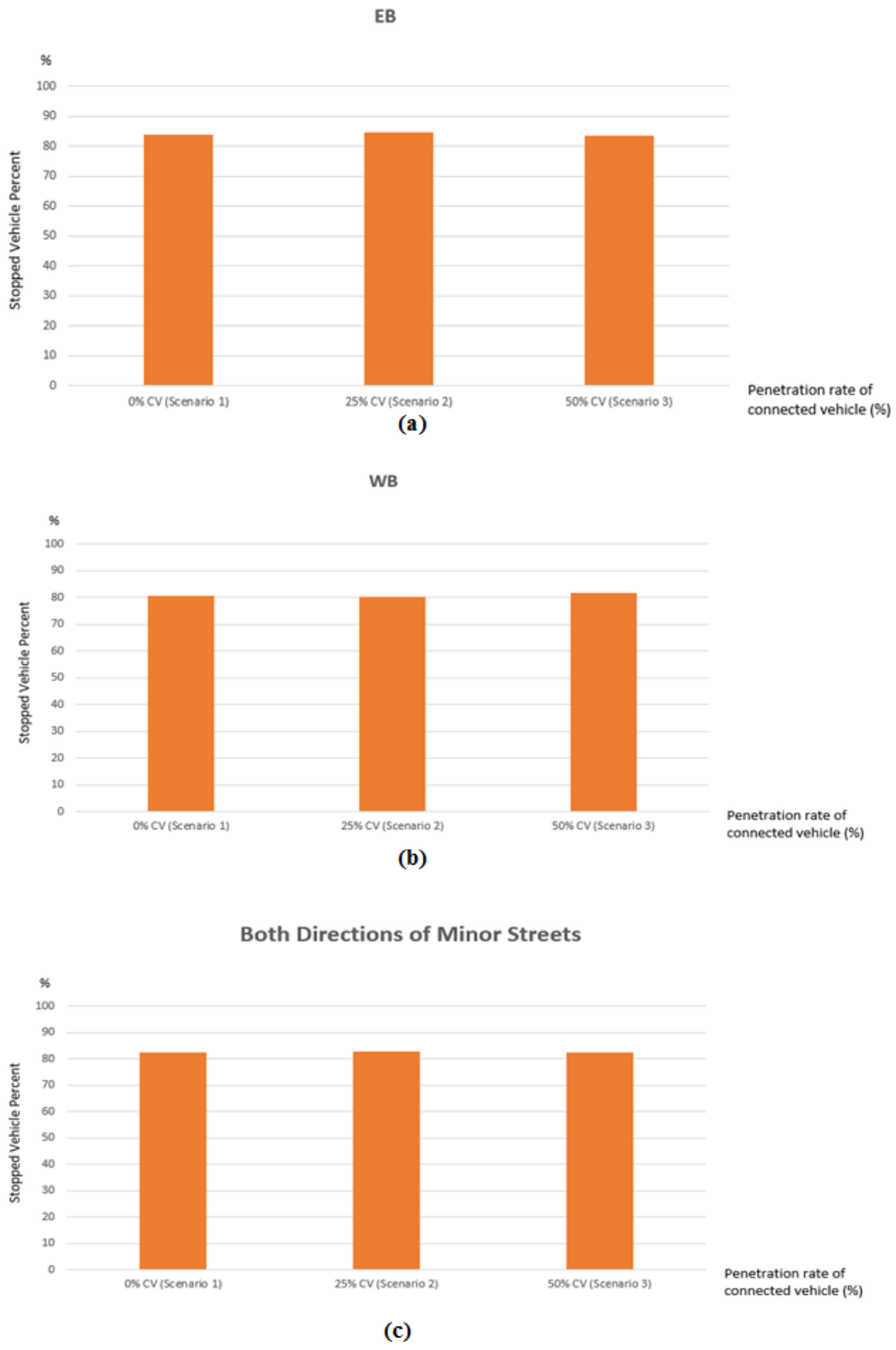

Figure 4.7 Stopped Vehicle Percent of Minor Streets

To investigate the penetration rates of connected vehicles requirement for ALTPOM, lower penetration rates of connected vehicle are utilized for evaluation. After analysis, 10% penetration rate of connected vehicle is the lowest penetration rate for ALTPOM. The reason is that estimated real-time turning percentages are an important input for the split adjustment module of ALTPOM. Real-time turning percentages are estimated according to real-time connected vehicle trajectories data. If connected vehicle penetration rates are very low, there is not enough connected vehicle trajectories data within a projection horizon to measure real-time turning percentages.

Table 4.3 shows the effects of ALTPOM for major streets when the penetration rate of connected vehicles is 10%. The same result as low and high penetration rate cases is found in that ALTPOM significantly decreased delays and improves mobility of the study arterial. For both directions of major streets, the control delay per vehicle reduced 58.5% and average speed improves 22.0% when compared with that of the base case. With respect to traffic progression, ALTPOM decreases stop vehicle percent for both the coordinated direction and its opposite direction. When comparing Table 4.3 with Table 4.1, it is found that the 10% penetration rate case has comparable performances with that of the low penetration rate case. For both directions of major streets, there are only 0.5 seconds control delay per vehicle and 0.4 mph average speed differences between 10% penetration rate case and the low penetration rate case.

Table 4.3 Results of 10% Penetration Rate of Connected Vehicle for Major Streets

			Control Delay Per Vehicle	Stop Delay Per Vehicle	Travel Time Per Vehicle	Average Speed	Stopped Vehicles Percent	Volume	LOS*
Unit			Seconds/Vehicle			MPH	%	VPH	----
Entire Arterial	Coordinated Direction	Base Case	48	42.9	89	13.1	53.5	4295	D
		10% Penetration Rate Case	21.8	17.3	57.7	15.8	45.2	4398	C
		Difference	-26.2	-25.6	-31.3	2.7	-8.3	103	----
		Difference (%)	-54.6%	-59.7%	-35.2%	20.6%	-15.5%	2.4%	----
	Opposite Direction	Base Case	64	52.3	98.5	11.2	43.8	3365	E
		10% Penetration Rate Case	24	19.4	54.8	13.9	42.9	3458	C
		Difference	-40	-32.9	-43.7	2.7	-0.9	93	----
		Difference (%)	-62.5%	-62.9%	-44.4%	24.1%	-2.1%	2.8%	----
	Both Direction of Major Streets	Base Case	55	47	93.2	12.3	49.2	7660	D
		10% Penetration Rate Case	22.8	18.2	56.4	15	44.2	7856	C
		Difference	-32.2	-28.8	-36.8	2.7	-5	196	----
		Difference (%)	-58.5%	-61.3%	-39.5%	22.0%	-10.2%	2.6%	----

Note: *LOS is determined according to Highway Capacity Manual 2010 [78].

Results of ALTPOM for minor streets under 10% penetration rates of connected vehicles condition are provided in Table 4.4. When the penetration rate of connected vehicle only reaches 10%, ALTPOM still notably increase mobility of minor streets. For both directions of minor streets, ALTPOM decreased 19.8% control delay per vehicle and increased 3.1% average speed when compared with results of the base case. After investigating Table 4.4 and Table 4.2 together, it is found that the 10% penetration rate case increased 4 seconds control delay per vehicle and decreased 0.3 mph average speed when compared with results of low penetration rate cases. With respect to the entire arterial, 10% penetration rate case increased control delay by 1861.1 seconds and

decreased throughput by 289 vehicles per hour when compared with results of low penetration rate cases.

Based on the analyses above, when penetration rates of connected vehicles increase ALTPOM can better predict/measure real-time traffic conditions of the study arterial to more effectively adjust splits and optimize offsets in order to further improve mobility of a signalized arterial. From Table 4.3 and Table 4.4, we can conclude that ALTPOM can significantly reduce delays and enhance mobility of a signalized arterial even when the penetration rate of connected vehicle reaches 10%.

Table 4.4 Results of 10% Penetration Rate of Connected Vehicle for Minor Streets

			Control Delay Per Vehicle	Stop Delay Per Vehicle	Travel Time Per Vehicle	Average Speed	Stopped Vehicles Percent	Volume	LOS*
Unit			Seconds/Vehicle			MPH	%	VPH	----
Entire Arterial	EB	Base Case	83.2	90.4	133.1	6	83.8	1954	F
		10% Penetration Rate Case	56.1	46.6	77.4	6.7	86.1	2227	E
		Difference	-27.1	-43.8	-55.7	0.7	2.3	273	----
		Difference (%)	-32.6%	-48.5%	-41.8%	11.7%	2.7%	14.0%	----
	WB	Base Case	41.7	34.2	58.9	6.8	80.6	1646	D
		10% Penetration Rate Case	44.8	37.1	62.3	6.5	81.6	1545	D
		Difference	3.1	2.9	3.4	-0.3	1	-101	----
		Difference (%)	7.4%	8.5%	5.8%	-4.4%	1.2%	-6.1%	----
	Both Direction of Minor Streets	Base Case	64.2	64.7	99.2	6.4	82.3	3600	E
		10% Penetration Rate Case	51.5	42.7	71.2	6.6	84.3	3772	D
		Difference	-12.7	-22	-28	0.2	2	172	----
		Difference (%)	-19.8%	-34.0%	-28.2%	3.1%	2.4%	4.8%	----

Note: *LOS is determined according to Highway Capacity Manual 2010 [78].

To further investigate the effects of penetration rate of connected vehicles for ALTPOM, the adjusted splits and optimized offsets are analyzed. Table 4.5 shows adjusted splits for 10%, low and high penetration rate cases. In the table, the fifth column's value is the same for all three cases. The reason is that, as mentioned before, the initial splits are optimized by TRANSYT-7F. These splits are used as the input for ALTPOM. From this table, it can be seen that splits are adjusted for each projection horizon to adapt traffic variations for all three cases. It is also found that less green times are assigned to minor streets in 10% penetration rate case than in the other two cases. For example, phases 4 and 8 of intersections 2 and 3. This situation also explains the results of Tables 4.3 and 4.4 where the 10% penetration rate case has worse performance for minor streets and better performances for major streets than that of the low penetration rate case. In addition, it can be seen that splits of low and high penetration rate cases are closer than that of 10% penetration rates. It is also indicates that low and high penetration rates have closer real-time traffic demand predictions for each phase.

Table 4.5 Adjusted Splits for 10%, Low and High Penetration Rate Cases

	Phase Number	Turning Movements	Simulation Case	Initial*	Time Interval 1	Time Interval 2	Time Interval 3	Time Interval 4	Time Interval 5
Intersection 1	Phase 1	NB-L	10% Penetration Rate Case	21	24	33	40	22	24
			Low Penetration Rate Case	21	13	26	38	34	31
			High Penetration Rate Case	21	18	33	32	28	36
	Phase 2**	SB-TR	10% Penetration Rate Case	51	50	51	43	58	56
			Low Penetration Rate Case	51	31	59	49	51	54
			High Penetration Rate Case	51	32	51	54	55	50

Table 4.5 (continued)

	Phase Number	Turning Movements	Simulation Case	Initial*	Time Interval 1	Time Interval 2	Time Interval 3	Time Interval 4	Time Interval 5
Intersection 1	Phase 5	SB-L	10% Penetration Rate Case	21	24	33	40	22	24
			Low Penetration Rate Case	21	13	26	38	34	31
			High Penetration Rate Case	21	18	33	32	28	36
	Phase 6	NB-TR	10% Penetration Rate Case	51	50	51	43	58	56
			Low Penetration Rate Case	51	31	59	49	51	54
			High Penetration Rate Case	51	32	51	54	55	50
	Phase 8	EB-LTR & WB-LTR	10% Penetration Rate Case	26	24	14	15	18	18
			Low Penetration Rate Case	26	54	13	11	13	13
			High Penetration Rate Case	26	48	14	12	15	12
Intersection 2	Phase 1	NB-L	10% Penetration Rate Case	7	14	10	18	13	10
			Low Penetration Rate Case	7	12	8	16	8	10
			High Penetration Rate Case	7	10	8	11	12	14
	Phase 2**	SB-TR	10% Penetration Rate Case	31	32	25	24	26	30
			Low Penetration Rate Case	31	35	25	25	34	27
			High Penetration Rate Case	31	36	27	26	24	22
	Phase 3	WB-L	10% Penetration Rate Case	42	21	36	30	28	17
			Low Penetration Rate Case	42	24	30	26	20	27
			High Penetration Rate Case	42	22	27	26	26	27
	Phase 4	EB-TR	10% Penetration Rate Case	18	31	27	26	31	41
			Low Penetration Rate Case	18	27	35	31	36	34
			High Penetration Rate Case	18	30	36	35	36	35
	Phase 5	SB-L	10% Penetration Rate Case	7	14	10	18	13	10
			Low Penetration Rate Case	7	12	8	16	8	10
			High Penetration Rate Case	7	10	8	11	12	14

Table 4.5 (continued)

	Phase Number	Turning Movements	Simulation Case	Initial*	Time Interval 1	Time Interval 2	Time Interval 3	Time Interval 4	Time Interval 5
Intersection 2	Phase 6	NB-TR	10% Penetration Rate Case	31	32	25	24	26	30
			Low Penetration Rate Case	31	35	25	25	34	27
			High Penetration Rate Case	31	36	27	26	24	22
	Phase 7	EB-L	10% Penetration Rate Case	42	21	36	30	28	17
			Low Penetration Rate Case	42	24	30	26	20	27
			High Penetration Rate Case	42	22	27	26	26	27
	Phase 8	WB-TR	10% Penetration Rate Case	18	31	27	26	31	41
			Low Penetration Rate Case	18	27	35	31	36	34
			High Penetration Rate Case	18	30	36	35	36	35
Intersection 3	Phase 1	NB-L	10% Penetration Rate Case	10	20	13	14	14	14
			Low Penetration Rate Case	10	15	19	21	14	19
			High Penetration Rate Case	10	14	12	14	20	19
	Phase 2**	SB-TR	10% Penetration Rate Case	27	29	26	31	26	30
			Low Penetration Rate Case	27	34	26	26	30	26
			High Penetration Rate Case	27	34	33	31	26	27
	Phase 3	WB-L	10% Penetration Rate Case	21	20	37	26	35	26
			Low Penetration Rate Case	21	21	26	24	24	26
			High Penetration Rate Case	21	20	23	25	23	24
	Phase 4	EB-TR	10% Penetration Rate Case	40	29	22	27	23	28
			Low Penetration Rate Case	40	28	27	27	30	27
			High Penetration Rate Case	40	30	30	28	29	28
	Phase 5	SB-L	10% Penetration Rate Case	10	20	13	14	14	14
			Low Penetration Rate Case	10	15	19	21	14	19
			High Penetration Rate Case	10	14	12	14	20	19

Table 4.5 (continued)

	Phase Number	Turning Movements	Simulation Case	Initial*	Time Interval 1	Time Interval 2	Time Interval 3	Time Interval 4	Time Interval 5
Intersection 3	Phase 6	NB-TR	10% Penetration Rate Case	27	29	26	31	26	30
			Low Penetration Rate Case	27	34	26	26	30	26
			High Penetration Rate Case	27	34	33	31	26	27
	Phase 7	EB-L	10% Penetration Rate Case	21	20	37	26	35	26
			Low Penetration Rate Case	21	21	26	24	24	26
			High Penetration Rate Case	21	20	23	25	23	24
	Phase 8	WB-TR	10% Penetration Rate Case	40	29	22	27	23	28
			Low Penetration Rate Case	40	28	27	27	30	27
			High Penetration Rate Case	40	30	30	28	29	28
Intersection 4	Phase 2**	SB-LTR & NB-LTR	10% Penetration Rate Case	34	66	48	62	59	58
			Low Penetration Rate Case	34	39	61	51	53	53
			High Penetration Rate Case	34	38	58	63	54	54
	Phase 4	EB-LTR & WB-LTR	10% Penetration Rate Case	64	32	50	36	39	40
			Low Penetration Rate Case	64	59	37	47	45	45
			High Penetration Rate Case	64	60	40	35	44	44
Intersection 5	Phase 1	SB-L & NB-L	10% Penetration Rate Case	25	23	30	31	31	26
			Low Penetration Rate Case	25	24	27	23	31	27
			High Penetration Rate Case	25	26	26	26	32	31
	Phase 2**	SB-TR & NB-TR	10% Penetration Rate Case	41	45	52	51	51	54
			Low Penetration Rate Case	41	41	55	56	49	55
			High Penetration Rate Case	41	40	55	55	48	50
	Phase 4	WB-LTR	10% Penetration Rate Case	32	30	16	16	16	18
			Low Penetration Rate Case	32	33	16	19	18	16
			High Penetration Rate Case	32	32	17	17	18	17

*Initial data is optimized splits by TRANSYT-7F; **Phase 2 is the coordinated phase.

Figures 4.8 and 4.9 show adjusted splits of major streets for 10%, low, and high penetration rate cases. It can be seen that differences between splits of low and high penetration rate cases are small. The splits for 10% penetration rate case are obviously differed with that of low and high penetration rates case. We also found that splits of all three cases for through and right movements of major streets are closer than that of left turn of major streets. The reason is that through and right turns of major streets have higher volumes than that of left turn, and there is more collected vehicle trajectory data provided for splits adjustment. In this condition, 10% penetration rate of connected vehicle can well predict traffic conditions. The trends of adjusted splits of high penetration rate case are smoother than that of 10% and low penetration rate cases. It seems that when the penetration rate of connected vehicle reaches 50%, there is enough connected vehicle data for each projection horizon to measure/estimate traffic conditions.

(a)

(b)

(c)

(d)

Figure 4.8 Adjusted Splits of Major Streets Left Turn

(a)

(b)

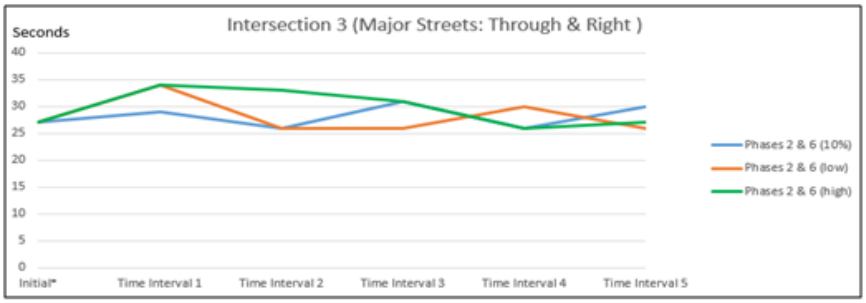

(c)

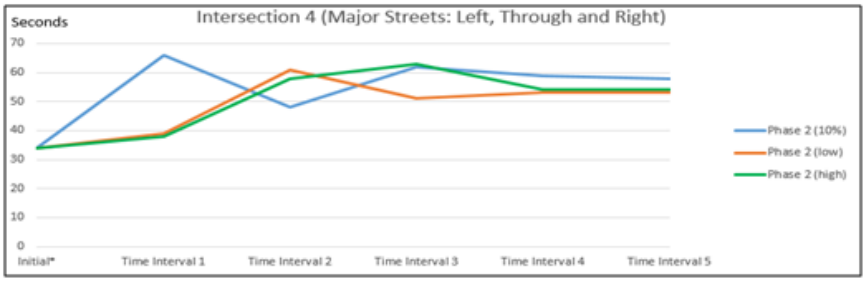

(d)

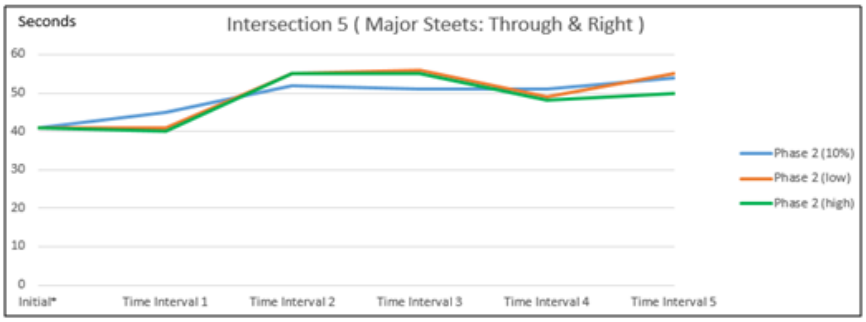

(e)

Figure 4.9 Adjusted Splits of Major Streets (Through and Right Turn)

Figures 4.10 and 4.11 show adjusted splits of minor streets for all three cases. It is the same as that of major streets that adjusted splits of low and high penetration rate cases are closer than that of 10% cases. For all three cases, their splits for through and right turn are closer than that of left turn. When comparing Figure 4.9 and Figure 4.11 for all three cases, splits of through and right turn in major streets are closer than that of minor streets, since major streets carry higher traffic volumes. It can then be concluded that penetration rates of connected vehicle has an obvious impact on splits adjustment of ALTPOM.

(a)

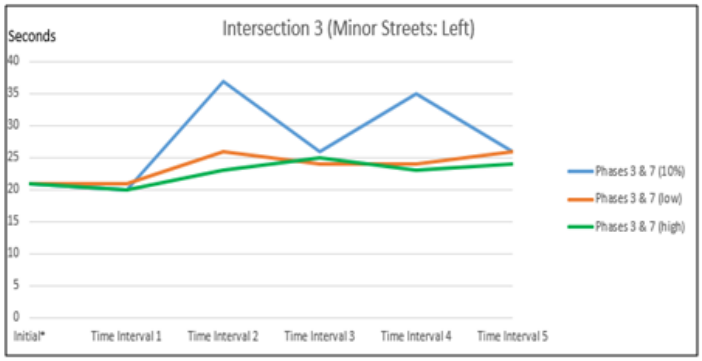

(b)

Figure 4.10 Adjusted Splits of Minor Streets Left Turn Only

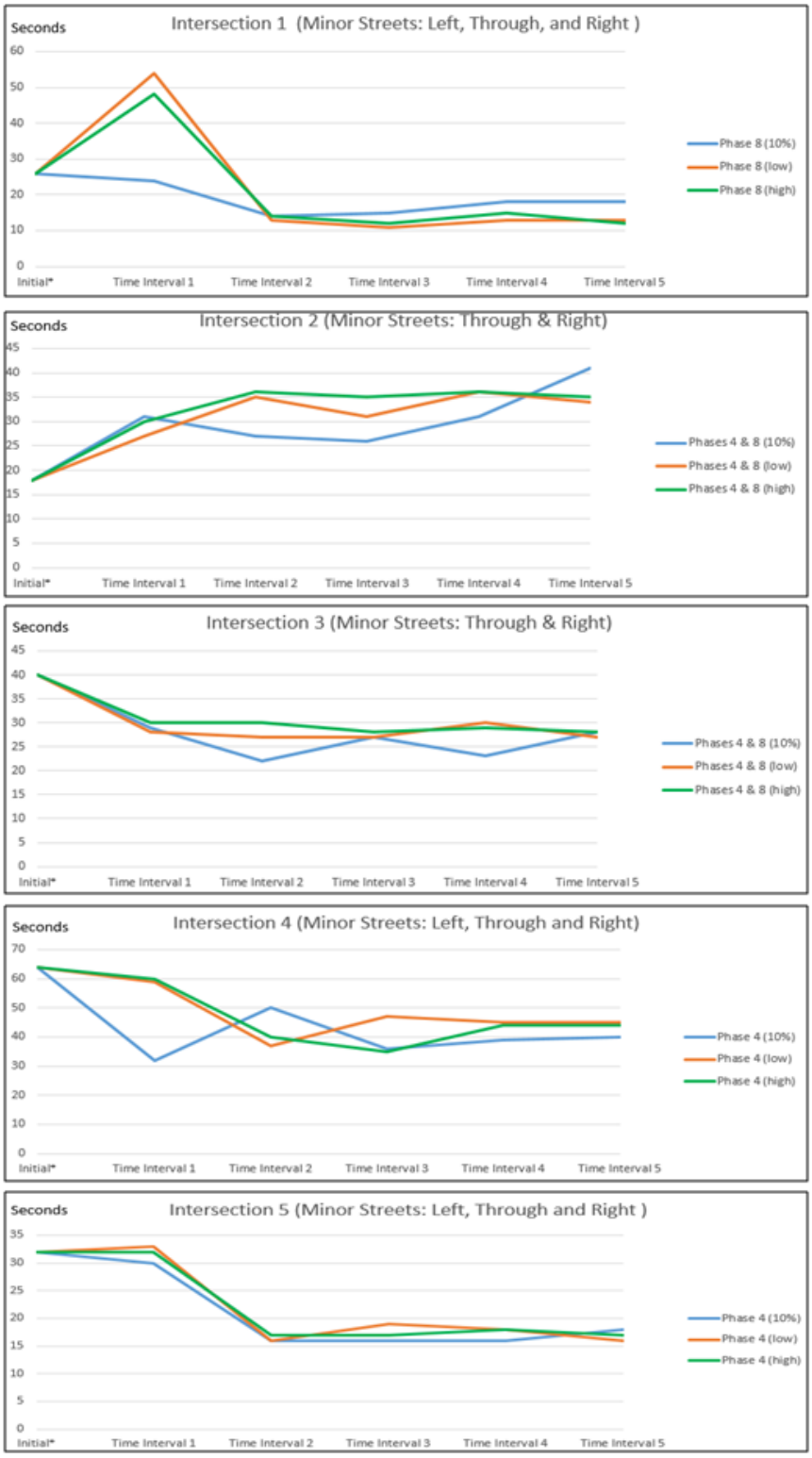

Figure 4.11 Adjusted Splits of Minor Streets Except Left Turn Only

Table 4.6 shows optimized offsets of ALTPOM for all three cases. The impacts of penetration rates of connected vehicles for offset optimization are not as clear as splits adjustment. All optimized offsets of the three cases are almost randomly distributed. According to standard deviation and the difference between minimum and maximum values, it can be seen that offsets in the first and last intersections are more widely distributed than the rest of intersections. Since ALTOPM was implemented five times during each simulation and the range of offset optimization during a projection horizon is [-5, +5] (based on the previous used offset), the maximum difference between minimum and maximum offsets is ±25. The contrast between minimum and maximum offsets for the 10% penetration rate case of intersection 1 and all three cases of intersection 5 is 19-20 (nearly 25). It indicates offsets of boundary intersections are less stable than that of the middle intersections of the study arterial. According to standard deviations, it can be found that the mean values of offsets for all three cases for an intersection are close. It points out that ALTPOM can effectively measure/predict traffic conditions when penetration rates are over 10%. For the final intersection, optimized offsets for low and high penetration rate cases are the same for all time intervals. In addition, for the final intersection the adjusted values in the last three intervals for all three simulation cases are the same.

Table 4.6 Optimized Offsets for 10%, Low and High Penetration Rate Cases

		Initial*	TI 1**	Difference between initial and TI1	TI 2	Difference between TIs 1 and 2	TI 3	Difference between TIs 2 and 3	TI 4	Difference between T TIs 3 and 4	TI 5	Difference between TIs 4 and 5	Mean	Standard Deviation	Minimum	Maximum	Difference between Min and Max
Intersection 1	10% Penetration Rate Case	42	37	-5	32	-5	27	-5	23	-4	28	5	32	7	23	42	19
	Low Penetration Rate Case	42	37	-5	38	1	35	-3	31	-4	34	3	36	4	31	42	11
	High Penetration Rate Case	42	37	-5	32	-5	32	0	34	2	29	-5	34	5	29	42	13
Intersection 2	10% Penetration Rate Case	26	31	5	27	-4	27	0	32	5	29	-3	29	2	26	32	6
	Low Penetration Rate Case	26	31	5	26	-5	31	5	34	3	29	-5	30	3	26	34	8
	High Penetration Rate Case	26	31	5	30	-1	25	-5	26	1	22	-4	27	3	22	31	9
Intersection 3	10% Penetration Rate Case	44	47	3	42	-5	41	-1	40	-1	39	-1	42	3	39	47	8
	Low Penetration Rate Case	44	39	-5	42	3	37	-5	39	2	34	-5	39	4	34	44	10
	High Penetration Rate Case	44	39	-5	44	5	44	0	39	-5	39	0	42	3	39	44	5
Intersection 4	10% Penetration Rate Case	72	67	-5	69	2	69	0	64	-5	64	0	68	3	64	72	8
	Low Penetration Rate Case	72	69	-3	64	-5	63	-1	58	-5	57	-1	64	6	57	72	15
	High Penetration Rate Case	72	67	-5	62	-5	63	1	64	1	60	-4	65	4	60	72	12
Intersection 5	10% Penetration Rate Case	43	47	4	47	0	52	5	57	5	62	5	51	7	43	62	19
	Low Penetration Rate Case	43	43	0	48	5	53	5	58	5	63	5	51	8	43	63	20
	High Penetration Rate Case	43	43	0	48	5	53	5	58	5	63	5	51	8	43	63	20

*Initial data is optimized splits by TRANSYT-7F.
**TI: Time Interval.

Figure 4.12 shows the optimized offsets for each time interval of each intersection. The optimized offsets for low and high penetration rates are closer than that of 10% penetration rate cases, especially for intersections 1, 4, and 5. When comparing Figures 4.8, 4.9, 4.10 and 4.11 with Figure 4.12, differences of optimized offsets among three cases are smaller than that of splits adjustment. The reason is that, as we mentioned above, the feasible offset optimization range of a projection horizon of ALTPOM is limited to [-5, +5] based on the utilized offset in the last projection horizon. Based on this procedure, the transition of an intersection due to offset changes could be completed immediately to alleviate impacts of signal timing transition. From the analysis above, we found that penetration rates of connected vehicle have more obvious impacts on split adjustment module of ALTPOM than that of offset optimization module.

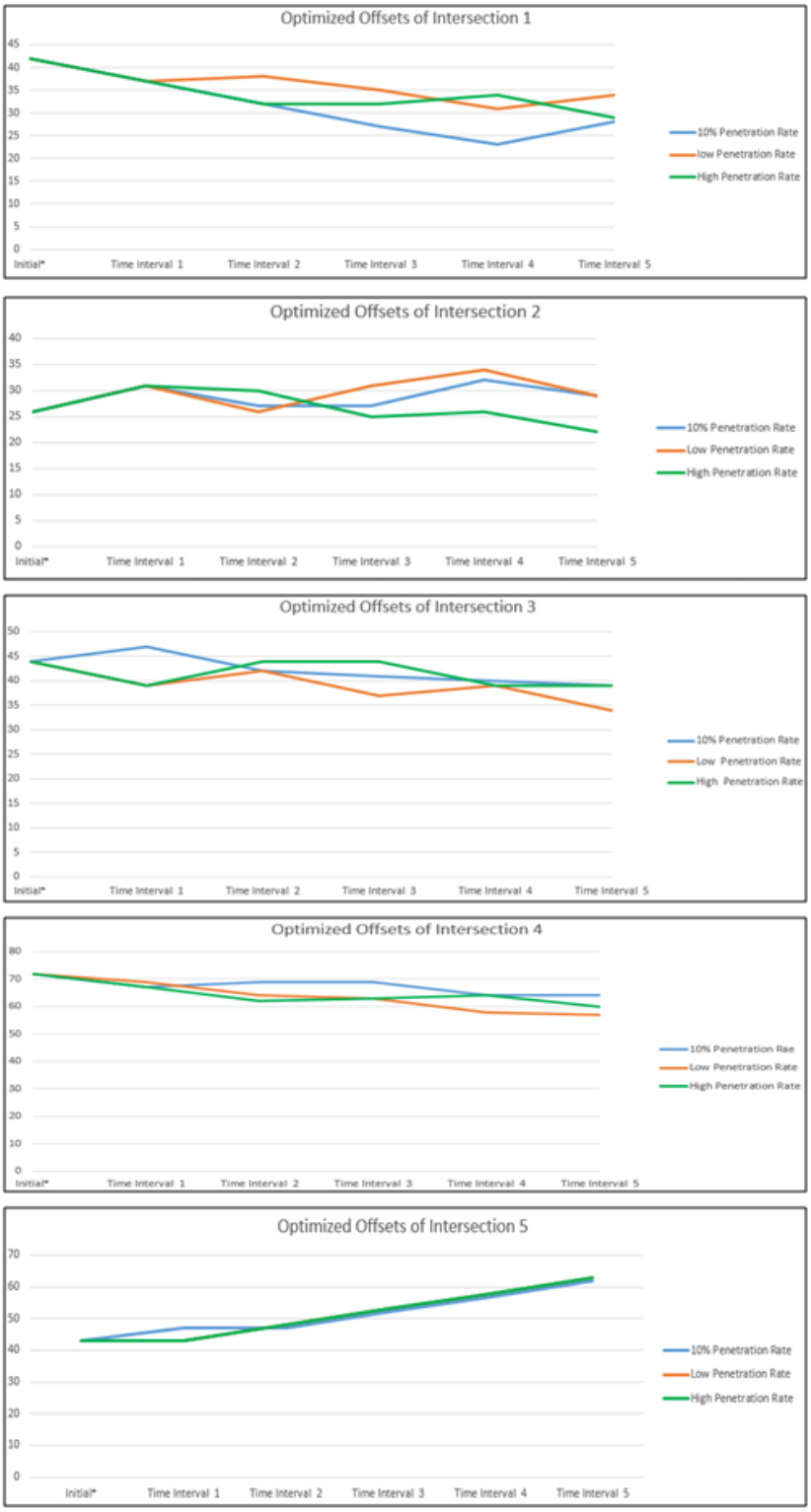

Figure 4.12 Optimized Offsets of All Intersections for Three Cases

4.2.4 Volume Sensitivity Study for the ALTPOM

To further analyze the effects of the proposed model under volume variations, volume sensitivity studies are conducted. Since the effects of different penetration rates of connected vehicle for ALTPOM are evaluated above, only the base case and low penetration rate case (25% penetration rate of connected vehicles) are performed for volume sensitivity studies. Two conditions are considered for the volume sensitivity studies. For the first condition, the entire arterial's volume is decreased by 20 %. There are two scenarios in this condition: base case with low volume, and low penetration rate with low volume. With respect to the second condition, volume of the entire arterial is increased 20%. The two scenarios in this condition are: base case with high volume, and low penetration rate with high volume.

Table 4.7 shows that under 20% volume reductions the proposed ALTPOM significantly reduces delays (control delay per vehicle and stop delay per vehicle), decreases travel time, and increases LOS for one level. When comparing Table 4.1 with Table 4.7, the benefits of the proposed model in Table 4.7 are not as good as that of the low penetration rate case in Table 4.1 when volume reduced 20%. For both directions of major streets, the benefits of implementing ALTPOM reduced 15.1% and 1.5% for control delay per vehicle and stopped vehicle percent in Table 4.7 than that of Table 4.1, respectively. The reason is that the entire network's delay is significantly lower when volume becomes lighter. As shown in Table 4.7, the LOS's of the base case with low volume and low penetration rate with low volume case are C and B, which indicates mobility of the study network is quite good. The proposed ALTPOM provides smooth

traffic progression for the coordinated direction without raising serious impacts on the opposite direction.

Table 4.7 Results of 80 % Volume for Base and Low Penetration Rate Cases

			Control Delay Per Vehicle	Stop Delay Per Vehicle	Travel Time Per Vehicle	Average Speed	Stopped Vehicles Percent	Volume	LOS*
Unit			Seconds/Vehicle			MPH	%	VPH	---
Entire Arterial	Coordinated Direction	Base Case with Low Volume	32.3	28.3	70.1	15.6	44.7	3573	C
		Low Penetration Rate with Low Volume	20	16.3	55	16.9	40	3473	B
		Difference	-12.3	-12	-15.1	1.3	-4.7	-100	---
		Difference (%)	-38.1%	-42.4%	-21.5%	8.3%	-10.5%	-2.8%	---
	Opposite Direction	Base Case with Low Volume	29	24.3	59	14	39.8	2803	C
		Low Penetration Rate with Low Volume	14.9	11.4	43.9	15.7	40.5	2785	B
		Difference	-14.1	-12.9	-15.1	1.7	0.7	-18	---
		Difference (%)	-48.6%	-53.1%	-25.6%	12.1%	1.8%	-0.6%	---
	Both Direction of Major Streets	Base Case with Low Volume	30.8	26.5	65.2	14.9	42.5	6376	C
		Low Penetration Rate with Low Volume	17.7	14.1	50.1	16.4	40.2	6258	B
		Difference	-13.1	-12.4	-15.1	1.5	-2.3	-118	---
		Difference (%)	-42.5%	-46.8%	-23.2%	10.1%	-5.4%	-1.9%	---

Note: *LOS is determined according to Highway Capacity Manual 2010 [78].

Table 4.8 provides the results for the base case and low penetration rate case when traffic volume increases 20%. It can be seen that congestion becomes more serious when volume increases 20%. However, ALTPOM remarkably decreases delays in all directions (coordinated direction, the opposite direction and both directions of major streets) of the study arterial when compared to the base case with high volume. When

Table 4.1 and Table 4.8 are compared, it was found that the proposed ALTPOM has better performance when congestion of the study arterial becomes more severe. ALTPOM increases throughputs at least 13.0% in all directions of the entire arterial as compared to that of base case with high volume. That is extraordinary!

Table 4.8 Results of 120 % Volume for Base and Low Penetration Rate Cases

			Control Delay Per Vehicle	Stop Delay Per Vehicle	Travel Time Per Vehicle	Speed Average	Stopped Vehicles Percent	Volume	LOS*
Unit			Seconds/Vehicle			MPH	%	VPH	----
Entire Arterial	Coordinated Direction	Base Case with High Volume	91.7	87.6	143.2	8.9	63	4231	F
		Low Penetration Rate with High Volume	40	34.9	80.5	13.1	53.8	5213	D
		Difference	-51.7	-52.7	-62.7	4.2	-9.2	982	----
		Difference (%)	-56.4%	-60.2%	-43.8%	47.2%	-14.6%	23.2%	----
	Opposite Direction	Base Case with High Volume	112	102	155.6	8.1	52.1	3582	F
		Low Penetration Rate with High Volume	49.1	39.1	82.7	11.8	47	4047	D
		Difference	-62.9	-62.9	-72.9	3.7	-5.1	465	----
		Difference (%)	-56.2%	-61.7%	-46.9%	45.7%	-9.8%	13.0%	----
	Both Direction of Major Streets	Base Case with High Volume	101	94.2	148.9	8.5	58	7813	F
		Low Penetration Rate with High Volume	44	36.7	81.5	12.5	50.8	9260	D
		Difference	-57	-57.5	-67.4	4	-7.2	1447	----
		Difference (%)	-56.4%	-61.0%	-45.3%	47.1%	-12.4%	18.5%	----

Note: *LOS is determined according to Highway Capacity Manual 2010 [78].

Figure 4.13 displays the changes of control delay per vehicle and LOS of the study arterial under 80%, 100%, 120% volume variations. ALTPOM decreases control delay per vehicle and improves LOS of the coordinated direction, opposite direction, and

both directions when volume rises. This improvement is more significant when congestion of the study arterial becomes high. With respect to LOS, ALTPOM improves one level under low and normal volumes, but it is found that the proposed model enhances two levels of LOS under high volume. The differences of control delay per vehicle between base case and low penetration rate cases are increased parallel to traffic volume increase. This indicates that the proposed model is effective under varying traffic demands. This feature is crucial since traffic volume in the field is always fluctuating. A new traffic signal control model with this feature is expected to have a better performance than existing models (such as TRASNYT-7F) under any traffic conditions.

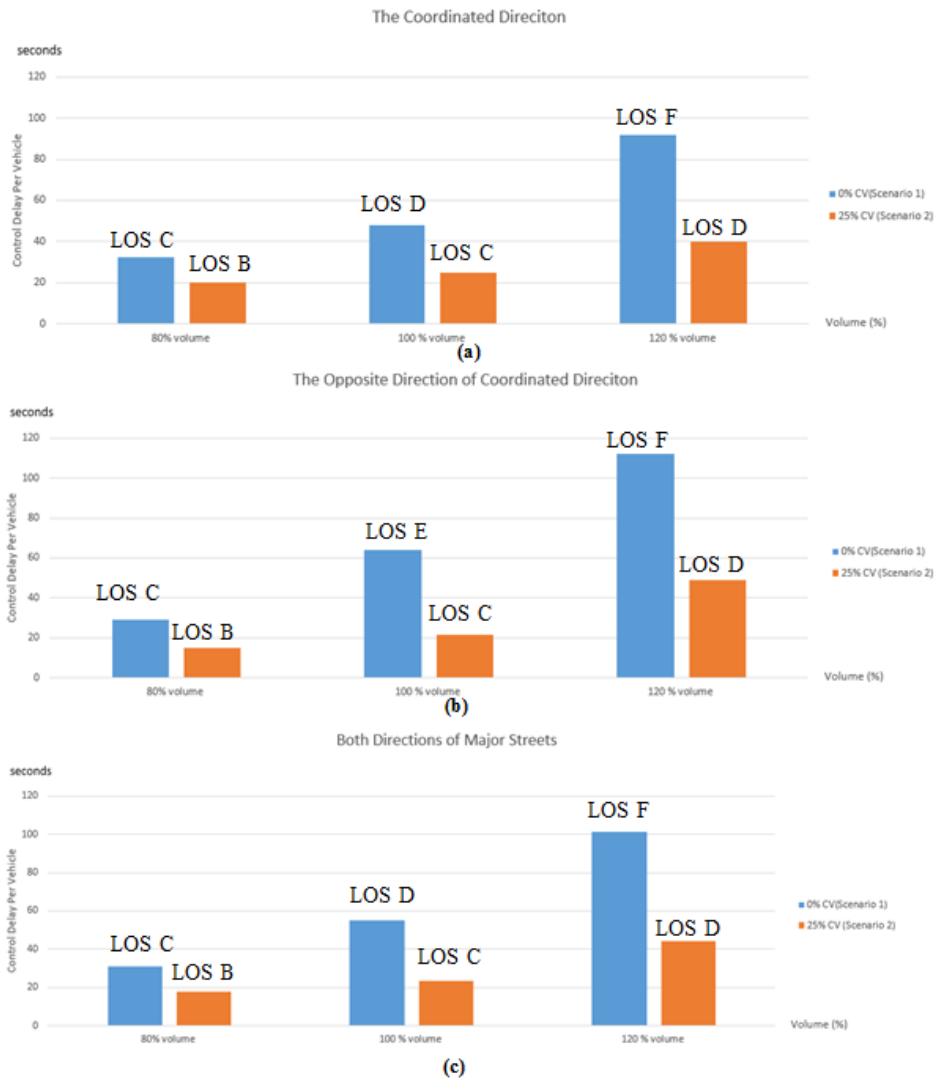

Figure 4.13 Control Delay per Vehicle and LOS of the Study Arterial under Volume Variations

Figure 4.14 shows changes of stopped vehicle percent of the study arterial under traffic volume variations. Figure 4.14 also proves that the proposed ALTPOM provides smooth traffic progression for the coordinated direction with little impact on performance of the opposite directions. With respect to both directions on major streets, the proposed model decreases stopped vehicle percent as compared with the base case. From Figure

4.13 and Figure 4.14, it is found that stopped vehicle percent is less sensitive to volume variations than control delay per vehicle.

Figure 4.14 Stopped Vehicle Percent of the Study Arterial under Volume Variations

Thus, according to the analysis above, it is concluded that the ALTPOM can significantly reduce delays and increase mobility of the study arterial. For both directions of major streets, ALTPOM can reduce 42.5%--61.5% of control delay per vehicle when

compared with that of the signal timing plan generated by TRANSYT-7F. In essence, ALTPOM belongs to adaptive traffic control system (ATCS), since ALTPOM adjusts signal control parameters according to upcoming traffic fluctuations. As indicated by a NCHRP report, an ATCS is hard to outperform in a well maintained traditional traffic signal control system over 10%-15% with respect to any one of all performance measures [79]. Based on the results of ALTPOM, we found that the benefits of ATCS significantly further improve based on connected vehicle technologies, compared to the conventional optimized traffic signal control. The reason is that predicted/measured real-time traffic data is more accurate based on connected vehicle technologies, which are crucial to an ATCS.

With respect to throughput, the effects of the proposed model are increased in relation to the increase of volume. The presented model offers traffic progression for the coordinated direction with little impact on the opposite direction. For the effects of penetration rates of connected vehicle, ALTPOM provides better performance as well as an increase in the penetration rate of connected vehicle. More importantly, ALTPOM is effective under traffic volume variations and performs even better when the study arterial is more congested.

CHAPTER V

ACTIVE TRAFFIC MANAGEMENT STRATEGIES FOR OVERSATURATED SIGNALIZED INTERSECTIONS[1]

Signal Phase and Timing (SPaT) is a critical component of V2I applications. SPaT interface works with legacy traffic signal control systems by adding a "black box" computer between a signal controller and other connected vehicle components such as Dedicated Short Range Communications (DSRC) Road Side Unit (RSU). When the Basic Safety Message (BSM) defined in J2735 [80] passes to the SPaT computer, there are countless applications that can be developed to improve the safety and mobility at signalized intersections. With the advent of connected vehicles, adding a low cost SPaT "black box" computer inside controller cabinets, State DOTs and cities will not have to upgrade their existing traffic signal controllers (even legacy NEMA controllers) as long as they are NTCIP compatible.

The objective of this chapter is to demonstrate the practicalities of using SPaT applications to improve mobility. The first effort under this endeavor is to explore a SPaT application to address rural and suburban saturated and/or oversaturated intersections. The short term demand surge or capacity reduction (primarily on major approaches)

[1] The major contents of this chapter are already published at ITS World Congress 2015 at Bordeaux, France (Zhitong Huang, Li Zhang, Deborah M. Curtis, Govindarajan Vadakpat, and Jia Hu, "SPaT and active traffic management strategies for oversaturated signalized intersection", ITS World Congress 2015, October 2015, Bordeaux, France).

causes the saturated or oversaturated traffic conditions and results in the intersection's failure. The ripple effect may cause queue spillback and gridlock at the corridor-level and potentially even a system-wide failure.

Given the information collected and the objectives, two queue length management based Active Traffic Management (ATM) strategies are proposed. Specifically, the second major module of the connected vehicle based traffic signal control model (CVTSCM), which could have the potential to seamlessly utilize BSM information. ATM is defined as "the ability to dynamically manage recurrent and non-recurrent congestion based on prevailing and predicted traffic conditions" [8]. The ATM strategies being proposed are analytically investigated first and then validated through field vehicle trajectory data.

The research of this chapter is unique, since it can be directly implemented to work with BSM on the SPaT hardware. All past studies reviewed in chapter 2 related to connected vehicles assumed that exact information fed into their algorithms and models directly. All algorithms reviewed are validated and developed using traffic simulation. This chapter takes one step further by applying the actual vehicle trajectory data collected from US DOT's Next Generation of SIMulation (NGSIM) program [10]. Currently there is a lack of available connected vehicle field data with enough penetration rates for the author to test and validate the proposed strategies.

5.1 Active Traffic Management Strategies

In this section, ATM strategies for oversaturated signalized intersection are proposed. In the actuated controller logic, after a phase services a minimum green, the green time will be extended with each upcoming vehicle's actuation. The green time

interval of the phase will be either gap out, max out or force off (coordination only). In the ideal scenario, it first clears resident queues accumulated during red time interval and any incoming vehicles during green time to clear the queue. The green time will be further extended if vehicles continue to come within gap out time before it maxes out. After that, the actuated controller would terminate that phase and assign green to the next phase.

Although the green extensions after queue dissipation grant vehicles right-of-way to traverse an intersection without stopping for vehicles at one approach, the benefit should be balanced against vehicle delays in the conflicting phases. Newell [71] indicated that the minimum intersection delay was achieved on the condition that a phase was switched when its queue is cleared. Newell's conclusion is based on an assumption that the intersection and the traffic flow are symmetric and arrival is stationary. However, for most intersections the major streets and minor streets usually carry different traffic volume and/or feature different capacities, which is opposes Newell's assumption. More importantly, traffic is stochastic and the direction of peak volumes is exhibited at diverse approaches during different times of the day. As a SPaT application, when the vehicle trajectory becomes known unparalleled advantages are gained to form ATM strategies, which will then address intersections operating at close to saturated or oversaturated traffic.

In this dissertation, analytic solutions are formed to illustrate the proposed strategies first. A one way two-approach intersection was used initially as a proof-of-concept. Without losing the generality, different v/s ratios (volume to saturation flow rate ratios) were assumed on different approaches. Furthermore, the v/s ratio differences

assumed on approaches are significant and the imbalanced v/s ratios provide room to better management queues even in the saturated or oversaturated intersections, as will be demonstrated. The imbalanced v/s ratios are widely observed at most major arterials intersected with minor streets. Even on the major approaches on arterials, the directional traffic volumes during peak hours are imbalanced. The presented ATM strategies should have wide applications.

In this chapter, the discharge rate of a lane group or an approach is defined as the summation of saturation flow rate across all lanes in that lane group or approach. For this dissertation, the effective green time and the effective red time are used to develop an analytical solution of proposed ATM strategies. The assumptions below are necessary for the analytic solutions, though some are not needed for numerical solutions when the vehicle trajectory becomes known. These assumptions are listed as:

- The actuated controller timing plan is up-to-date and configured efficiently.
- Imbalanced v/s ratios. While the entire intersection is at v/c>1 (volume to capacity ratio), the queue of major streets cannot be cleared even when the maximum green time of corresponding phases has been reached. For minor streets, the queues could be completely dissipated during green.
- Saturation flow rate of each lane is the same for both major and minor streets.
- There are more lanes on major streets than minor streets.

- Uniform arrivals and uniform departure are assumed (i.e. D/D/1 queue) since traffic conditions of an intersection are usually not significantly changed for a short time period, e.g. 5 minutes.

5.1.1 Minimizing Delay

Figure 5.1 shows queue accumulations on two approaches of an oversaturated intersection with assumed characteristics. Phase 1 is on minor streets and Phase 2 is on major streets. The average arrival and departure rates of a short term time period are represented by λ and ρ. Since this is the oversaturated intersection with actuated control, it will focus on finding the time to terminate Phase 1 in $C - t'$ where t' is the effective green time in Phase 2 and C is cycle length. Strategies that minimize delay are of most interest. The delays for minor and major streets are the areas under the queue length curves.

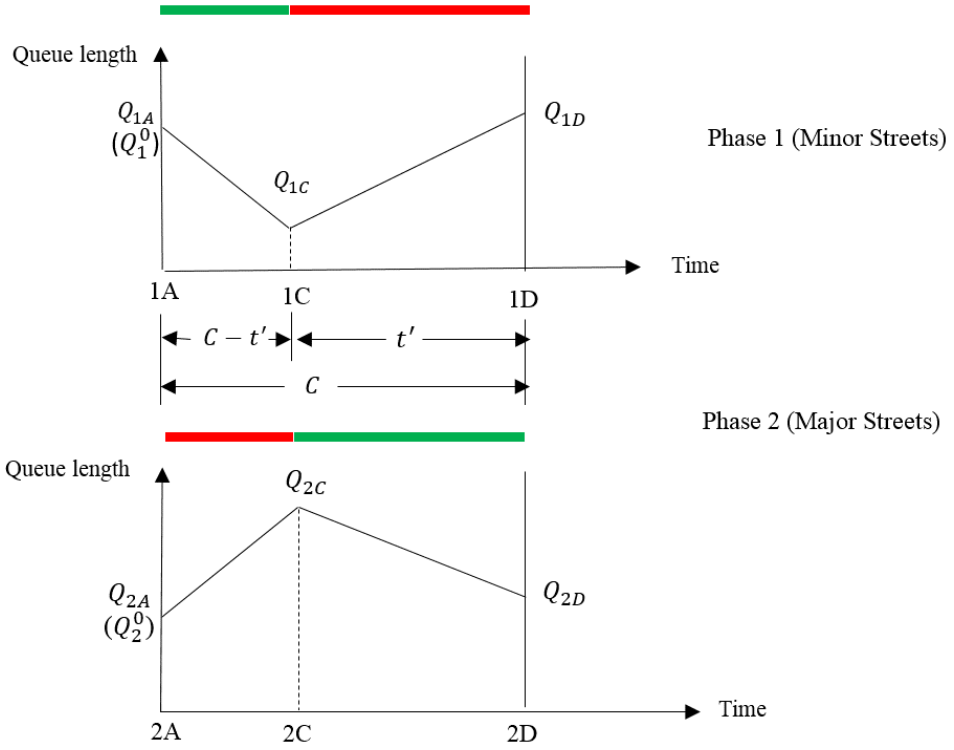

Figure 5.1 Delay and Queue Length Diagram of One Cycle

From Figure 5.1, the following equations show the total stop delays of the entire intersection:

$$D_{total} = D_1 + D_2 = \frac{1}{2}(\rho_1(t')^2 + 2Q_1^0 C + \lambda_1 C^2 - \rho_1 C^2) + \frac{1}{2}(-\rho_2(t')^2 + 2Q_2^0 C + \lambda_2 C^2) \quad (5.1)$$

$$0 \le C - t' \le G_{max,1} \le C \quad (5.2)$$

$$0 \le t' \le G_{max,2} \le C \quad (5.3)$$

Where,

Q_1^0, Q_2^0: Initial queue length of phases 1 and 2 (vehicles),

$Q_{1A}, Q_{1C}, Q_{1D}, Q_{2A}, Q_{2C}, Q_{2D}$: Queue length of phases 1 and 2 at time stamps A, C, D (vehicles),

D_1, D_2: Stop delays of phases 1 and 2 (seconds),

λ_1, λ_2: Arrival rate of phases 1 and 2 for a short term period (vehicle/seconds),

ρ_1, ρ_2: Saturation discharge rate of phases 1 and 2 (vehicle/seconds),

C: Cycle length (seconds),

t': The optimal effective green time for major streets (seconds).

D_{total}: Total stop delays of an entire intersection (seconds),

$G_{max,1}, G_{max,2}$: Maximum effective green times of phases 1 and 2 (seconds).

To obtain the extreme values and identify these values as maximum or minimum values, D_{total} is differentiated with respect to t' for the 1st and 2nd order of differentials. These equations are listed below.

$$\frac{dD_{total}}{dt'} = t'(\rho_1 - \rho_2) \tag{5.4}$$

$$\frac{d^2D_{total}}{d(t')^2} = \rho_1 - \rho_2 \tag{5.5}$$

The total saturation discharge rate (ρ_2) on major streets is assumed to be larger than that of minor streets (ρ_1) since major streets usually have more lanes than minor streets. Therefore, the total saturation discharge rate on major streets is larger than that of minor streets, i.e. $\rho_1 < \rho_2$.

$$\frac{dD_{total}}{dt'} = t'(\rho_1 - \rho_2) \leq 0 \tag{5.6}$$

$$\frac{d^2D_{total}}{d(t')^2} = \rho_1 - \rho_2 < 0 \tag{5.7}$$

To get potential minimized values, equation (5.4) is assigned to 0. It is solved and obtained for $t' = 0$ which is the maximum value, since $\frac{d^2D_{total}}{d(t')^2} < 0$. Because $\frac{dD_{total}}{dt'} < 0$ when $t' \neq 0$, then D_{total} is a monotonically decreasing function for $t' \in (0, C]$. So, the

intersection would obtain minimum stop delays when all green time of a cycle is assigned to major streets, i.e. $t' = C$. However, in reality it is not feasible to assign all green time to major streets when minor streets could have demand.

From the above analysis, the first ATM strategy is formed to allocate as much green time as possible to the lane groups or approaches with a higher saturation discharge rate when an intersection is oversaturated. This would result in less overall delay at the entire intersection. On the other hand, when major traffic moves across a lane group with lower discharge capacity, it is not beneficial to assign additional green time to this lane group at the cost of increasing resident queue in competing phases which was also pointed out by Newell [71].

5.1.2 Queue Management

Another important factor to be considered is queue length on each approach for oversaturated intersections, even though it is ideal to allocate more green time to lane groups with a higher discharge rate. When significant queues are formed over time during oversaturated conditions, the queue will spillback to the upstream intersection and create serious gridlock. Queue spillback or gridlock will cause the traffic to come to a standstill and result in serious area/corridor wide congestion for an extended period of time.

The second strategy is that the green splits of a signal timing plan are adjusted to balance each phase's queue length at the end of *k*th cycle to an allowable queue length at both major and minor streets in order to prevent spillbacks. Figure 5.2 shows queue length changes after implementing the proposed queue management strategy. t^* is the actuated effective green time for minor streets. Queue could be completely cleared without excessive green time during t^*. This timing plan is referred to as the original

timing plan. t_1 is the effective green time of minor streets generated by the proposed queue management strategy. In Figure 5.2, the blue and black lines show the evolving queue procedures for original and queue management timing plans. The proposed queue management strategy is formulated in the following paragraphs.

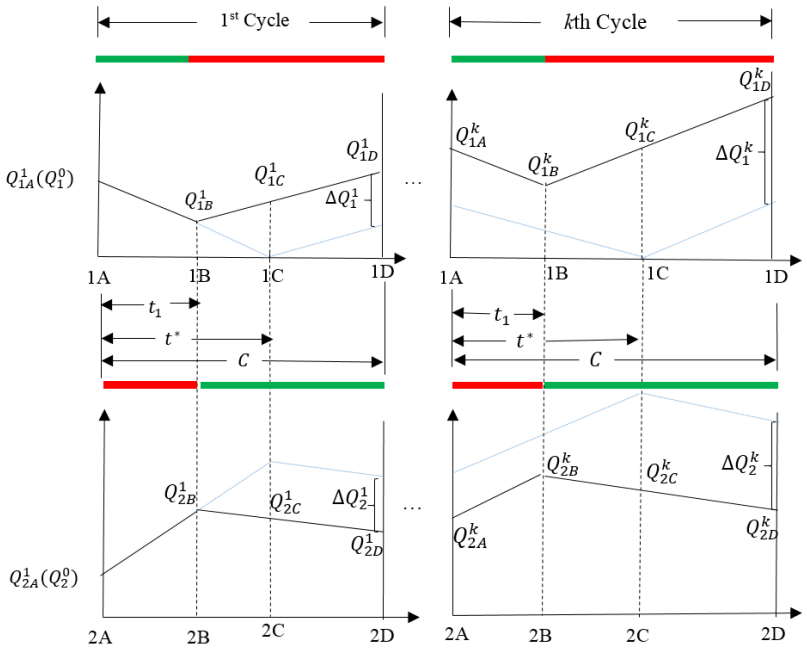

Figure 5.2 Queue Management Strategies for kth Cycle

The queue management strategy is derived for one cycle and gradually expands to k cycles. The effective green time for minor streets, t_1, prevents queue spillback or gridlock and can be computed as follows:

$$t^* = \frac{\lambda_1}{\rho_1} * C \tag{5.8}$$

$$Q_1^0 = (\rho_1 - \lambda_1) * t^* \tag{5.9}$$

$$\delta = \frac{N_m L_m}{N_s L_s} \tag{5.10}$$

$$t_1 = \frac{\delta\lambda_1(k+1)C - \delta\lambda_1 t^* - Q_2^0 - \lambda_2 kC + k\rho_2 C}{\delta k\rho_1 + k\rho_2} \tag{5.11}$$

$t_1 \in [0, C]$

Where,

k: The kth cycle,

δ: A weighted parameter, ratio of vehicles stored on major streets and minor streets allowed,

N_s, N_m : Number of lanes of side streets and major streets, respectively,

L_s, L_m: The predefined maximum allowable queue length for side streets and major streets, respectively (vehicles).

Based on equation (5.11), the effective green time can be calculated for minor streets when a signalized intersection is oversaturated due to demand surges and/or loss capacities for major streets. For the selection of k values, it depends on existing queue lengths of major streets and/or choice of transportation professionals. When selecting k, one important factor should be noted. Although we can get an accurate calculation of current queue length from SPaT system, the average queue arrivals and departures will be less accurately forecasted as the k value increases.

5.2 Field Data Validations

All of the strategies proposed are based on the average arrival rate of a short term period under the deterministic traffic. This section is focused on examining the strategies under real world stochastic arrivals while using the trajectory data from the field. The performance of the proposed strategies is then evaluated and validated in three scenarios. In the first scenario, the first strategy is validated. In the second scenario, the second strategy is applied in the de-queueing process. In this case, for the oversaturated

intersection significant queue length already has been formed at major streets. For the third scenario, the second strategy is applied in the queue formulation process. All of these strategies are examined under the intersection v/c ratio that is greater than 1 (oversaturated intersection) or around 1.0 (saturated intersection).

Although the proposed two ATM strategies are expected to develop as a SPaT application, connected vehicle technologies are still in rudimentary stages. Since there is a lack of connected vehicle field data, what is needed in our algorithms is primarily the vehicle trajectory data decoded from BSM messages which is extracted from RSU on a SPaT computer. The actual field vehicle trajectory is a good alternative to test the proposed strategies.

In this chapter, Microsoft Excel is used to simulate queue accumulation and dissipation procedures second by second. To simplify the calculations in Excel, stop delay is used instead of control delay as the performance measurement. Again, an assumed one-way two movement intersection was used to illustrate these strategies.

5.2.1 Brief Summary of NGSIM Data

Sample data sets of NGSIM vehicle trajectory data at Lankershim Blvd are pre-processed. There are two 15 minute trajectory data sets at Lankershim Blvd. The vehicle trajectory data of Campo De Cahuenga Wy/Universal Hollywood Dr at Lankershim Blvd intersection from 8:30 a.m. to 8:45 a.m. is utilized in this research [81]. The vehicle trajectory data of two lanes of the SB and one lane of NB of the selected intersection are extracted and referred to for the vehicle trajectory data of the major and minor streets of a hypothetical one-way two movement intersection.

Based on the investigation of major and minor streets, the traffic conditions of major streets are not congested enough in the original data. For two lanes of major streets, original inter-arrival time or arrival headway is scaled at factors of 0.5 and 0.3. Vehicles with arrival headway on major and minor streets equal to or larger than 20 seconds are discarded. After adjusting vehicle arrival headway, corresponding volumes of major streets are 1107 and 1382 vehicles/hour/lane (scale factor: 0.5) (1419 and 1668 vehicles/hour/lane for scale factor 0.3). With respect to minor streets, corresponding volume is 550 vehicles/hour/lane. Due to a relatively short time interval on data collected and the condensing of the data, only 300 seconds vehicle trajectory data is qualified and selected for this study.

As indicated by the report of Cambridge Systematics Inc, the vehicle trajectory data of the chosen segment of Lankershim Blvd was collected by digital video cameras installed on a 36 story building [81]. To obtain capacity per lane of the study site, the saturation headway per lane of North and South bounds are measured by the author by watching video streams of the intersection. The author selected one lane of NB and of SB to measure the data needed. Based on analysis, the saturation headway of SB and that of NB are 1.99 and 1.96 seconds/vehicle, or is 2.0 seconds/vehicle in this research which corresponds to saturation rate per lane of 1800 vehicles/hour.

5.2.2 Scenario 1: Green Time/Split for Minimizing Delay

In scenario 1, validating the first strategy is to distribute as much green time as possible to the lane group or approach with higher discharge rate at an oversaturated intersection. The vehicle headway from field trajectory data of major streets scaled by a factor of 0.3 and processed original vehicle trajectory data of minor streets are used for

this scenario. The corresponding arrival rate of major and minor streets are 0.858 and 0.153 vehicle/seconds. The departure rates of major and minor streets are 1 and 0.5 vehicle/seconds. The v/s ratios of major and minor streets are 0.858 and 0.306. The intersection critical v/c ratio is 1.164. The cycle length of the assumed intersection is chosen as 80 seconds. Based on equations (5.8) and (5.9), the initial queue length of minor streets at the beginning of green interval is 8 vehicles. A total of 30, 60 and 90 vehicles are assumed to accumulate on both lanes of major streets. An incremental interval of 2 seconds is applied to green time of minor streets from 0 to 80 seconds in order to generate intersection delay profiles.

Figure 5.3 shows delay profiles of different initial queue lengths at major streets. From Figure 5.3, it is found that with a notable initial queue length the intersection stop delay achieves the minimum values when effective green time of minor streets is zero or all effective green time is assigned to major streets. With the increase of effective green time on minor streets, the intersection stop delays also increase correspondingly. It reaches the maximum value when all effective green time is allocated to minor streets. Hence, the analytical conclusion we described in the last section is validated under the stochastic field arrival data.

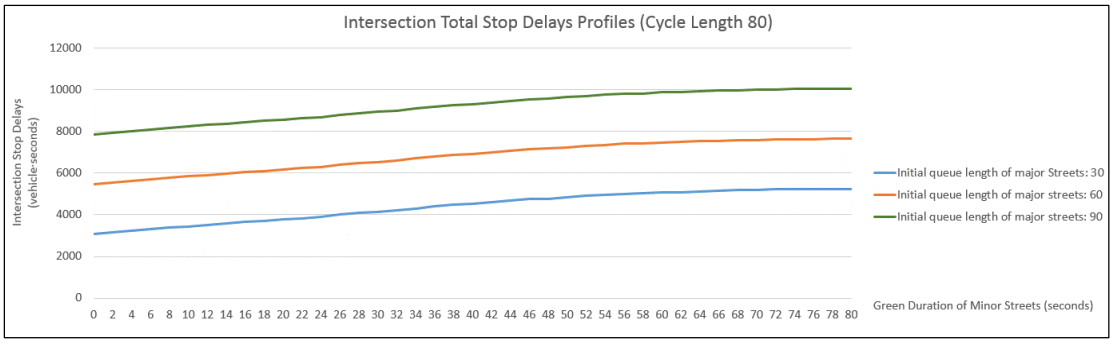

Figure 5.3 Delay Profiles of an Oversaturated Intersection (Cycle Length 80 seconds)

5.2.3 Scenario 2: Queue Management at Queue Dispersion Process

In this scenario, we evaluate the performance of the proposed second strategy for dissipating significant accumulated queue. Trajectory data and volume is explained in the Brief Summary of NGSIM Data subsection. With arrival headways scaled to 0.5 and 0.3, intersection v/c ratios are 0.997 and 1.164. A total of 90 vehicles are assumed to accumulate on both lanes of major streets left over from the previous cycle. The initial queue length of minor streets at the start of green is accumulated from red time interval calculated by equations (5.8) and (5.9). The allowable queue length per lane for both major and minor streets is assumed to be 50 vehicles. Cycle length of 80, 100, and 120 seconds are chosen to test the sensitivity of this strategy.

Table 5.1 shows the results of the queue dispersion processes. For Table 5.1, the 1st column indicates implemented scale factors for major street vehicle arrival headway and the 2nd column is cycle length. Since a total of 300 seconds of processed vehicle arrival data is implemented for scenario 2, there are 3, 3 and 2 complete cycles with cycle length at 80, 100 and 120 seconds.

Table 5.1 Results of Scenario 2: Queue Dispersion Process

1	2	3	4	5	6		7	
Arrival Headway Scale Factor at Major streets	Cycle Length		Effective Green time of Minor Streets (seconds)	Intersection Total Stop Delay per Minute (seconds)	Delay Reduction Per Minute		Final Queue Ratios	
					Total (seconds)	(%)	Major Streets	Minor Streets
0.5	80	Original Timing	24	5775.5	-------	------	0.82	0.26
		Queue Management Timing	12	5134.3	641.2	11.10	0.46	0.62
	100	Original Timing	31	6173.9	-------	------	0.94	0.23
		Queue Management Timing	19	5542.1	631.8	10.23	0.58	0.59
	120	Original Timing	37	6237.5	-------	------	0.84	0.34
		Queue Management Timing	21	5631.5	606	9.72	0.52	0.66
0.3	80	Original Timing	24	7184	-------	------	1.24	0.26
		Queue Management Timing	6	6201.9	982.1	13.67	0.70	0.80
	100	Original Timing	31	7778.5	-------	------	1.43	0.23
		Queue Management Timing	11	6701.5	1077	13.85	0.83	0.83
	120	Original Timing	37	7646	-------	------	1.26	0.34
		Queue Management Timing	11	6628.8	1017.2	13.30	0.74	0.86

It is assumed that the actuated controller at the hypothetical intersection is properly set and the minor street is gapped out when the queue on minor streets is dissipated. The green time in major streets uses the time left in a cycle and it refers to the original timing plan which is considered as the benchmark. For the second case, the queue management strategies are implemented. Equation (5.11) computes green times for

minor streets with the average arrival rates of major and minor streets. In column 4, it shows effective green time of minor streets for cases 1 and 2 calculated by equation (5.8) and (5.11). Columns 5 and 6 provide intersection total stop delay per minutes and corresponding delay reduction. For the final column, we present the ratio of queue length at the end of the computing period (300 seconds for cycle length 100 and 240 seconds for cycle lengths 80 and 120) to assume allowable queue length per lane.

Table 5.1 indicates the queue length is controlled to the desirable length under the proposed strategies, while in the actuated control (original timing plan) the queue length exceeds the assumed allowable queue length. By implementing the proposed queue management strategies, the intersection total stop delays significantly reduce within the range from 9.72% to 13.85%. In column 5 of Table 5.1, it is shown that utilizing the short cycle length produces less intersection total stop delays per minute under the saturated conditions.

From Figure 5.4, we can see that the major streets with original timing plan exceed the targeted allowable queue length frequently when the queue length ratios are plotted at different approaches vs. the seconds in the cycle. The situation is more serious when an intersection becomes more congested. However, by performing the proposed queue management strategies the queue length of major streets is controlled and no queue spillback occurs.

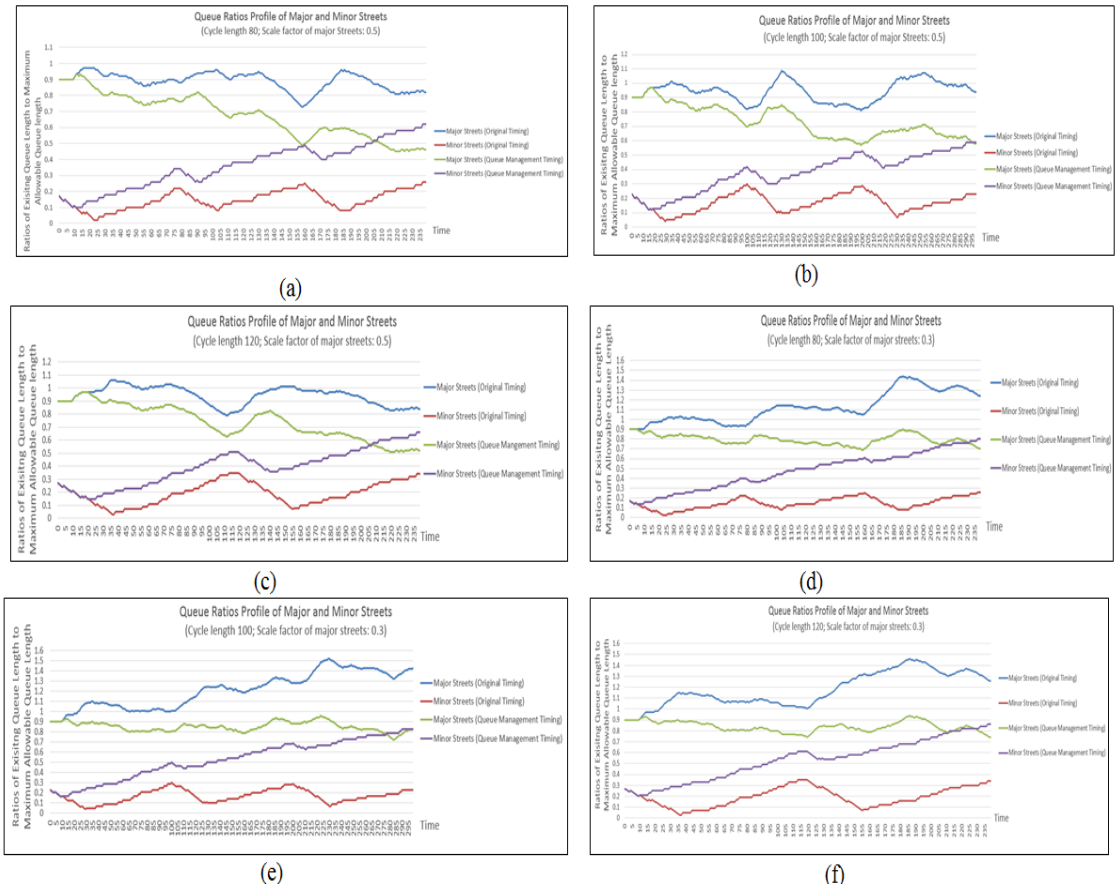

Figure 5.4 Effects of Queue Management Strategies for Queue Dispersion Process

5.2.4 Scenario 3: Queue Management in Queue Formulation Process

In this scenario, the effects of the queue management strategies for queue formulation process of an oversaturated intersection are evaluated. The same hypothetical intersection in Scenario 2 is still used for this scenario. It is assumed that the capacities of both lanes on major streets are reduced by 40%. The total departure rate of major streets becomes 0.6 vehicle/seconds, i.e. the total saturation discharge rate of major streets is 2160 vehicles/hour with two lanes. It is also assumed that there is no residual queue on major streets left from the previous cycle. For the minor streets, the initial queue length is computed by the same method in Scenario 2. The vehicle trajectory data of major streets

is scaled by a factor 0.3 in arrival headway and is used in this scenario. Effective green time distribution and assumed maximum queue length limits in Scenario 2 are also applied. Table 5.2 shows the results of scenario 3.

Table 5.2 Results of Scenario 3: Queue Formulation Process

1	2	3	4	5	6	7		8	
Capacity Loss of Major streets (%)	Intersection v/c ratio	Cycle Length		Effective Green time of Minor Streets (seconds)	Intersection Total Stop Delay per Minute (seconds)	Delay Reduction per Minute		Final queue Ratios	
						(seconds)	(%)	Major Streets	Minor Streets
40%	1.736	80	Original Timing	24	3606.8	-------	------	1.01	0.26
			Queue Management Timing	6	3549.9	56.9	1.58	0.71	0.80
		100	Original Timing	31	4614.1	-------	------	1.36	0.23
			Queue Management Timing	7	4457.9	156.2	3.39	0.94	0.95
		120	Original Timing	37	3939.2	-------	------	1.02	0.34
			Queue Management Timing	12	3744.2	195	4.95	0.72	0.84
30%	1.532	100	Original Timing	31	4055.2	-------	------	1.15	0.23
			Queue Management Timing	13	3669.6	385.6	9.51	0.77	0.77
20%	1.379	100	Original Timing	31	3496.3	-------	------	0.94	0.23
			Queue Management Timing	18	3084.5	411.8	11.78	0.63	0.62

Case 1 has signal timing determined by the simulated actuated control logic and case 2 has timing determined by the proposed second strategy. Column 2 shows intersection v/c ratios. For the assumed conditions, when the capacity of major streets

loses 40% the stop delay reductions in the scenario is found to be less significant than those of scenario 2 (less than 5%). To understand the sensitivity of the strategies with different capacity losses, a cycle length of 100 seconds was used to conduct two additional situations at 30% and 20% capacity losses in major streets. From Table 5.2, the proposed queue management strategies could effectively balance queue length of major and minor streets. When the capacity is reduced by 20% and 30%, the delay reductions are quite noticeable at around 10%.

Figure 5.5 also shows the effects of proposed queue management strategies for queue formulation processes of an oversaturated intersection. It can be seen that the speed of queue accumulation at major streets becomes slower than that of original timing plans by implement the proposed strategies. No queue exceeds assumed allowable length by using the developed strategies. In contrast (except (f)), under actuated controller logic major street queue length during the study periods in all other figures of Figure 5.5 was over the maximum queue limits. Hence, the second strategy is effective in managing queue growth during queue formulation process to avoid spillback. It can also reduce stop delays in an oversaturated intersection when comparing with results of the original timing case.

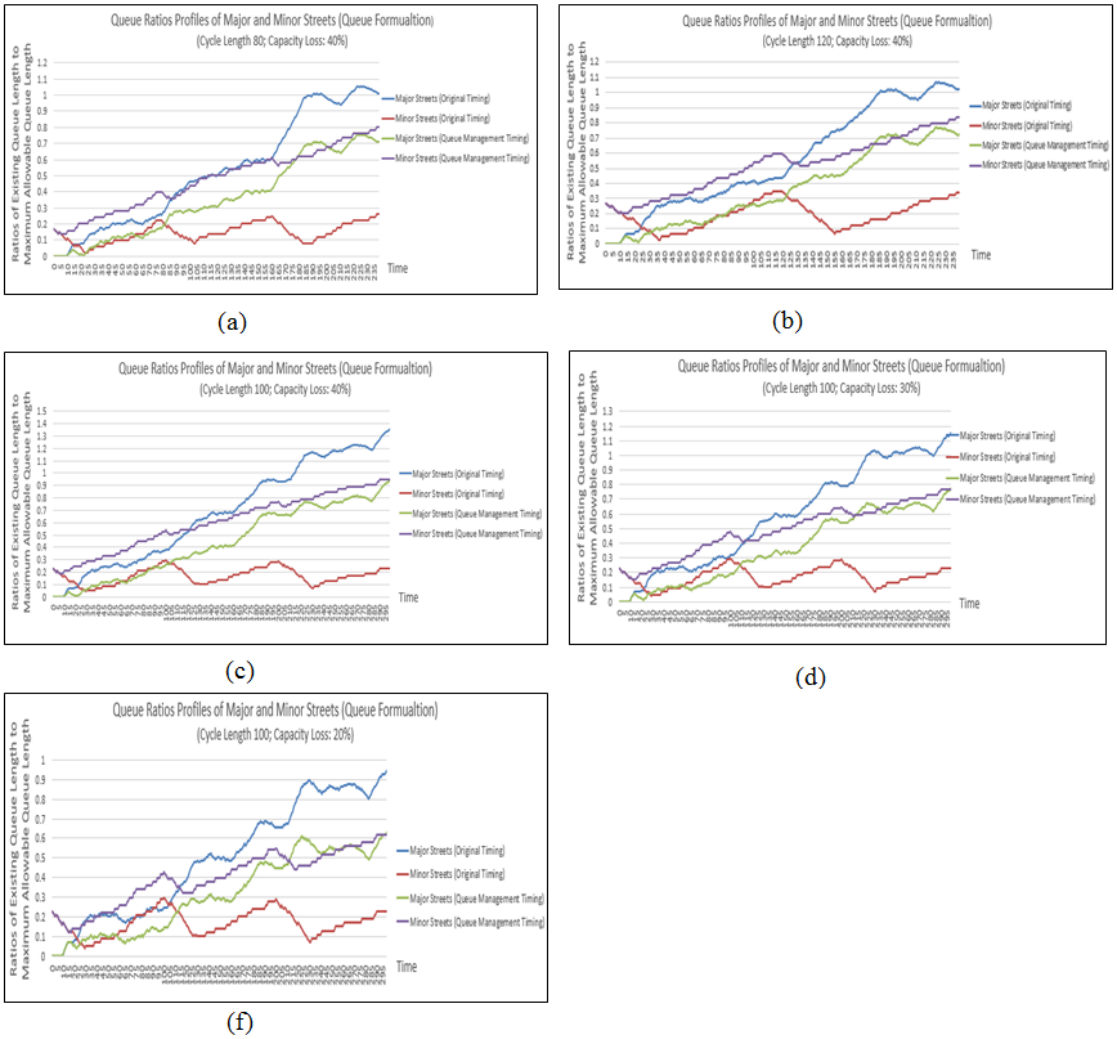

Figure 5.5 Effects of Queue Management Strategies for Queue Formulation Process

CHAPTER VI

CONCLUSIONS AND RECOMMENDATIONS

6.1 Conclusions

The connected vehicle program, a U.S. Department of Transportation major research initiative, is one of the most promising technologies to mitigate traffic congestion and enhance mobility for transportation system users. Connected vehicle technologies are still in the simulation and experimental stages, and the full implementation of connected vehicle technologies on all vehicles (i.e. penetration rates of connected vehicles at 100%) is still decades to come. However, traffic signal models and algorithms based on connected vehicle technologies can still generate obvious benefits when the penetration rate of connected vehicles reaches a minimum value. For example, a 20-30% penetration rate is helpful and could be achieved within 5-7 years as indicated by Goodall [6].

Therefore, a solution at the beginning stage of connected vehicle deployment that can utilize these technologies with a low cost upgrade for existing infrastructures is important to study in order to find ways to mitigate congestion on signalized arterials. In this dissertation, a connected vehicle based traffic signal control model (CVTSCM) was presented. There are two modules: an arterial-level traffic progression optimization model (ALTPOM) for under-saturated conditions, and two queue length management based ATM strategies for saturated/oversaturated conditions. The prominent feature of

ALTPOM is that it simultaneously optimizes traffic progression for an entire signalized arterial instead of one intersection by one intersection. To optimize offsets, the splits of coordinated intersections are first adjusted to balance predicted upcoming demands of all approaches. Then, a traffic propagation model based on the fusion data from connected vehicle and loop detectors is used to predict upcoming vehicles' trajectories. Based on predicted vehicle trajectories for the entire arterial, ALTPOM maximizes the total number of arrivals on green after clearing the existing queue. Dynamic programming is then utilized to solve the ALTPOM. ALTPOM is recursively implemented in real time for a user defined projection horizon.

To build, debug and evaluate the performance of ALTPOM, a connected vehicle simulation environment with DSRC communication simulation capacity called ETFOMM was selected. ETFOMM has integrated Trajectory Conversion Algorithm (TCA) software. TCA is produced by Noblis, Inc. It can simulate DSRC communication between Road Side Units (RSUs) and vehicle on-board equipment (OBUs), and it can transfer Basic Safety Message (BSMs) [9]. The interface of ALTPOM with ETFOMM is carefully designed, programmed and tested.

Then case studies are conducted to evaluate the performance of ALTPOM within a connected vehicle environment. An urban signalized arterial with 5 signals in Jackson, Mississippi was selected. The field signal timing plans were collected and then were optimized by TRANSYT-7F as the benchmark. Two additional scenarios were performed: 1) ALTPOM under 25% penetration rate of connected vehicle; and 2) ALTPOM under 50% penetration rate of connected vehicle. According to the results, ALTPOM significantly outperforms TRANSYT-7F. When compared to TRANSYT-7F

at under 25% (50%) penetration rates of connected vehicles, ALTPOM reduces 57.6% (61.5%) control delay per vehicle, increases 18.7% (23.6%) average speed, and improves 4.9% (4.4%) throughput for both directions of major streets. ALTPOM also provides smooth traffic progression for the coordinated direction with little impact on the opposite direction. Within 25% (50%) penetration rates of connected vehicles environment, ALTPOM decreases 12.3% (14.6%) stopped vehicle percent of the coordinated direction while stopped vehicle percent of the opposite direction increases 1.4% (decreases 0.2%), which is almost unchanged. The control delay in the opposite direction also considerably decreases.

In traditional traffic signal coordination, smoothing the major street traffic generally results in the performance of minor streets degrading. This is not the case in the proposed models. ALTPOM not only optimizes the offset but also proactively and dynamically adjusts splits of all phases. This overcomes the traditional shortfalls of previous methods where increased performance of major streets come at the sacrifice of performance on minor streets. In addition to substantially enhancing the performance of the major streets, ALTPOM also significantly improves performance of the minor streets. Compared with TRANSYT-7F at under 25% (50%) penetration rates of connected vehicles, ALTPOM reduces 26.0% (31.8%) control delay per vehicle, increases 7.8% (10.9%) average speed, and improves 7.7% (7.4%) throughput for both directions of minor streets.

This dissertation also conducted a volume sensitivity study for ALTPOM. Two traffic conditions were considered: 1) volume of the entire arterial decreases 20%; and 2) volume of the entire arterial increases 20%. Since the effectiveness of ALTPOM under

different penetration rates of connected vehicle was validated in the last case study, ALTPOM is implemented with a 25% penetration rate of connected vehicles for these two additional traffic conditions. Based on the results, ALTPOM also outperforms TRANSYT-7F under different levels of traffic demand variations and has better performance when the study arterial is more congested.

In essence, ALTPOM belongs to adaptive traffic control system (ATCS), since ALTPOM adjusts signal control parameters according to upcoming traffic fluctuations. As indicated by a NCHRP report, an ATCS is hard to outperform in a well maintained traditional traffic signal control system over 10%-15% with respect to any one of all performance measures [79]. Based on results analyses of ALTPOM above, the benefits of ATCS can significantly further improve based on connected vehicle technologies, compares to the conventional optimized traffic signal control. The reason is that predicted/measured real-time traffic data is more accurate based on connected vehicle technologies, which are crucial for an ATCS.

With respect to saturated or over-saturated conditions, queue lengths need to be well managed in order to prevent queue spillback to upstream intersections or network gridlock. Two queue length management based Active Traffic Management (ATM) strategies based on connected vehicle technologies for an oversaturated intersection, which is typical at rural and suburban arterials, are proposed. The first strategy allocates as much effective green time as possible to the approach or the lane group with higher discharge capacity to reduce delays. The second approach allocates effective green time of a cycle, thus balancing queue length of major and minor streets to prevent queue spillback and reduce intersection stop delays.

Both strategies were theoretically investigated and experimentally validated. A hypothetical intersection with different capacities on major and minor streets was modeled to operate under the simulated actuated control logic. The first strategy is validated by enumerating all possible effective green time combinations of minor and major streets. Two scenarios were developed to evaluate the effectiveness of the second approach. One is queue dispersion and the other is the queue formulation process. Based on the results, the second strategy more effectively manages and balances queue lengths of both major and minor streets to avoid queue spillback.

By implementing the second strategy, intersection stop delays are reduced as well. The stop delays significantly decrease for the queue dispersion process when significant residual queue is present during the first cycle, from 9.72% to 13.85%. With respect to the queue formulation process, the saturation discharge rate loss of the major streets is assumed to be 40%, 30% and 20%. Under all of the scenarios, by performing the second strategy queue lengths are well balanced. While under actuated control logic, queues are extended over the allowable maximum length. The delay reduction is not significant when saturation discharge rate reduction of major streets is 40% (slightly less than 5%). When capacity drops on major streets are 20% and 30%, the delay reduction becomes more noticeable at around 10%.

Therefore, the effectiveness of the proposed ALTPOM and two queue length management based ATM strategies based on connected vehicle technologies are validated by the case studies. These two traffic signal control model/strategies are major modules of CVTSCM, and as such the effectiveness of CVTSCM is proven. Specifically, when traffic conditions are under-saturated, ALTPOM is used to provide smooth

progression for upcoming traffic. When traffic conditions become saturated, queue length management based ATM strategies are applied to control queue length dynamics in order to prevent queue spillback and gridlock. Thus, the CVTSCM proposed in this dissertation can handle all traffic conditions of an arterial.

Since the developed CVTSCM is verified by simulated Basic Safety Messages (BSMs) and BSM equivalent data, it is expected that CVTSCM could be implemented in the field without significant revisions or numerous field experimentations. CVTSCM is also expected to be implemented in a "black box" computer with NTCIP compatible field controllers to increase the mobility of signalized arterials in the future.

6.2 Recommendations for Future Studies

The developed CVTSCM within the connected vehicle environment is only validated by simulation studies. It is preferred to assess CVTSCM in a hardware-in-the-loop study and a field study if future funding and resources are available.

The effects of large trucks on mobility and safety of signalized arterials are a potential future focus that could improve the proposed CVTSCM. Large trucks can still be identified by the occupancy of upstream loop detectors. Large trucks need longer distance to acceleration and deceleration than personal vehicles. When several large trucks are predicted to arrive at an approach of an intersection, longer green time may be considered to allocate to that approach to decrease the number of stops of large trucks and ensure large trucks could safely traverse the intersection. By considering the effects of large trucks, the explored CVTSCM in this dissertation could be expanded to multi-modes traffic signal control model, which is a hot research topic within the traffic signal control field.

Based on connected vehicle technologies, the real-time partial or complete vehicle trajectory of connected vehicles within signalized arterials are available. This data could be utilized to estimate real-time Original and Destination (OD) data. Traffic signal control based on real-time OD data is expected to further improve the performance of traffic signal coordination which is a desired research topic for future studies.

REFERENCES

1. Schrank, D., B. Eisele, and T. Lomax, *TTI's 2012 URBAN MOBILITY REPORT Powered by INRIX Traffic Data*. 2012: College Station, Texas. p. 131.

2. Federal Highway Administration. *Congestion Reduction Toolbox: Improve Service on Existing Roads*. [cited 2015 Dec 5th, 2015]; Available from: https://www.fhwa.dot.gov/congestion/toolbox/service.htm.

3. Federal Highway Administration. *Connected Vehicle*. January 24, 2012 [cited 2012 Feb 16th, 2012]; Available from: http://www.its.dot.gov/research/v2i.htm.

4. Research and Innovative Technology Administration. *Vehicle-to-Infrastructure (V2I) Communications for Safety*. Connected Vehicle Applications January 12, 2012 [cited 2012 Feb 16th, 2012]; Available from: http://www.its.dot.gov/research/v2i.htm.

5. SAE International, *SAE J2735 Dedicated Short Range Communications (DSRC) Message Set Dictionary (Apr 2015)*. 2015, SAE International: Warrendale, PA. p. 402.

6. Goodall, N.J., *Traffic Signal Control with Connected Vehicles*, in *Civil Engineering*. 2013, University of Virginia: Charlottesville, VA. p. 224.

7. Office of Operations Federal Highway Administration, *Traffic Signal Timing Manual*. 2009, U.S. Department of Transportation: Washitongton D.C.

8. Federal Highway Administration *Lankershim Boulevard Dataset*. 2007.

9. Deurbrouck, T., et al., *Trajectory Conversion Algorithm Software User Manual Version 2.3*. 2015: Washington, DC p. 31.

10. Federal Highway Administration. *Next Generation Simulation (NGSIM)*. 2015 July 24, 2015 [cited 2015 August 2015]; Available from: http://ops.fhwa.dot.gov/trafficanalysistools/ngsim.htm.

11. Li, P., et al. *A Monte Carlo Simulation Procedure to Search for the Most-likely Optimal Offsets on Arterials Using Cycle-by-Cycle Green Usage Reports*. in *Transportation Research Board 90th Annual Meeting*. 2011.

12. Shoup, G.E. and D. Bullock, *Dynamic offset tuning procedure using travel time data.* Transportation Research Record: Journal of the Transportation Research Board, 1999. **1683**(1): p. 84-94.

13. Liu, H.X. and H. Hu. *A Data-Driven Approach to Arterial Offset Optimization*. in *Transportation Research Board 2011 Annual Meeting*. 2011. Washington D.C.: Transportation Research Board.

14. Day, C.M., et al. *Visualization and assessment of arterial progression quality using high resolution signal event data and measured travel time*. in *TRB 2010 Annual Meeting*. 2010. Washington D.C.: Transportation Research Board.

15. Gettman, D., et al. *Data-driven algorithms for real-time adaptive tuning of offsets in coordinated traffic signal systems*. in *TRB 2007 Annual Meeting*. 2007. Washington D.C.: Transportation Research Board.

16. Abbas, M., D. Bullock, and L. Head, *Real-time offset transitioning algorithm for coordinating traffic signals.* Transportation Research Record: Journal of the Transportation Research Board, 2001. **1748**(1): p. 26-39.

17. Liu, G., et al. *Adaptive Model-based Offsets Optimization for Congested Arterial Network*. in *TRB 93rd Annual Meeting*. 2014. Washington D.C.: Transportation Research Board.

18. Abbas, M.M., Y.-S. Jung, and Y. Zhang. *Offset Performance Evaluation Using Stop Bar Detector Data and Microscopic Shockwave Theory*. in *Transportation Research Board 85th Annual Meeting*. 2006. Washington D.C.: Transportation Research Board.

19. Takahashi, S., et al. *Genetic algorithm approach for adaptive offset optimization for the fluctuation of traffic flow*. in *The IEEE 5th International Conference on Intelligent Transportation Systems*. 2002. Singapore: IEEE.

20. Little, J.D., *The synchronization of traffic signals by mixed-integer linear programming.* Operations Research, 1966. **14**(4): p. 568-594.

21. Little John, D., M.D. Kelson, and N.H. Gartner, *MAXBAND: A Versatile Program for Setting Signals on Arteries and Triangular Network*. 1981, Alfred P. Sloan School of Management, Massachusetts Institute of Technology: Cambridge, MA. p. 1-30.

22. Gartner, N.H., et al., *A multi-band approach to arterial traffic signal optimization.* Transportation Research Part B: Methodological, 1991. **25**(1): p. 55-74.

23. Gartner, N.H., J.D. Little, and H. Gabbay, *Optimization of traffic signal settings by mixed-integer linear programming: Part I: The network coordination problem.* Transportation Science, 1975. **9**(4): p. 321-343.

24. Gartner, N.H., J.D.C. Little, and H. Gabbay, *Optimization of Traffic Signal Settings by Mixed-Integer Linear Programming Part II: The Network Synchronization Problem.* Transportation Science, 1975. **9**(4): p. 344 - 363.

25. Wallace, C.E. and K.G. Courage, *Arterail progression--new design approach.* Transportation Research Record, 1982. **881**(HS-034 940): p. 53-59.

26. Bleyl, R.L., *A practical computer program for designing traffic-signal-system timing plans.* Highway Research Record, 1967(211): p. 19-33.

27. Lieberman, E.B., J. Chang, and E.S. Prassas, *Formulation of real-time control policy for oversaturated arterials.* Transportation Research Record: Journal of the Transportation Research Board, 2000. **1727**(1): p. 77-88.

28. Messer, C.J., et al., *A variable-sequence multiphase progression optimization program.* Highway Research Record, 1973(445): p. 10.

29. Mirchandani, P. and L. Head, *A real-time traffic signal control system: architecture, algorithms, and analysis.* Transportation Research Part C: Emerging Technologies, 2001. **9**(6): p. 415-432.

30. Sen, S. and K.L. Head, *Controlled optimization of phases at an intersection.* Transportation science, 1997. **31**(1): p. 5-17.

31. Luyanda, F., et al., *ACS-lite algorithmic architecture: Applying adaptive control system technology to closed-loop traffic signal control systems.* Transportation Research Record: Journal of the Transportation Research Board, 2003. **1856**(-1): p. 175-184.

32. Robertson, D.I. and R.D. Bretherton, *Optimizing networks of traffic signals in real time: The SCOOT method.* IEEE Transactions on Vehicular Technology. , 1991. **40** (1): p. 11-15.

33. Jhaveri, C.S., J.J. Perrin, and P.T. Martin. *Effectiveness of SCOOT Adaptive Control on Networks and Corridors*. in *TRB 2004 Annual Meeting*. 2004. Washington D.C.: Transportation Research Board.

34. Wilson, C., G. Millar, and R. Tudge. *Microsimulation Evaluation of the Benefits of SCATS Coordinated Traffic Control Signals*. in *TRB 2006 Annual Meeting*. 2006. Washington D.C.: Transportation Research Board.

35. Gartner, N.H., F.J. Pooran, and C.M. Andrews, *Optimized policies for adaptive control strategy in real-time traffic adaptive control systems: Implementation and field testing.* Transportation Research Record: Journal of the Transportation Research Board, 2002(1811): p. 148-156.

36. Chandra, R. and C. Gregory, *InSync Adaptive Traffic Signal Technology: Real-Time Artificial Intelligence Delivering Real-World Results*. 2012: Lenexa, Kansas.

37. Panda, D.P., *An integrated video sensor design for traffic management and control*, in *IMACS IEEE CSCC '99 International Multiconference* 1999, World Scientific and Engineering Press. p. 176-185.

38. Oh, J. and J.D. Leonard, *Vehicle Detection Using Video Image Processing System: Evaluation of PEEK VideoTrak.* Journal of transportation engineering, 2003. **129**(4): p. 462-465.

39. Sharma, A., et al. *Detection of Inclement Weather Conditions at a Signalized Intersection using a Video Image Processing Algorithm*. in *12th Digital Signal Processing Workshop*. 2006. Wyoming: IEEE.

40. Grenard, J.L., D.M. Bullock, and A.P. Tarko, *Evaluation of selected video detection systems at signalized intersections*. 2002, Joint Transportation Research Program, Purdue University: West Lafayette, Indiana. p. 199.

41. Rhodes, A., et al., *Evaluation of Stop Bar Video Detection Accuracy at Signalized Intersections*. 2006, Joint Transportation Research Program, Purdue University: West Lafayette, Indiana. p. 418.

42. Rhodes, A., K. Jennings, and D.M. Bullock, *Impact of Camera and Lighting Position on Video Detection Precision*. 2006, Joint Transportation Research Program, Purdue University: West Lafayette, Indiana. p. 23.

43. Unal, O. and M. Cetin. *Estimating Queue Dynamics and Delays at Signalized Intersections from Probe Vehicle Data*. in *Transportation Research Board 93rd Annual Meeting*. 2014. Washitong D.C.: Transportation Research Board.

44. Cheng, Y., et al. *An exploratory shockwave approach for signalized intersection performance measurements using probe trajectories*. in *Transportation Research Board 89th Annual Meeting*. 2010. Washington D.C.: Transportation Research Board.

45. Izadpanah, P., B. Hellinga, and L. Fu. *Automatic traffic shockwave identification using vehicles' trajectories*. in *Transportation Research Board 88th Annual Meeting*. 2009. Washington D.C.: Transportation Research Board.

46. Lu, X.-Y. and A. Skabardonis. *Freeway traffic shockwave analysis: exploring the NGSIM trajectory data*. in *Transportation Research Board 86th Annual Meeting* 2007. Washington, DC: Transportation Research Board.

47. Cheng, Y., et al., *Cycle-by-cycle queue length estimation for signalized intersections using sampled trajectory data.* Transportation Research Record: Journal of the Transportation Research Board, 2011(2257): p. 87-94.

48. Quiroga, C.A. and D. Bullock, *Measuring control delay at signalized intersections.* Journal of Transportation Engineering, 1999. **125**(4): p. 271-280.

49. Liu, H.X. and W. Ma, *A virtual vehicle probe model for time-dependent travel time estimation on signalized arterials.* Transportation Research Part C: Emerging Technologies, 2009. **17**(1): p. 11-26.

50. Ni, D. and H. Wang, *Trajectory reconstruction for travel time estimation.* Journal of Intelligent Transportation Systems, 2008. **12**(3): p. 113-125.

51. Herrera, J.C., et al., *Evaluation of traffic data obtained via GPS-enabled mobile phones: The Mobile Century field experiment.* Transportation Research Part C: Emerging Technologies, 2010. **18**(4): p. 568-583.

52. Sun, Z. and X.J. Ban, *Vehicle trajectory reconstruction for signalized intersections using mobile traffic sensors.* Transportation Research Part C: Emerging Technologies, 2013. **36**: p. 268-283.

53. Ban, X., et al. *Delay pattern estimation for signalized intersections using sampled travel times*. in *Transportation Research Board 88th Annual Meeting*. 2009. Washington D.C.: Transportation Research Board.

54. Ban, X.J., P. Hao, and Z. Sun, *Real time queue length estimation for signalized intersections using travel times from mobile sensors.* Transportation Research Part C: Emerging Technologies, 2011. **19**(6): p. 1133-1156.

55. Hao, P., X. Ban, and J. Whon Yu, *Kinematic Equation-Based Vehicle Queue Location Estimation Method for Signalized Intersections Using Mobile Sensor Data.* Journal of Intelligent Transportation Systems, 2014: p. 1-17.

56. Hao, P. and X. Ban. *Long queue estimation using short vehicle trajectories for signalized intersections*. in *Transportation Research Board 92nd Annual Meeting*. 2013. Washington D.C.: Transportation Research Board.

57. Lee, J., *Assessing the Potential Benefits of IntelliDrive-based Intersection Control Algorithms*, in *Civil and Environmental Engineering*. 2010, University of Virginia: Charlottesville, VA.

58. Smith, B.L., et al., *IntelliDrive^{SM} Traffic Signal Control Algorithms*. 2011: Charlottesville, VA. p. 73.

59. Rhythm Engineering. *HOW INSYNC WORKS.* [cited 2014 Feb 2014]; Available from: http://rhythmtraffic.com/how-insync-works/.

60. Cesme, B. and P.G. Furth. *Self-Organizing Control Logic for Oversaturated Arterials*. in *Transportation Research Board 92nd Annual Meeting*. 2013. Washington D.C.: Transportation Research Board.

61. He, Q., K.L. Head, and J. Ding, *PAMSCOD: Platoon-based arterial multi-modal signal control with online data.* Transportation Research Part C: Emerging Technologies, 2012. **20**(1): p. 164-184.

62. Priemer, C. and B. Friedrich. *A decentralized adaptive traffic signal control using V2I communication data*. in *12th International IEEE Conference on Intelligent Transportation Systems*. 2009. St. Louis, MO, USA: IEEE.

63. Feng, Y., et al. *A Real-time Adaptive Signal Phase Allocation Algorithm in a Connected Vehicle Environment*. in *Transportation Research Board 94th Annual Meeting*. 2015. Washington D.C.: Transportation Research Board.

64. He, Q., K.L. Head, and J. Ding, *Multi-modal traffic signal control with priority, signal actuation and coordination.* Transportation Research Part C: Emerging Technologies, 2014. **46**: p. 65-82.

65. Intelligent Transportation Systems Joint Program Office. *ICM Pioneer Sites*. Integrated Corridor Management 2013 December 4, 2013 [cited 2013 December 24, 2013]; Available from: http://www.its.dot.gov/icms/pioneer.htm.

66. Christofa, E., J. Argote, and A. Skabardonis. *Arterial Queue Spillback Detection and Signal Control Based on Connected Vehicle Technology*. in *Transportation Research Board 92nd Annual Meeting*. 2013. Washington, D.C.: Transportation Research Board.

67. Khoshmagham, S., et al. *Travel Time Observation in Privacy Ensured Connected Vehicle Environment Using Partial Vehicle Trajectories and Extended Tardity*. in *Transportation Research Board 94th Annual Meeting*. 2015. Washington D.C.: Transportation Research Board.

68. Arnaout, G.M., et al. *An IntelliDrive application for reducing traffic congestions using agent-based approach*. in *Systems and Information Engineering Design Symposium (SIEDS), 2010 IEEE*. 2010. Charlottesville, VA: IEEE.

69. Koonce, P., et al., *Traffic Signal Timing Manual*. 2008: Washington, DC. p. 265.

70. Battelle and Texas A&M Transportation Institute, *SIGNAL PHASE AND TIMING AND RELATED MESSAGES FOR V-I APPLICATIONS CONCEPT OF OPERATIONS DOCUMENT*. 2013: McLean, VA p. 122.

71. Newell, G.F., *The rolling horizon scheme of traffic signal control.* Transportation Research Part A: Policy and Practice, 1998. **32**(1): p. 39-44.

72. Roess, R.P., E.S. Prassas, and W.R. McShane, *Traffic Engineering (Fourth Edition)*. 2010, New Jersey: Pearson Higher Education.

73. New Global Systems *Enhanced Transportation Flow Open-source Microscopic Model (eTFOMM) A Tool for Advanced Research Projects such as Connected Vehicle Applications*.

74. Zhang, L. *Clound, Distributed, and Parallel Computing Practice Workshop Session I: Theories (Presentation)*. in *South District ITE Meeting*. 2015. Biloxi, Mississippi: South District ITE.

75. New Global Systems for Intelligent Transportation Management, *API Report*. p. 40.

76. Zhang, L., *etFomm API*. p. 12.

77. Zhang, L., et al., *I-55 Integrated Diversion Traffic Management Benefit Study*. 2014: Jackson, MS. p. 148.

78. Transportation Research Board, *Highway Capacity Manual 2010*. 2010, Washington D.C.: Transportation Research Board.

79. Stevanovic, A., *Adaptive traffic control systems: domestic and foreign state of practice*. 2010, Washington D.C.: Transportation Research Board.

80. SAE International, *J2735. SAE International. Dedicated short-range communications (DSRC) message set dictionaty (nov. 2009)*. 2009, SAE International: Warrendale, PA. p. 359.

81. Cambridge Systematics Inc., *NGSIM Lankershim Data Analysis (8:30 a.m. to 8:45 a.m.) summary report*. 2006: Washington D.C. p. 25.

APPENDIX A

PARAMETERS DEFINICAITON IN CHAPTERS 3 AND 5

A.1 Parameters Deification in Chapter 3

TM: Turning movement (left =1, through =2, and right=3);

j: The time index of a projection horizon (j =1, 2, ⋯, T),

d: Approach of each intersection (d= 1 2, 3, ⋯, and TD)

TD: Total number of approaches for an intersection,

p: The index of phases for an intersection (p =1, 2, 3, ⋯, and TP),

TP: Total number of phases for an intersection,

m: The index of coordinated intersections (m= 1, 2, 3, ⋯, M),

M: Total number of coordinated intersections in a signalized arterial,

T: The duration of a projection horizon (seconds),

$TP_{TM,d,m}\%$: Turning Percentage of turning movement TM for approach d at intersection m (%),

$CQ_{TM,d,m}$: Number of connected vehicle in the queue at the beginning of a projection horizon for turning movement TM of approach d at intersection m (vehicles),

$NCV_{j,TM,d,m}$: Number of connected vehicles discharged at time index j from turning movement TM of direction d at coordinated intersection m (vehicles),

$\alpha_{TM,p,m}$: The binary variables, ($\alpha_{TM,p,m} = 1$,if phase p severs turning movement TM of approach d at intersection m; $\alpha_{TM,p,m} = 0$, otherwise),

$TP_{p,m}\%$: Turning percentage of phase p at intersection m (%),

$DM_{p,m}$: Total demand for phase p at intersection m (vehicles),

$N_{j,d,m}$: Number of vehicles actuated the upstream detector at the jth time index of the direction d at coordinated intersection m (vehicles),

$DC_{p,m}$: The discharge capacity of phase p at intersection m (vehicles),

C: The cycle length (seconds),

$NL_{p,m}$: Number of lanes for phase p at intersection m,

$dp\%$: Desired cumulative percentages that a selected discharge headway should cover (%),

$\mu_{d,m}^{dp\%}$: The selected discharge headway to estimate desirable green time (seconds/vehicle/lane),

$G_{de_{p,m}}$: The duration of desirable effective green time of phase p at intersection m (seconds),

$G_{a_{p,m}}$: Maximum green time of phase p at intersection m (seconds),

$y_{p,m}$: Yellow time of phase p at intersection m (seconds),

$ar_{p,m}$: All red time of phase p at intersection m (seconds),

$l_{1_{p,m}}$: Startup lost time of phase p at intersection m (seconds),

$l_{2_{p,m}}$: Clearance lost time of phase p at intersection m (seconds),

$Split_{p,m}$: Split of phase p at intersection m (seconds),

$L_{p,m}$: Total lost time of phase p at intersection m (seconds),

$G_{e,min_{p,m}}$: The minimum effective green time of phase p at intersection m (seconds),

TG_{e_m}: Total available effective green time of a cycle at intersection m (seconds),

L_m: Total lost time of a cycle at intersection m (seconds),

TG_{de_m}: Total desirable effective green time of a cycle at intersection m (seconds),

O_m: Offset of intersection m which will be implemented in the next projection horizon (second),

$O_{current,m}$: Current offset of intersection m (second),

ΔO_m: Offset adjustment factor (seconds),

$-\beta_m, \beta_m$: The lower and upper bound of offset adjustment for intersection m defined by users (seconds),

t_{ss}^a: The travel time of connected vehicle a from the location it stops first time to the stop bar (seconds),

$DS_{d,m}^a$: The distance between the location that connected vehicle a completely stop first time and the stop bar (ft),

$UV_{d,m}$: The free flow speed of approach d at intersection m (mph),

$T_{d,m}^a$: Travel time of connected vehicle a at approach d of intersection m (seconds),

t_{enter}^a: The time instant that connected vehicle a arrives at the upstream detector on the approach d of intersection m (second),

t_s^a: The time instant that connected vehicle a completely stops for the first time within DSRC communication zone i at approach d of intersection m (t_s^a is the time instant that connected vehicle a traverses the stop bar of intersection m, if the vehicle doesn't completely stop),

$T_{d,m}$: Average travel time at approach d of intersection m (seconds),

A: Total number of connected vehicles which complete vehicle trajectories are available at approach d of intersection m for the last projection period (vehicles),

i: The time index in a cycle($i = 0,1,2,\cdots,C-1$),

$Arr\_sb_{i,d,m}$: Stop bar arrival profiles for time index i at approach d of intersection m (vehicles),

$Arr\_up_{i,d,m}$: Upstream arrival profiles for time index i at approach d of intersection m (vehicles),

$TNVL_{d,m}$: Total number of vehicle travel on approach d of intersection m currently (vehicles),

$AccV_{up_{d,m}}$: Accumulative traffic counts for the upstream detector on approach d of intersection m currently (vehicles),

$AccV_{stop_{d,m}}$: Accumulative traffic counts for the stop bar detector on approach d of intersection m currently (vehicles),

$MNVL_{d,m}$: Maximum number of vehicles may travels on link (vehicles),

veh: The index of all vehicles,

$VA_{veh,d,m}$: Arrival time of vehicle veh at the upstream detector on approach d of intersection m (second),

$VD_{veh,d,m}$: Scheduled departure time of vehicle veh at approach d of intersection m (second),

$RG_{cp,m}$: The remaining green time of the coordinated phase cp at intersection m (seconds),

t_{yield_m}: The time instant of the yield point at intersection m, i.e. the last second of the coordinated green (second),

$t_{curre\,t}$: The current time (second),

$W_{d,m}$, $E_{d,m}$, $Q_{d,m}$: variables which indicate estimated total number of vehicles in the queuing region, deceleration region, and free flow region 1 of approach d at intersection m, respectively, (vehicles),

N_v: A binary variable,

v: The index of vehicles,

$VIQ0_{p,m}$: Estimated number of vehicles in the queuing region for of phase p at intersection m (vehicles) and these vehicles could be released during remaining green time (vehicles),

$DR_{p,m}$: The discharge rate per second per lane for phase p at intersection m (vehicles),

$NL_{p,m}$: Number of lanes for phase p at intersection m,

$VIQC_{p,m}$: Estimated number of vehicles in the queuing and deceleration region for phase p at intersection m which could be released during the remaining green time (vehicles),

$VFFRC_{p,m}$: Estimated Number of vehicles in the free flow region 1 could be discharged during the remaining green time (vehicles),

$rq_{0,p,m}$: The initial queue length of the phase p at intersection m for the next projection horizon (vehicles),

$rq_{i,p,m}$: The queue length of time index i for phase p at intersection m of the next projection horizon (vehicles),

$DC_{i,p,m}$: The discharge capacity of time index i for phase p at intersection m of the next projection horizon (vehicles),

$QDH_{p,m}$: Queue discharge headway per lane for phase p at intersection m (seconds/vehicle),

$SI_{i,p,m}$: Signal indication for time index i of phase p at intersection m ($SI_{i,p,m} =$ 1: green light; $SI_{i,p,m} = 0$: red light),

NC: Number of cycles within a projection horizon,

$dis_{i,p,m}$: The discharge profiles of time index i for phase p at intersection m of the next projection horizon (vehicles),

$NAG_{O_m,cp,m}$: Total number of arrivals on green after existing queue dispersed for coordinated phase cp of intersection m for next projection horizon (vehicles),

$VSplit_m$: The split vector which contains splits of 8 phases of intersection m (seconds),

$f(O_m, VSplit_m)$: Number of arrivals on green after existing queue cleared when the offset of an intersection is O_m and splits of the intersection are $VSplit_m$ (vehicles),

$cf(O_m, VSplit_m)$: Cumulative number of arrivals after existing queue cleared from intersection 1 to m (vehicles). The offsets and splits of intersection m and $m-1$ are ($O_m, VSplit_m$) and ($O_{m-1}, VSplit_{m-1}$), respectively,

Z: The maximum number of arrivals on green after the existing queue is cleared in the coordination direction for the entire arterial (vehicles).

A.2 Parameters Definition of Chapter 5

Q_1^0, Q_2^0: Initial queue length of phases 1 and 2 (vehicles),

$Q_{1A}, Q_{1C}, Q_{1D}, Q_{2A}, Q_{2C}, Q_{2D}$: Queue length of phases 1 and 2 at time stamps A, C, D (vehicles),

D_1, D_2: Stop delays of phases 1 and 2 (seconds),

λ_1, λ_2: Arrival rate of phases 1 and 2 for a short term period (vehicle/seconds),

ρ_1, ρ_2: Saturation discharge rate of phases 1 and 2 (vehicle/seconds),

C: Cycle length (seconds),

t': The optimal effective green time for major streets (seconds).

D_{total}: Total stop delays of an entire intersection (seconds),

$G_{max,1}, G_{max,2}$: Maximum effective green times of phases 1 and 2 (seconds),

k: The kth cycle,

δ: A weighted parameter, ratio of vehicles stored on major streets and minor streets allowed,

N_s, N_m : Number of lanes of side streets and major streets, respectively,

L_s, L_m: The predefined maximum allowable queue length for side streets and major streets, respectively (vehicles),

t^* : The actuated effective green time for minor streets (seconds),

t_1: The effective green time of minor streets generated by the second queue management strategy (seconds).